Modelling a small-scale rainwater harvesting system for irrigation using SWAT

A thesis presented in partial fulfilment of the requirement for the degree of Masters of AgriScience

Masters
in
Agricultural Science

at Massey University, Manawatu,
New Zealand

Jiajia Liu
2018

Abstract

In many regions, the water available for allocation to irrigation has reached its limit and that there is a need to identify alternative sources. Large scale irrigation schemes are available for farmers to buy in in certain part of the country. However, not all farmers will have access to water from large scale irrigation schemes and this has led some hill country farmers to consider the potential to construct their own, relatively small, dams on their properties to capture and store water for irrigation. The major challenge to estimating the potential benefits of water storage for irrigation is reliably simulating the likely volume of water that can be captured.

This thesis models the rainwater harvesting potential of a hill country farm in the Wairarapa region (Riverside Farm). Soil Water Assessment Tool (SWAT) has been selected to model the water harvesting potential due its ability to separate runoff, lateral flow, and the ground water contribution to the harvestable water according to the local topographic, soil and land use properties. This allows the modeller to consider a wide range of scenarios.

A SWAT model was set up for the water harvesting catchment (WHC) on the case study farm. The WHC is ungauged, however it is nested within a larger catchment called the Calibration and Validation Catchment (CVC). CVC is gauged and therefore flow data can be obtained. Improved parameters obtained through CVC calibration is transferred to the WHC, this process of donating calibrated parameters to a hydrologically similar ungauged catchment is called parameter regionalization.

The model suggests that the storage scheme can meet the average irrigation demand of 43 ha of land 90% of the time. The predicted water harvesting potential decreases with regionalized parameters when compared to the default settings which suggests that there is a risk that some modelling may overestimate the volume of water that can be captured.

The economic impact of irrigation was also assessed in this study. The cost of one extra kilogram of pasture dry matter production is estimated to be between 39-44 cents/kg. Nitrogen fertilizer application can increase pasture yield but it is not a perfect substitution to irrigation because nitrogen fertilizer is not to be applied during drought. However, purchasing supplement feed from outside the farm might be a cheaper alternative to building a small-scale dam.

Acknowledgment

I'd like to acknowledge my supervisor Dave Horne. Me Wang for providing help with SWAT model calibration and validation. Ahmed Elwan for help with R.

Table of Contents

Table of Figures

Chapter 1 Introduction

The climate in New Zealand varies both spatially and temporally. The spatial variability is in part due to the long and narrow shape of the country and the mountains that run mostly lengthwise down the islands. These features play a role in the spatial variability of climates they encourage the formation of microclimatic systems. The prevailing wind direction in New Zealand is westerly, The windward side of New Zealand receives much higher precipitation than the leeward side (Salinger, 1980), with a recent study suggesting that this precipitation difference is increasing, particularly in the South Island (Caloiero, 2015). On average, New Zealand receives between 600 mm to 1600 mm of rainfall per year. Typically, the rainfall is spread throughout the year with a dry period during the summer. In the North Island, more rain falls in winter than summer, and most of the south western part of New Zealand, winter is often the driest season (Mackintosh, 2001). The greatest seasonal variation in rainfall is observed in Northland, East Cape, and the Wairarapa region, where winter rainfall nearly doubles the rainfall in summer (Duncan & Woods, 2013). Rainfall also varies on a year-to-year basis. For example at Lincoln, Canterbury, the long term (1975-2007) mean annual rainfall was 627 mm/year but the minimum rainfall was 308 mm in 1988 and the maximum rainfall was 1015mm recorded in 1978 (Moot, Mills, Lucas, & Scott, 2009). Climate change further aggravates such variation: it has been observed that the winter and spring seasons are getting wetter, and summers and autumn are getting dryer (Caloiero, 2015).

The variation of the New Zealand climate is both ‘a blessing and a curse.' On the one hand, the variability of New Zealand’s climate allows for the cultivation of a wide range of agricultural products. As a result, New Zealand horticultural production is concentrated in areas that are favorable to specific crops, such as avocado in the Bay of Plenty and Northland, and cherries in the Central Otago. On the other hand, the variability in climate (especially precipitation), creates uncertainty and risk for agricultural producers. According to NIWA (National Institute of Water and Atmospheric Research), a drought would occur in New Zealand every year or two. With ongoing climate change, this variability is likely to continue or become exacerbated. NIWA projects that by 2080, under a medium-high climate change scenario, the frequency of severe drought (equivalent to a current day ‘one-

in-twenty year' drought) are projected to quadruple in North Otago, Canterbury, Marlborough, and much of the Wairarapa, Bay of Plenty, Coromandel, Gisborne, and Northland regions (Mullan, Porteous, Wratt, & Hollis, 2005). In 2015, the North Canterbury region was hit by the worst drought in 20 years, which resulted in nearly all of the farmers in this region struggling for many months.

Irrigation provides some level of relief from variable climatic patterns. In addition, irrigation contributes to the economic growth of New Zealand. According to a report by the New Zealand Institute of Economic Research, irrigation contributes about $2.2 billion dollars to net farm gate GDP. This accounting does not consider the flow-on impacts of irrigation. The same study also concludes that if irrigation had never occurred, the New Zealand GDP would be 2.4% lower (Corong, Hensen, & Journeaux, 2014).

Hill country pasture is particularly important to the New Zealand sheep and beef industry. Hill country sheep and beef enterprises occupy about 4.1 million ha of land or about 15.2% of the total land area in New Zealand (Moot et al., 2009). Despite improvements in irrigation techniques that reduce potential risks of soil erosion and nutrient loss, few hill country farms are irrigated (Hedley, Laurenson, Mclndoe, & Reese, 2014). The low adoption rate of irrigation in hill country is a limitation to New Zealand pastoral system, as it is estimated that irrigated pastures may produce on average 28% more biomass than unirrigated pasture during the dry months between December and April, and twice as much biomass in a particularly dry year (Scotter, Clothier, & Turner, 1979). Summer pasture production on a sheep and beef farm is often particularly important because with irrigation, summer pasture production is likely to exceed animal demand and feed can be stored for winter use. The feed surplus generated during the summer period, to some extent, determines the number of animals a farm can carry through winter. Horne and Gray (2014) conducted a case study analysis on the profitability of irrigation in hill country and found that by strategically utilizing the extra biomass produced from irrigation, a farm may generate a net advantage of $1200/ha to $1125/ha after accounting for the annual cost of irrigation.

In response to drought and the economic benefit of utilizing irrigation systems, there is increasing interest in, and adoption of, irrigation across New Zealand. This is increasing the demand for water and placing increasing pressure on valuable and limited fresh water resources. Groundwater reserves and summer flow in rivers is not sufficient to support

marked increases in the irrigated area and so alternative sources of water must be identified before this expansion can occur. One such alternative is to harvest surplus river flow in winter when rivers are often carrying very large volumes of water. Many large-scale irrigation schemes have been constructed or proposed. These irrigation schemes collect and store river water behind a dam during high flow and release the water stored during periods of low rainfall, for irrigation purposes.

The majority of such large-scale irrigation schemes are located in the East Coast of South Island due to drier climates, but there are also projects at different stages of development and feasibility study in the North Island. For example, a dam has been proposed in the Ruataniwha Basin in Central Hawkes Bay to store water for irrigation purposes. The dam would capture water from the Makaroro River near the Ruahine range and has the potential to irrigate 20,000 ha of land. However, these schemes are expensive to build and maintain and they are not available everywhere. For instance, the Hawkes Bay Regional Council dedicated $80 million to the longterm plan of the Rutaniwha Water Storage scheme alone, however, the scheme also needs investment from private parties and MPI (Hendery, 2015). There is a scheme proposed in the Wairarapa Valley, the feasibility of which is still being evaluated. Therefore, currently there is no large-scale water harvesting scheme for irrigation in the lower North Island.

The reliability of some of the rivers and streams for irrigation purposes can be low, due to minimum flow requirements imposed by regional councils. For example, the Waipoua River, which flows through the Wairarapa region only irrigates 57 ha of agricultural land, but on average there are 18-25 days of a year that irrigation is restricted. In a particularly dry year, consent holder may experience up to 45-61 days of irrigation restriction (Thompson, 2015). Prolonged irrigation restrictions have serious economic consequences. It has been estimated that in an average year, water restrictions reduce farm operating profit in the Waipoua catchment by 7% (Harris, 2015).

Small-scale rainwater harvesting and irrigation systems have been proposed as a novel tool that could allow New Zealand hill country farmers to increase their resilience to seasonal climatic variation. Rainwater harvesting (RWH) uses small-scale structures to collect and store runoff and drainage as a water source for irrigation. It does not involve storing river water in large reservoirs or the mining of ground water. Critchley, Siegert, Chapman, and

Finkel (1991) summarized some of the small-scale water harvesting schemes being used worldwide.

The key function of RWH, as it is more widely understood, is to convert that part of the precipitation that would be surface runoff or drainage into soil moisture, either by reducing surface runoff/drainage and increasing soil water storage at the crop growth site or by increasing surface runoff to maximize the amount of water entering the water storage system. The rainwater harvesting scheme proposed in this study belongs to the latter case. The proposed small-scale rainwater harvesting (on-farm) scheme will consist of two parts. The first component part of the small-scale rainwater harvesting scheme is the natural catchment basin. Some of the surface runoff and drainage that exits the catchment is intercepted, collected and stored behind a dam at the catchment outlet. The second part of the water harvesting scheme involves irrigating this stored water to a command area. Unlike large-scale dams that are expensive to build, small scale on-farm dams (up to approximately 15 meters high) can be constructed using relatively unsophisticated design procedures and equipment (Stephens, 2010). A typical dam includes three parts; the reservoir area, the embankment structure, and spillways. The reservoir area of the proposed water harvesting scheme overlaps with the water harvesting catchment. The embankment is the barrier used for water storage; this is often referred to as the dam. An example of an embankment is shown Figure 1-1. Spillways are exit passages for surplus water and perform an essential role by allowing excess water to be released in a controlled manner and thus avoiding a breach of the dam.

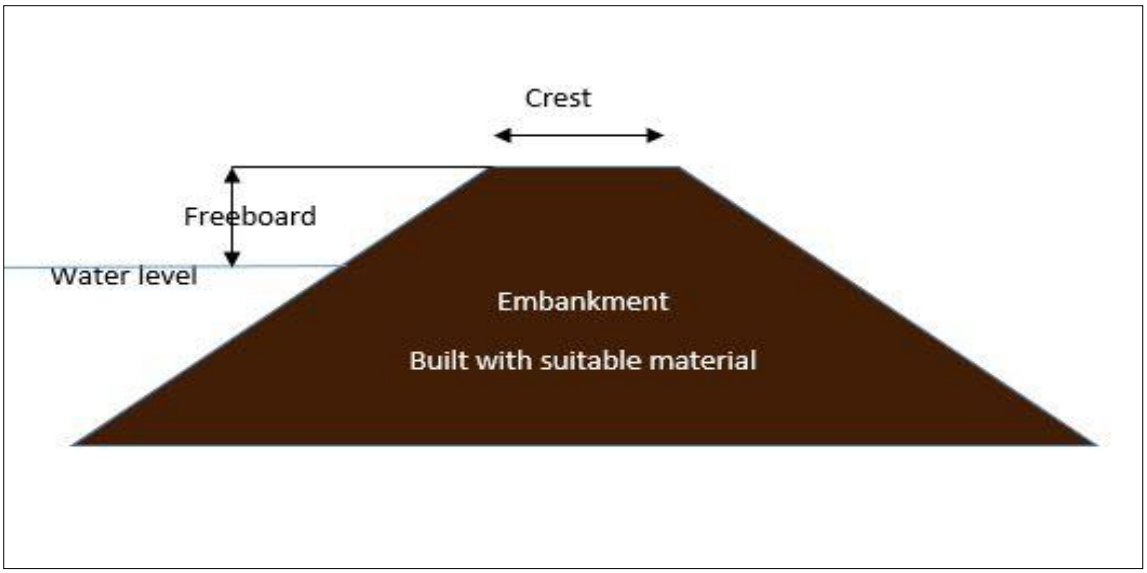

Figure 1-1 Cross-Sectional View of a typical embankment.

This study seeks to model the dynamic balance of water supply and demand for irrigation water on the case study farm to investigate the long-term feasibility and reliability of a small-scale water harvesting system.

1.1 Water Supply

Rain Water Harvesting Potential

Rain water harvesting potential or (RWHP) is the amount of water a catchment can collect for storage purpose during a given period. Traditionally, RWH potential is estimated using a simple water balance method, for example, Horne and Gray (2014) used this approach to estimate the water harvesting potential of a case study sheep and beef farm in the Huatokitoki catchment in the southern Hawkes Bay. The simple water balance is expressed below in Equation 1-1:

$$SW_t = SW_0 + \sum_{i=1}^{t} (R_{day} - E_a - Q_{loss})$$

Equation 1-1 A simple water balance

Where $\boldsymbol{SW_t}$ is the final soil water content (mm), $\boldsymbol{SW_0}$ is the initial soil water content on day i (mm), t is the time (days), $\boldsymbol{R_{day}}$ is the precipitation on day i (mm) , $\boldsymbol{E_a}$ is the evapotranspiration on day i (mm) , $\boldsymbol{Q_{loss}}$ is the combination term for amount of surface runoff and drainage on day i (mm)

Rain Water harvesting Potential (RWHP) of a catchment is therefore expressed as:

$$RWHP = \sum_{i=1}^{t} (R_{day} - E_a - (SW_t - SW_0)) * k_h * area$$

Equation 1-2 Equation to calculate rain water harvesting potential of a catchment

Where $\boldsymbol{k_h}$ is the water harvesting efficiency, representing the portion of water which will end up in the water storage structure, and area is the catchment size.

The water balance method has the advantage of being easy to use and only climate data, basic soil data and the area of the farm is required. However, the water balance model is often too simplistic to realistically model a water harvesting scheme in hill country landforms as that proposed for the case study farm (Riverside farm near Masterton in the Wairarapa region). The water harvesting scheme proposed is only able to capture and store runoff generated within the catchment as it does not intercept any streams. Runoff and

drainage is governed by soil type, slope, land use, and temporally variable soil moisture conditions (Andersson, Zehnder, Jewitt, & Yang, 2009). Simple water balance methods cannot partition runoff and drainage and may lead to an overestimation of water harvesting potential. For the proposed scheme, RWH potential is determined by a number of factors including runoff/drainage generation potential and water storage potential. The SWAT (Soil Water Assessment Tool) has been selected to model the runoff/drainage generation potential as it incorporates the CN (Curve Number) rainfall-runoff partitioning method, which accounts for the dynamic runoff potential change under different soil water conditions. A detailed introduction to SWAT model will be given in Chapter 4

1.2 Water Demand:

Command Area irrigation demand

The objective of irrigation is (Siddique, Belford, & Tennant, 1990) to maintain the soil moisture deficit in a certain range so as to prevent a reduction in plant growth or performance during a dry period. In this way, irrigation provides a boost to pasture productivity, particularly during the summer when soil moisture is often the primary factor limiting pasture growth.

Irrigation demand is calculated as:

$$IWD = \sum_{i=1}^{t} (CWR - SW - R_{day}) * command\ are$$

Equation 1-3 Irrigation water demand for the command area

Where IWD (m3) is the irrigation water demand of the command area and CWR is the crop water requirement (mm) for optimal pasture growth, SW is water stored in the profile above some critical value and $\boldsymbol{R_{day}}$ is the rain on day i (mm). Of course, the smallest value IWD can take on any day is 0.

The irrigation demand of the command area depends on the critical value for SW. On some occasions this critical value corresponds to the readily available water and so irrigation takes place once this portion of soil water has been depleted. Other farmers irrigate at some point between field capacity and the value for readily available water for example at 80% of

available water. The setting of the critical point at which irrigation commences is often based, arbitrarily, on farmer's experience. For this study, the irrigation demand of the command area is calculated using the soil water balance method due to its relative success and widespread use in predicting the response of pasture to irrigation.

1.3 Site Description

Riverside farm

The case study has been carried out using Riverside Farm to investigate the feasibility of a small scale water harvesting schemes for hill country in New Zealand. Riverside farm is situated 14 km north of Masterton in the Wairarapa region. It has a total area of 696 ha (shown in Figure 1-2) The Riverside farm is dominated by Kohinui and Tauherenikau soils, while the Greytown series, Konini and Mikimiki soils are also present. Riverside farm hosts 3200 Romney breeding ewes, 950 Romney breeding hoggets, 30 Romney rams, 10 blackface terminal rams as well as 300-350 trade steers. Waipoua River and Mikimiki stream runs through the farm before joining each other before Mikimiki Bridge ("Riverside Farm," 2016). The 30-year mean annual precipitation is 1350 mm, with higher precipitation during winter months and lower precipitation during the summer months as summarized in Figure 1-3. The mean annual temperature is at 12.8 °C, with January being the hottest month and July being the coldest. Both El Nino and La Nina cause low seasonal rainfall in the Wairarapa region where the farm is located. El Nino enhances westerly weather patterns and exacerbates low rainfall in the summer. La Nina affects the region to a lesser extent by causing dry summers interspersed with heavy rainfall events (Watts, 2005).

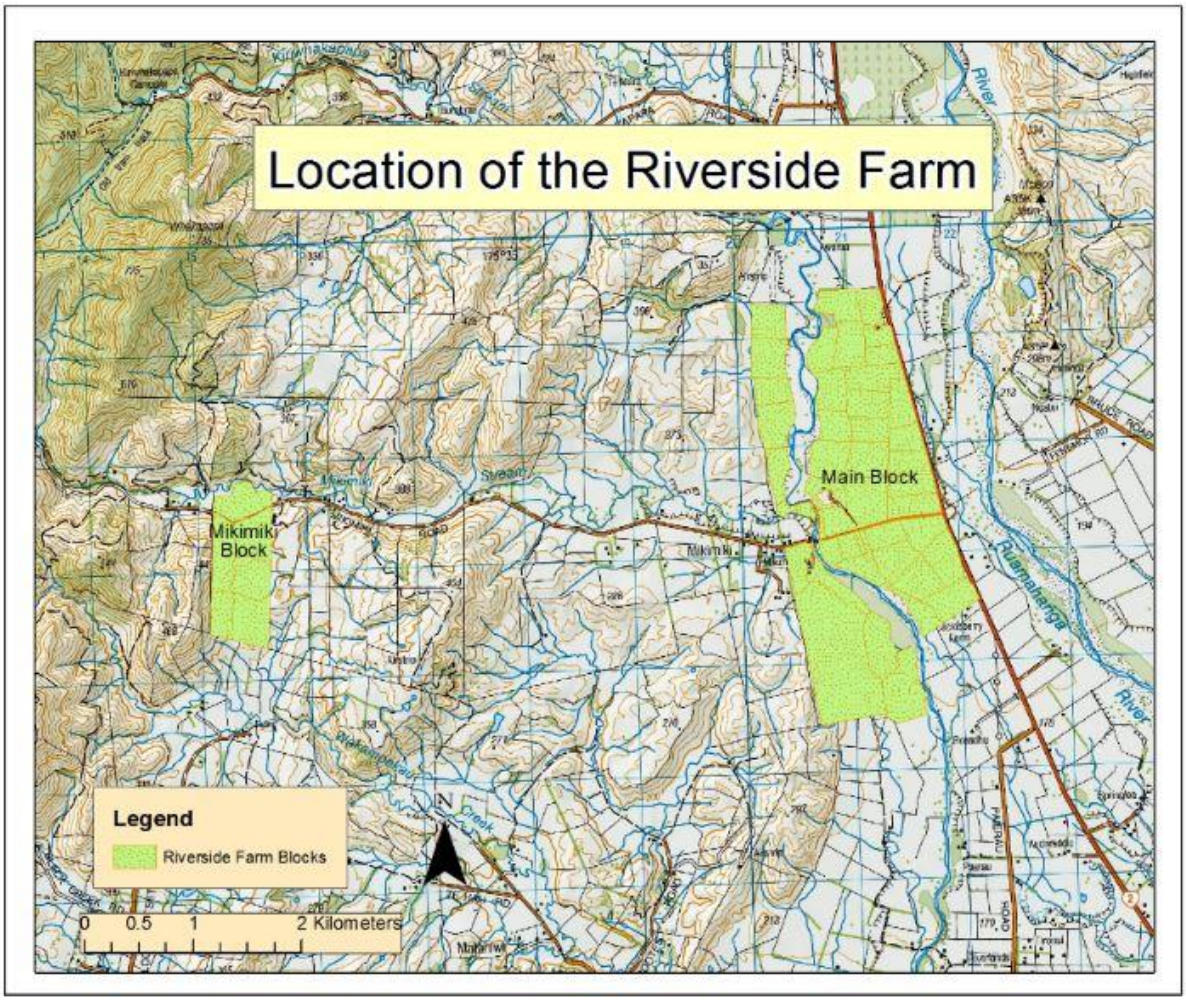

Figure 1-2 Location of the 'Main block' and ' Mikimiki block' on Riverside farm

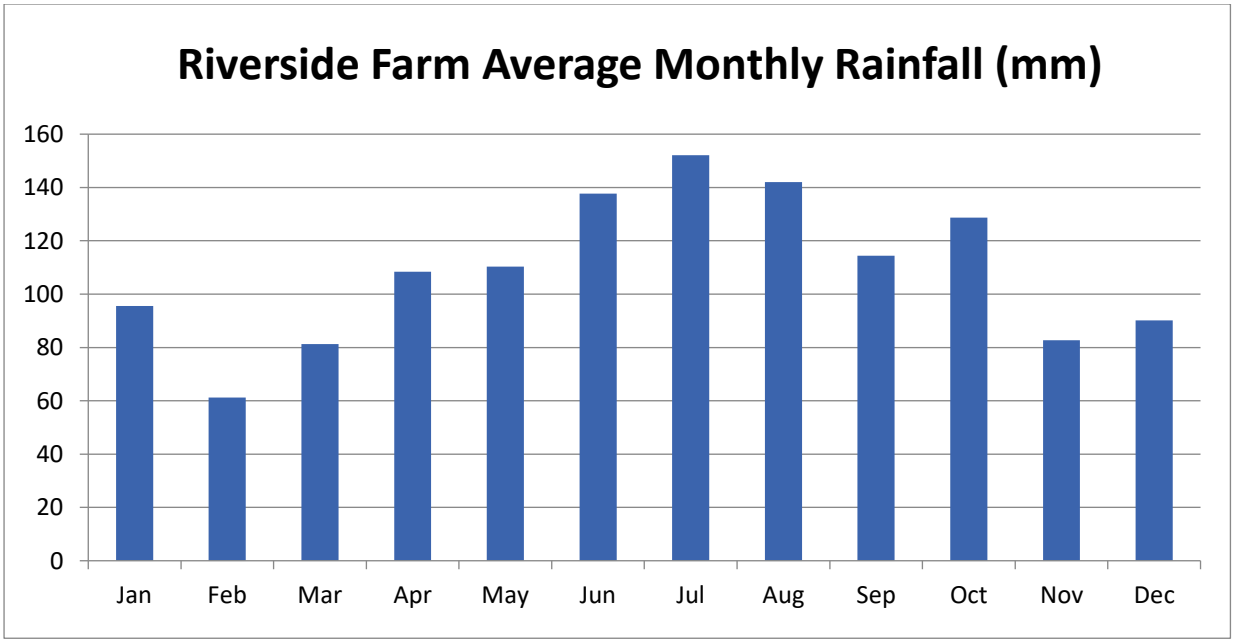

Figure 1-3 Thirty-year (1984-2014) Average Monthly Rainfall (mm) at the riverside farm

Calibration, Validation Catchment

The CVC is 7774 ha in area. Together, pasture and forest occupy about 90% of the total catchment area. Rimutaka, Ruahine, and Konini are the three main soil types within the catchment. The average annual rainfall of the CVC varies greatly according to the location. The mountainous west side of the catchment receives more rainfall than the flat eastern plain.

Command Area

Water collected and stored in the WHC is then applied to a flat pasture covered area on Riverside farm. The soil in the command area is assumed to be Kohinui soil series. A pedo-transfer function was used to derive soil water properties from a detailed description of the soil. The area is assumed to be homogenous, flat, and free draining.

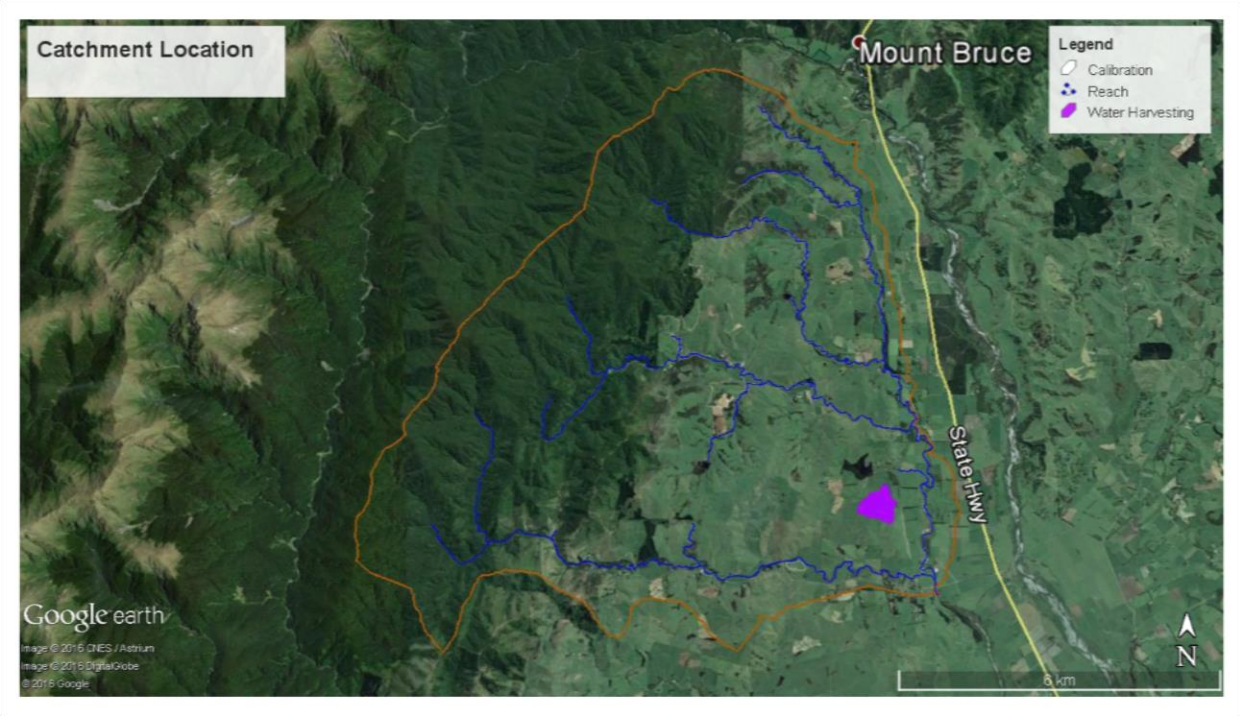

Figure 1-4 Aerial Photos of the Calibration and Validation Catchment. The water harvesting catchment is nested within the Validation catchment.

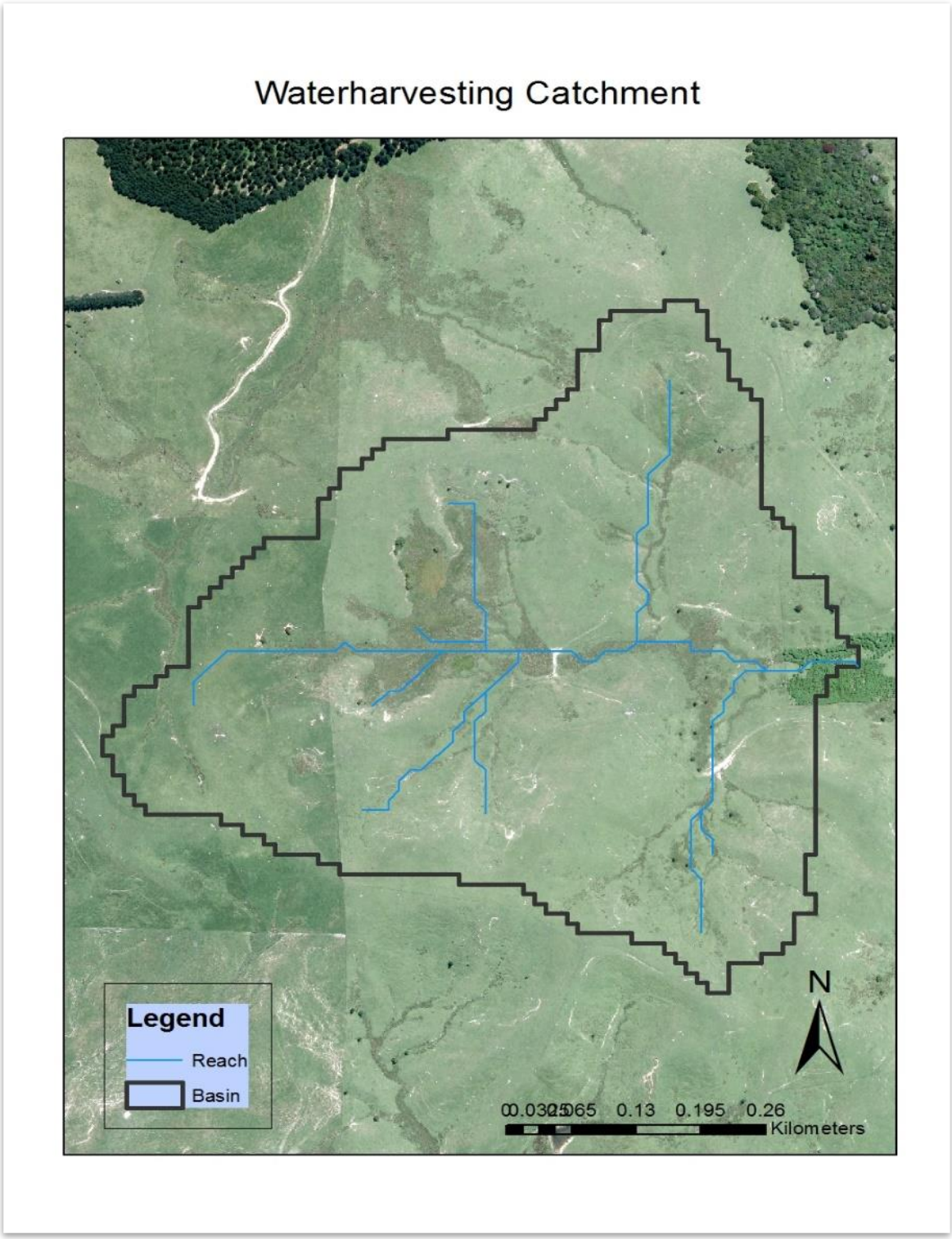

Figure 1-5 Aerial photo of the Water Harvesting Catchment

1.4 Research Objective

In this study, the technical and financial feasibility and reliability of a small-scale water harvesting scheme is investigated on a case study farm, which is representative of summer-dry hill country in New Zealand. SWAT is used to answer the question about water supply: how much water can be harvested and stored in a dam constructed near the outlet of the water harvesting catchment? Next, a soil water balance and a pasture growth model is used to answer the question of how much water is needed for irrigation and what is the pasture response to irrigation using harvested water? Finally, the supply and demand side of the equation are balanced to answer the last question: What is the cost to supply water for irrigation and what is the cost of extra pasture? These three questions will be addressed in later chapters

Chapter 2 Literature Review

2.1 Hill Country Farming

The New Zealand grassland system is divided into three categories based on topography and productivity. High country which is characterized by hilly terrain, high altitude and low pasture production (2.0 tonnes dry matter per ha). Hill country which is defined as 'all lowland and montane hill and steeplands (slope >15°) with average pasture production reaching 7.0 tonnes dry matter per hectare per year (Kemp & Lopez, 2016). Flat to rolling country often has good year-round pasture production, producing, on average approximatey 11 tonnes dry matter per ha per year or in some areas significantly more. Flat to rolling land supports most of the dairy production and over half of the total sheep and beef production due to its high productivity: this land can carry in excess of 14 SU per ha. High country is the least productive type of all; it is mainly used for fine wool production. Hill country farms carry approximately 40% of sheep and 39% of beef cattle in New Zealand with an average of stocking rate of 7.5 SU per ha. (Machado, Morris, Hodgson, & Fathalla, 2005).

Hill country farming contributes significantly to the New Zealand economy. The New Zealand meat and wool sector generates $7.5 billion export earnings annually. Notably, New Zealand produced 47% of the lamb traded in the global market and 12% of global wool production. New Zealand also exported 82% of beef produced within the country, generating $2.2 billion in the year ending in September 2012 (Morris & Dymond, 2013). Improving the productivity of hill country farms can have a considerable impact on the economic prosperity of the nation as a whole.

B. Zhang, Valentine, & Kemp (2007) conducted a meta-analysis of the factors influencing annual herbage production in hill country. They found that slope and spring rainfall are the most important factors influencing hill country annual herbage production. In some areas sufficient rainfall during the spring and summer allows hill country farms to achieve high herbage production. In other regions, pasture production is significantly constrained by low rainfall in late spring and/or summer. It has been proposed that storing water from winter precipitation and applying it to the pasture during the critical spring-summer period might improve overall hill country farm productivity.

In order to model the potential benefit that irrigation can have on a hill country farm, it is important to understand the basic production principles of a typical hill country sheep and beef farm.

In New Zealand, sheep and beef cattle are often kept on the same farm. Beef cattle can be used to control secondary growth and thus prevent sward deterioration. The ideal ratio of sheep to beef cattle changes depending on the economic situation. The challenges of hill country pastoral farming vary depending on local/regional climatic conditions. In wet North Island hill country, the major challenge is to keep enough stock over winter, when pasture production is very low, to consume the spring and summer pasture growth. By adjusting the number of livestock in the autumn and making sure each animal attains a certain body condition score by the beginning of the winter, these livestock can be overwintered and rationed enough pasture for body maintenance requirements. The rationing of pasture allows rapid pasture growth recovery during spring and summer when lambing and finishing occurs. In the East Coast (where Riverside farm is located), where the summer is particularly dry, the goal is to ensure maximum production during spring and early summer and then to reduce demand when the summer dry spell starts by selling off lambs. Figure 2-1 shows the daily pasture growth rate in the Wairarapa region; summer pasture production suffers due to soil water deficiency. The dry summer is problematic for the beef cattle breeding cycle, as this season coincides with peak lactation demand.

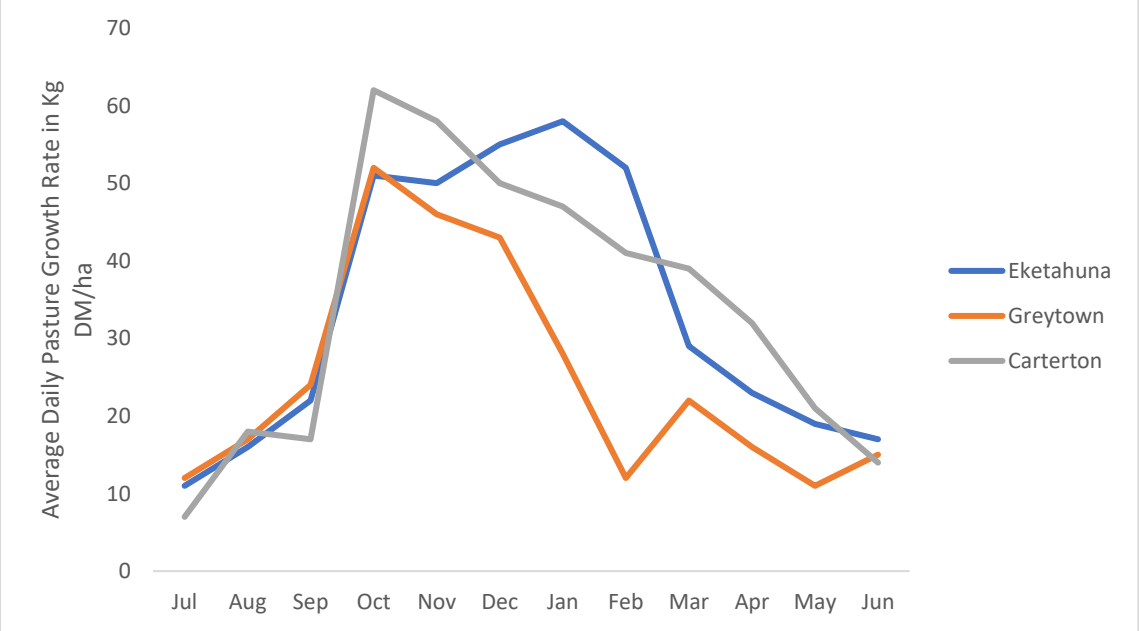

Figure 2-1 Average Daily pasture growth rate in Kg DM/ha in three Wairarapa site (DairyNZ, 2010)

Scotter et al. (1979) found that irrigation can nearly double the pasture growth rate during a particularly dry summer in Central New Zealand. Studies conducted in Canterbury show that up to 80% increased dry matter yield annually can be obtained through irrigation (McBride, 1994). Since 95% of the sheep and beef cattle diet is pasture, irrigation may mitigate the limitations that dry summers impose on pasture production on East Coast hill country farms and thus allow for a more productive pastoral system.

Improvement in hill country farm productivity may provide additional benefits by improving hill country farm sustainability. In the rare cases where irrigation is used on hill country farms, it is often applied to flatter areas of the farm, which have a higher land use capacity (LUC) class and are less prone to erosion. Increased productivity in these areas can reduce the demand for feed from more vulnerable land types. Retiring low LUC land from pasture production can reduce soil erosion and the quantity of sediments entering waterways (Cameron, Di, & Moir, 2013). In addition, there has been evidence showing that plots under long-term irrigation have higher soil carbon concentration (Srinivasan & McDowell, 2009).

In conclusion, the adoption of irrigation in Hill country New Zealand can be beneficial both economically and ecologically. There is a strong interest among both the central government and farmers in irrigation of hill country farms.

Water requirement of pasture

Plant water requirement is defined as the total water required for optimal pasture growth i.e. the water requirement of pasture is calculated as the quantity of water that will allow maximum pasture growth in a year when other factors such as soil nutrition are optimized. There are many theories on the relationship between plant biomass production and soil water content. Howell, Cuenca, and Solomon (1990) summarized the factors that affect biomass production using a sequence of five equations:

$$ET = f\ (I, \theta, C, W, M)$$

Equation 2-1 Evapotranspiration is a function of Irrigation, soil physical and chemical properties crop biological properties, weather conditions, and miscellaneous factors.

$$T = f\ (ET, C, W, M)$$

Equation 2-2 Transpiration is a function of evapotranspiration, crop biological properties, various weather vectors, and miscellaneous factors

$$A = f\ (T, C, W, M)$$

Equation 2-3 Carbon assimilation is a function of transpiration, crop biological properties, and miscellaneous factors

$$P = f\ (A, C, M)$$

Equation 2-4 Plant dry matter production is a function of plant carbon assimilation, crop biological properties, and miscellaneous factors.

$$Y = f\ (P, C, M)$$

Equation 2-5 Economic yield is a function of the plant dry matter production, crop biological properties, and miscellaneous factors.

Dry matter production is linearly related to the quantity of evapotranspiration. Howell summarized this relationship as:

$$P\ P_m{}^{-1} = T\ T_m{}^{-1}$$

Equation 2-6 The ratio between actual dry matter production and potential dry matter production equals to that of the ratio between actual transpiration and the potential evapotranspiration.

Where P is the dry matter production and Pm is the potential dry matter production. T is the transpiration, Tm is the potential transpiration when yield is not affected.

Nearly all evapotranspiration is transpiration under full pasture cover. In order to achieve maximum dry matter production, the soil water deficit must not limit transpiration. McAneney and Judd (1983) further suggested a hypothesis that production is maximized when the soil water deficit is below a critical point, which is equal to the readily available soil water.

$$T\ T_m{}^{-1} = 1 \quad When\ SD_i \leq SD_c$$

Equation 2-7 Transpiration is maximized when soil water deficit is below the critical point SD_c

When the soil water deficit is greater than this critical point, transpiration is limited by the extent of the soil water deficit.

$$T\ T_m{}^{-1} = (AWC - SD_i)(AWC - SD_c)^{-1} \quad When\ SD_i > SD_c$$

Equation 2-8 when soil water deficit is greater than the critical point, the ratio between the actual and potential transpiration is equivalent to the ratio between actual water available in the soil profile for plant extraction and water available in the soil profile at critical point.

Where $\boldsymbol{SD_i}$ is the current soil water deficit, $\boldsymbol{SD_c}$ is the critical soil water deficit, $\boldsymbol{AWC}$is the total plant available water in soil.

McAneney and Judd (1983) found that the critical soil water deficit that affected transpiration lies between 60 and 70 mm for the Horotiu sandy loam in the Waikato. The same study measured the effect of soil water deficit on pasture yield and discovered that the critical point is much lower at 34 mm. This suggests that pasture yield starts to decrease

before transpiration decreases and that Equation 2-6 is likely to over-predict dryland pasture production. The authors recommend irrigating smaller quantities at higher frequencies to fully realize the dry matter production response to irrigation. However, the sample size of data in this experiment is small, and therefore caution is needed in interpreting the results of this experiment. Turner (1990) suggested that leaf enlargement is more sensitive than leaf photosynthesis to larger soil water deficits, which might explain the difference in critical points for transpiration and pasture yield observed by McAneney and Judd (1983).

2.2 Overview of SWAT

History and Development of SWAT

SWAT (Soil and Water Assessment Tool) (Neitsch, Arnold, Kiniry, & Williams, 2011) is a physically-based, daily time step, distributed watershed model developed by Jeff Arnold for the USDA-ARS (United States Department of Agriculture- Agricultural Research Service). SWAT was developed to predict the impact of land management practices on water, sediment, nutrients, and agricultural chemical yields in watersheds with varying soil types, land use, and management conditions over time.

SWAT was created in the early 1990s and was a direct improvement of the SWRRB model (Simulator for Water Resources in Rural Basins). SWRRB was developed using components of other models including CREAMS (Chemical, Runoff, and Erosion from Agricultural Management Systems), GLEAMS (Groundwater Loading Effects on Agricultural Management Systems), EPIC (Erosion-Productivity Impact Calculator), and ROTO (Routing Outputs to Outlet). CREAMS was included to allow daily rainfall and hydrology simulation in SWRRB. A function of GLEAMS was used to simulate the fate of pesticides in SWRRB. EPIC was used to simulate crop growth in SWRRB. ROTO (Routing Outputs to Outlet) was then used to simulate the downstream effects of management practice in SWRRB. However, SWRRB was difficult to use and it only allowed a maximum computing of 10 sub-basins. Development was made allowing multiple outputs of SWRRB run to be fed into ROTO, but it was still required the tedious task of managing input and output datasets. Finally, SWAT was developed by merging ROTO and SWRRB to allow the simulation of multiple sub-basins.

Since its inception, SWAT has been under constant review and development. Over eight major updates have been issued since the first version published in 1994. In addition to updates to the model, interfaces have also been developed for QGIS, ArcGIS, and Visual Basics. As of 2016, there are over 2400 peer-reviewed journal articles published regarding the development and application of the model.

SWAT is a physically based model

SWAT is a physically-based model. Rather than relying on regression equations to describe the relationship between model input and output, SWAT uses specific information about soil, land-use, topography, climate data, and land management to model the physical processes related to water movement, sediment movement, plant growth, nutrient cycling, etc. A physically-based modeling approach has a number of advantages compared to regression based models;

1) SWAT can be applied to a watershed with no monitoring data (ungauged catchment). For example, Srinivasan et al., (2010) modeled crop yields and hydrologic budgets with SWAT for the Upper Mississippi River basin without calibration. The uncalibrated SWAT model was able to predict annual stream flow at 11 USGS (United States Geological Survey) gauges and crop yield at a four-digit hydrologic unit scale. However, the time scale of the simulation was a concern. The stream flow prediction is comparatively poor at a monthly time scale when compared with the annual flow. This study also shows that uncalibrated SWAT can predict base flow contribution reasonably well. The author summarized by saying that SWAT can provide a satisfactory prediction of the hydrologic budget and crop yield in the Upper Mississippi region without calibration given that accurate spatial input data are used.
2) The relative impact of alternative input data such as changes in management practices, climate, and vegetation on the model output can be quantified. For example, studies have been conducted on the impact of land use change on total water yields, groundwater flow, and quick flow in the Moteuka River Catchment in New Zealand. In this study, the model was calibrated and validated to historical flow records for current land use conditions; the model is then applied to two alternative land cover scenarios; prehistoric land cover and a potential maximum pine

plantation. The result shows that quick flow and base flow for the prehistoric and potential pine forest are both moderately smaller than the quick flow and base flow under current land use. There is no significant difference in terms of water balance for potential pine land cover and prehistorical land use (Cao, Bowden, Davie, & Fenemor, 2009).

SWAT model hydrologic cycles

Within SWAT, a watershed can be divided into sub-basins for modeling purposes. Each sub-basin is then divided into many hydrologic response units (HRUs). Each HRU is an area within the basin that contains a unique combination of land cover, soil, and slope class. "The water balance is the driving force behind everything that happens in the watershed" (Neitsch et al., 2011). The model has to simulate the hydrologic cycle well to reflect reality within the watershed. In order to achieve this, SWAT models the hydrologic cycles in two phases; the land phase and the water routing phase.

The land phase of the hydrologic cycle controls the amount of water, sediment, nutrient and pesticide loading to the main channel in each sub-basin. The water routing phase defines the movement of water, sediments, etc. through the channel network of the watershed to the outlet.

Land phase hydrologic cycle

The land phase of the hydrologic cycle is based on the water balance equation:

$$SW_t = SW_0 + \sum_{i=1}^{t} \left(R_{day} - Q_{surf} - E_a - w_{seep} - Q_{gw}\right)$$

Equation 2-9 Soil water balance in the land phase of the hydrologic cycle in SWAT

Where $\boldsymbol{SW_t}$ is the final soil water content (mm), $\boldsymbol{SW_0}$ is the initial soil water content on day i (mm), t is the time (days), $\boldsymbol{R_{day}}$ is the precipitation on day i (mm) , $\boldsymbol{Q_{surf}}$ is the amount of surface runoff on day i (mm), $\boldsymbol{E_a}$ Is the evapotranspiration on day i (mm), $\boldsymbol{w_{seep}}$ is the amount of water entering the vadose zone from soil profile on day i (mm), and $\boldsymbol{Q_{gw}}$ is the amount of return flow on day i (mm).

Precipitation is either captured by the vegetation canopy or falls onto the soil surface. Water on the soil surface can either enter the soil surface or become runoff. Runoff enters the stream system, and increases stream flows in the short term. Water infiltrated into the

soil can be stored and then evapotranspired or forming lateral flow and then enter the surface water system or percolate into a shallow or deep aquifer. Water entering a shallow aquifer may enter the stream as base flow, or return to the soil profile, or enter a deep aquifer. In addition to the soil, stream, and groundwater system, SWAT also has the capacity to take ponds/reservoirs into account. This allows more dynamic and realistic modeling of the water balance. The movement in, out, and between the water systems is summarized in Figure 2-2:

Figure 2-2 SWAT hydrologic modeling processes flow chart (Neitsch et al., 2011)

***Precipitation*:** Precipitation is a primary driver of the hydrologic cycle. It is a required input for the SWAT model. When daily climatic data is not available, SWAT generates daily climate data from historical statistics of monthly climatic data in combination with a weather generator.

Evapotranspiration: Evapotranspiration is the collective term for the processes of evaporation and transpiration. Evaporation is the simple processes of liquid water becoming

atmospheric water vapor. Transpiration is the process by which moisture enters the roots from the soil and is carried through the vascular system of plants then exits into the atmosphere through stomata on leaf surfaces. Within SWAT, evaporation and transpiration are calculated separately. Leaf area index (LAI) plays a crucial role in the modeling of evaporation and transpiration.

***Potential Evapotranspiration (PET)*:** Potential Evapotranspiration is the rate at which soil water evapotranspiration occurs from a large, uniform cover crop area with an unlimited supply of soil water. SWAT offers three alternative methods for estimating PET: Hargreaves, Priestly-Taylor, and Penman-Monteith.

Canopy Storage: Before rain falls on the soil, a part of it is intercepted by the plant canopy. This part of the water is available for evaporation. Maximum canopy storage at maximum leaf area index for a given land cover can be manually entered into the SWAT model. This value is then used to calculate the maximum canopy storage at any given stage of plant growth. Canopy storage is taken into account when using the SCS (USDA Soil Conservation services) curve number for calculation. When calculating evaporation, water is first removed from canopy storage.

Infiltration: Infiltration is the process by which water on the ground enters the soil profile. This process is controlled by rainfall intensity, soil characteristics, soil saturation, land cover type, and slope of the land. However, when the SCS curve method was used in SWAT to calculate surface runoff, infiltration was not directly calculated, but rather SWAT estimates infiltration by calculating the difference between rainfall and surface runoff.

Redistribution*:* Redistribution describes the processes by which water continues to move through soil profile after water has infiltrated the soil surface. This movement is governed by heterogeneity in the soil water potential in the soil profile. Once soil water potential has equilibrated, redistribution stops. SWAT uses a storage routing technique to predict flow through each soil layer in the root zone. Percolation only happens when field capacity of the soil profile has been exceeded and the lower profile is not saturated.

Surface runoff: surface runoff is the flow of water on a sloping surface. SWAT can simulate surface runoff volumes with daily rainfall or peak runoff rates using sub-daily rainfall amounts. One of two methods can be selected to estimate surface runoff; the Green & Ampt infiltration method and the SCS curve number method. The Green & Ampt infiltration

method requires sub-daily rainfall data and therefore is not realistic for the catchment of interest in this thesis. Therefore, the CS curve method is selected.

The SCS curve method predicts the surface runoff volume using the equation below:

$$Q_{surf} = \frac{(R_{day} - 0.2S)^2}{(R_{day} + 0.8S)}, R > 0.2S$$

Equation 2-10 Equation calculating the surface runoff using the retention parameter

Where $\boldsymbol{S}$ is the retention parameter, $\boldsymbol{R_{day}}$ is the rainfall for the day in mm, Runoff will only occurs once $\boldsymbol{R_{day}}$ exceeds $\boldsymbol{0.2S}$

The retention parameter varies due to land use, slope, management, and soil water content. It is expressed as the equation below:

$$S = 25.4(\frac{1000}{CN} - 10)$$

Equation 2-11 the retention parameter is a function of the runoff curve number

Where CN is the runoff curve number for the day

Lateral Flow: Lateral flow is the flow of water below the soil surface but above the zone where rocks are saturated with water. SWAT uses a kinematic storage model to predict lateral flow in each soil layer when accounting for variations in hydraulic conductivity, slopes, and soil water content.

Base Flow: Base flow is the amount of stream water that originates from ground water. SWAT models ground water as two separate pools; shallow ground water, which can contribute to base flow within the catchment; and deep ground water, which may contribute to base flow outside the catchment. Once water has entered the deep ground water system, this water is considered to be lost from the catchment system.

Plant growth and Land cover: SWAT simulates plant growth to reflect the reality of land cover. The plant growth module of SWAT differentiates between annual and perennial plants by allowing perennial plants to become dormant in the winter months. Simulated dormancy is controlled by the air temperature and the minimum temperature required for plant growth.

Routing Phase of the Hydrologic Cycle

Once the land phase of the hydrologic cycle is completed, the second phase of the hydrologic cycle starts. The loading of water, sediment, nutrients, and pesticides then enters the main channel and routes through the network of streams within the watershed. In addition to calculating the movement of water within the network of streams, SWAT also models in-streams processes involving sediment, nutrient, and pesticides.
The routing phase of sediment is governed by two simultaneous processes, deposition, and degradation. Stream power which is a product of water density, flow rate, and water surface slope is used to estimate deposition and degradation. Available stream power is used to deposit material while excessive stream power causes bed degradation. The in-stream nutrient modeling module of SWAT was adapted from the QUAL2E model. This model assumes that dissolved nutrients travel with water and those absorbed to the sediment may be deposited onto the stream channel with the sediment. Pesticide is modeled in a similar fashion as in-stream dissolved nutrients.

2.3 Application of SWAT

Application of SWAT in New Zealand

To date, there are over 2400 peer-reviewed publications on the application, development of SWAT globally. Despite the global adoption and adaptation of SWAT, there are only three published peer- reviewed journal articles on the application of SWAT in New Zealand. In addition to the Journal publications, there has been some Masters and Honours thesis that used SWAT. The following is a table summarising the scope of the current publications on the application of SWAT in New Zealand and this is followed by a brief summary of the peer-reviewed journal articles.

Publication name	Author	Type
Multi-Variable and multi-site calibration and validation of SWAT in a large mountainous catchment with high spatial variability	W. Cao W.B. Bowden T. Davie A. Fenemor	Journal article published on Hydrological Processes

Modelling impacts of land cover change on critical water resources in Motueka River Catchment, New Zealand	W. Cao W.B. Bowden T. Davie A. Fenemor	Journal article published in Water Resources Management
Effects of hydrologic conditions on SWAT model performance and parameter sensitivity for a small, mixed land use catchment in New Zealand	W. Me J.M. Abell D.P. Hamilton	Journal article published in Hydrology and Earth System Science
Modelling water, sediment and nutrient fluxes from a mixed land use catchment in New Zealand: Effects of hydrologic condition on SWAT model performance	W. Me J.M. Abell D.P. Hamilton	Conference presentation on Hydrology and Earth System Science discussion
Nitrogen Yields into the Tauranga Habour based on sub-catchment land use	C.P. Morcom	Thesis for Masters of Science degree in the University of Waikato
Modelling the hydrological impacts of land use change and integrating cultural perspectives in the Waikouaiti Catchment, Otago New Zealand	E. Reeves	Thesis for Masters of Science degree in the University of Otago.

Table 2-1 Summary of the current publications on the use of SWAT in New Zealand

Multi-Variable and multi-site calibration and validation of SWAT in a large mountainous catchment with high spatial variability

SWAT is a distributed model and calibration is often conducted by adjusting parameters and then comparing the simulated basin outlet stream flow to observed data. However, this single variable approach is misleading because the calibration of the complex and spatially distributed model using a single variable (i.e. outlet streamflow) often has multiple acceptable calibration results. This is called the equifinality or non-uniqueness problem. Cao et al. (2006) explored the options of calibrating the SWAT model using data of multiple variables from multiple sites. The modified version of the SWAT model was set up for the Motueka River basin situated in the South Island of New Zealand. This site is located in a mountainous region with high spatial variability particularly regarding precipitation. By calibrating the hydrological component of the SWAT model including PET, water yield, stream flow, and base flow, the calibration was able to produce a realistic set of parameters. Despite high spatial variability in precipitation within the catchment, SWAT was able to

produce excellent hydrological simulations of the Motueka Catchment, with the predicted daily stream flow matching the observed stream flow with an NSE (Nash-Sutcliffe efficiency) of 0.78 during calibration and 0.72 during validation. However, the results for sub-catchments were less ideal, with an NSE ranging from 0.31 to 0.67 during calibration and ranging from 0.36 to 0.52 during validation. Model prediction of soil moisture performed poorly. The model predicts 50% extra soil water storage compared to the recorded data, and this is likely to be the result of over-prediction of precipitation in the modified version of SWAT. This study highlights the importance of good climatic data in New Zealand. In mountainous regions of New Zealand, climatic variability can be large. Reliable climate data is necessary for the application of SWAT.

Modelling impacts of land cover change on critical water resources in Motueka River Catchment, New Zealand

After the calibration and validation of the modified version of SWAT model were conducted, a further study tested the effect of alternative land cover (potential pine forest and prehistorical indigenous forest) on total water yields, ground water flow, and quick flow in the Motueka Catchment. The study identified that the annual water balance for potential pine forest was similar to that of prehistorical land use. Low flows for both potential pine cover and prehistorical forest cover were reduced compared with the low flow under current land use. This study demonstrated the ability of SWAT to predict the influence of changes to model inputs.

Effects of hydrologic conditions on SWAT model performance and parameter sensitivity for a small, mixed land use catchment in New Zealand

A SWAT model was set up for the Puarenga Stream catchment, Rotorua, New Zealand. The model was subsequently calibrated using SWAT-CUP (SWAT- Calibration and Uncertainty Program) to identify unknown parameter values. On the one hand, the model performed well in predicting suspended sediments during validation with <1% bias, and an R2 and NSE both above 0.75. On the other hand, the model performed poorly in predicting total phosphorus and total nitrogen concentrations. The discrepancy between the model prediction and reality is most likely the result of an underestimation of the concentration of suspended sediment and total phosphorus in stream during high rainfall periods,

highlighting the need for high frequency, event-based monitoring data for better calibration and validation. Sensitivity analysis has been conducted for both base flow and quick flow. Base flow is more sensitive to a change in parameters related to channel processes while quick flow is more sensitive to parameters related to overland processes.

Advantages and Disadvantages of SWAT

Compared with the popularity of the model overseas, some factors may explain the lack of application of SWAT within New Zealand. First of all, in addition to hydrological modelling, another important function of SWAT is to model the fate of nutrients and pesticides. However, in New Zealand, programs such as Overseer and CLUES (Catchment Land Use for Environmental Sustainability) have been developed for these purposes. These models are close substitutions for SWAT and they are regionally calibrated for New Zealand. Secondly, a large quantity of data is required for SWAT modelling. SWAT requires inputs of topography, soil, land use, and long-term climate data to set up. Due to its complexity, SWAT also requires the model user to possess a high level of computer literacy and understanding of soil water processes. It has been estimated that a SWAT project would need over six months to complete. Thirdly, local calibration is usually needed and the SWAT model calibration process is very challenging. Finally, even after calibration, the model occasionally performs poorly under daily time step simulations.

Although SWAT modelling is data intensive, time-consuming, and difficult to run, SWAT also possesses advantages over other programs. Firstly, SWAT is a physically-based program which draws a clearer picture of the details of the fundamental processes. Secondly, SWAT is an open-source program. This provides the opportunity to localize SWAT for New Zealand use. Thirdly, SWAT is a multi-function model that can be used to model many aspects of soil water interactions. SWAT has been applied to model surface runoff, nutrient transport, sediment load, climate change scenarios, etc. Finally, the integration of SWAT and GIS interface allows easy representation of spatially variable data.

Application of SWAT for water harvesting

There have been only a few studies modelling the water harvesting potential of catchments using SWAT. SWAT has been identified as an “interesting candidate” for modelling the impact of a rainfall water harvesting system by the authors (Glendenning, Van Ogtrop, Mishra, & Vervoort, 2012), who highlighted the potential for SWAT to integrate spatially

variable data such as satellite data and the potential of SWAT to be applied in ungauged basins. Currently, there are a few studies assessing the possibility and impact of water harvesting in local regions using SWAT modelling outside New Zealand. These examples are described below.

Ouessar et al. (2009) evaluated a modified version of the SWAT to model a water harvesting system in arid Tunisia. SWAT was first modified to allow better simulation of the water harvesting methods called jessour and tabias by changing the SWAT irrigation operations. SWAT was then modified to adjust the crop model parameters to represent Mediterranean arid cropping system by changing the initialization of heat unit accumulation and by removing crop dormancy. The model underwent sensitivity analysis, and the most sensitive parameters were selected for calibration and validation. The model produced satisfactory results with an R2 at calibration of 0.77 and R2 at validation of 0.44, the NSE during calibration was 0.73 and 0.43 during validation period, MAE (mean absolute error) at 2.6 mm and 3.0 mm at calibration and validation, respectively.

Kelkar, Narula, Sharma, and Chandna (2008) combined SWAT and MODFLOW to investigate the vulnerability and adaptive capacity of the Lakhwar watershed in India to climate variability and water stress. The hydrological model showed high average daily runoff (water yield) in the Lakhwar catchment, The authors suggested that rain water harvesting at the catchment level with local dams might increase local communities' resilience to drought.

Andersson et al. (2009) tested the reliability of in situ water harvesting in smallholder agriculture in the Thukela River Basin, South Africa, using SWAT. The authors considered both the supply and demand of water in the catchment and calibrated the model using both the stream discharge and maize crop yield and concluded that the reliability of in situ water harvesting was low in the basin but considerable variation exists between the different areas.

2.4 SWAT model Calibration

Calibrating for ungauged catchments:

SWAT contains many default parameters. However these default parameters may not be suitable for the catchment of interest. Although some of the parameters can be directly measured, other parameters, due to their non-physical and/or scale-dependent nature,

cannot be directly measured (Her & Chaubey, 2015). Therefore, SWAT must undergo calibration in order to estimate the parameter range and to increase model performance. Calibration is the 'process of estimating model parameters by comparing model prediction for a given set of assumed conditions with observed data for the same conditions' (Moriasi et al., 2007). However, usually the catchment of interest is ungauged and therefore lacks 'observed data' for calibration. Modelling stream flows in an ungauged basin is considered one of the most challenging tasks in surface water hydrology because of the lack of data and the heterogeneity of the system (Cibin, Athira, Sudheer, & Chaubey, 2014).
Nevertheless, there are potential solutions to the ungauged basin problem. Blöschl (2005) stated that physically-based parameters can be derived either by measuring or inferring from physical reality. Non-physically based parameters that rely on calibration are often estimated by transposing calibration parameters from a gauged, hydrologically similar 'donor catchment.' This process is also called parameter regionalization. Blöschl (2005) further defined 'hydrologically similar' catchments as being 1) located close to one another. Sites that are close to one another often have similar hydrological behaviour, because the controls for hydrological behaviour are likely to vary smoothly in space and therefore spatial proximity can be a good indicator of the similarity of catchment response. 2) Having similar measurable catchment attributes such as the same soil type, vegetation type, and topographic characteristics (useful indicators for hydrologic similarity). 3) Having similar 'similarity indices' which are a dimensionless number that defines the structure of hydrologic responses. This method is also referred to as a regression approach by other authors (Gitau & Chaubey, 2010; Y. Zhang & Chiew, 2009).
When a 'hydrologically similar' donor gauged catchment has been identified, calibration can be carried out using observed data from the donor catchment. Once calibrated parameters have been identified, the parameters can be transferred to the catchment of interest to make predictions.

Comparing parameter regionalization methods

Gitau and Chaubey (2010) compared two regionalization methods for ungauged catchments in SWAT. The first method, termed 'global averaging,' involves applying the mean of the calibrated parameter values of multiple donor catchments in the region. Catchment characteristics were not considered. The second method tested was the regression

approach. This approach establishes a relationship between donor catchment attributes and calibrated parameter values and then the parameter values for the ungauged catchment is estimated from the regression. Global averaging and regression based regionalization produced comparable and acceptable results at monthly time steps but the regression-based method provided 'good' results (NSE>0.75) more frequently. Y. Zhang and Chiew (2009) tested the merits of several regionalization methods for runoff prediction using SIMHYD and XInanjiang models and confirmed that differences between methods were small. The biggest improvement in output came from making an "educated selection" of donor catchments. (Merz & Blöschl, 2004) measured the "loss" of model efficiency by transferring parameters from calibrated catchments to the ungauged catchment. The smallest efficiency loss ocurred when regionalization methods used the average parameters of immediate upstream and downstream (nested) neighbouring catchments.

Efficiency Criteria

The comparison between the simulated and the observed values is measured by the 'efficiency criteria' which assesses the 'closeness' of simulated outputs to measurements. These efficiency criteria provide a quantitative estimate of how well the model performs. They also give insight into the improvements of the model masde by adjusting parameters (Krause, Boyle, & Bäse, 2005). Efficiency criteria that are commonly used in hydrological modelling are the Nash-Sutcliffe Efficiency (NSE), the coefficient of determination (R2), percent bias (PBIAS), etc. These are described below.

NSE is defined as one minus the sum of the absolute squared difference between the predicted and observed values, normalized by the variance of the observed value during the period under investigation. NSE indicates how well the plot of observed and the predicted values fit the 1:1 line. NSE is one of the most widely adopted measures for hydrological modelling. It is the most objective function to reflect overall fit of hydrographs.

$$NSE = 1 - \frac{\sum_{i=1}^{n}(O_i - P_i)^2}{\sum_{i=1}^{n}(O_i - \bar{O})^2}$$

Equation 2-12 Equation for calculating the NSE

Where $\boldsymbol{O_i}$ is the observed value, $\boldsymbol{P_i}$ is the predicted value, $\boldsymbol{\bar{O}}$ is the mean observed value

Possible values of NSE range between -∞ to 1.When NSE<0, the mean value of the observed time series would be a better prediction than the model. When NSE=1, the model is a perfect fit.

Because the observed and predicted value are squared during the calculation, NSE has the tendency to overestimate larger values, whereas lower values are neglected. In a hydrology model, NSE has the tendency to overestimate model performance during peak flows and underestimate model performance during low flow. NSE is also insensitive to the system over/under estimation.

R2 is the squared ratio between the covariance and the multiplied standard deviations of the observed and predicted value. It describes the degree of collinearity between observed and predicted data.

$$R^2 = \left(\frac{\sum_{i=1}^{n}(O_i - \bar{O})(P_i - \bar{P})}{\sqrt{\sum_{i=1}^{n}(O_i - \bar{O})^2}\sqrt{\sum_{i=1}^{n}(P_i - \bar{P})^2}}\right)^2$$

Equation 2-13 Equation for calculating R^2

Where: $\boldsymbol{O_i}$ is the observed value $\boldsymbol{P_i}$ is the predicted value $\boldsymbol{\bar{O}}$ is the mean observed value $\boldsymbol{\bar{P}}$ is the mean predicted value

R2 ranges between 0 and 1, the closer R2 is to 1, the better the prediction. As with NSE, R2 is more sensitive to high and extreme values. R2 only measures the degree of collinearity. Therefore R2 is not sensitive to proportional or additional difference between observed data and predicted values. This means poor model performance model may result in a high R2. When using R2, it is important to pay close attention to the gradient and intercept of the regression.

PBIAS or percentage bias is an error index. Compared to the NSE and R2 described above, it measures the average tendency of a predicted value to be larger or smaller than its observed counterpart.

$$PBAIS = \frac{\sum_{i=1}^{n}(O_i - P_i) * 100}{\sum_{i=1}^{n}(O_i)}$$

Equation 2-14 Equation for calculating the PBIAS

Where: $\boldsymbol{O_i}$ is the observed value $\boldsymbol{P_i}$ is the predicted value

The optimal PBIAS is 0, and when PBIAS is positive, it indicates that there is an underestimation bias, whereas when PBIAS is negative, there is an overestimation bias.

Efficiency Criteria	Unsatisfactory	Satisfactory	Good	Very Good
R^2	<0.5	0.5-0.6	0.6-0.7	0.7-1
NSE	<0.5	0.5-0.65	0.65-0.75	0.75-1
PBIAS	>25	15-25	10-15	<10

Table 2-2 performance ratings for different efficiency criteria for SWAT calibration/ validation (Moriasi et al., 2007)

Performance rating for the three main efficiency criteria used in SWAT calibration and validation are listed in Table 2-2.

Review of SWAT-CUP

It is important to note that the calibration process is always conditional in nature. The domain of use and the uncertainty of the model must be clearly addressed for both the decision maker and the analyst. Due to the distributed nature of the SWAT model, calibration may be particularly difficult due to the large model structure uncertainty, input uncertainty, parameter non-uniqueness, and output uncertainty. SWAT-CUP (SWAT Calibration and Uncertainty Program) was developed to facilitate the difficult task of calibrating a SWAT model.

SWAT-CUP has three general calibration methods which include: Generalized Likelihood Uncertainty Estimation (GLUE), parameter Solution (ParaSol), and Sequential Uncertainty Fitting (SUFI-2). Of the three methods offered by SWAT-CUP, SUFI-2 can be run with the smallest number of model runs to achieve good prediction results (Yang, Reichert, Abbaspour, Xia, & Yang, 2008). All of the calibration methods are 'Inverse modelling' (IM) methods, which describes the process for which measured data is used to optimize an objective function for the purpose of finding the 'best' parameters. A unique set of 'best' parameters is usually not available from the limited number of observations that can possibly be obtained; this problem is often referred to as the 'equifinality' or 'nonuniqueness' problem. This equifinality or nonuniqueness problem may be more severe in the calibration for distributed parameter models such as SWAT (Her & Chaubey, 2015). Therefore, SWAT-CUP inverse modelling aims to "characterize a set of models by assigning distributions (uncertainties) to the parameters which fit the data and satisfy presumptions as well as prior information". Addressing uncertainty of a calibrated model is crucial to the

calibration process. One must note that the equifinaility problem is inevitable and cannot be prevented unless the model is fully physically based and observations for hydrologic processes are error-free.

In SUFI-2, parameter uncertainty accounts for all the uncertainties such as uncertainty in the driving variables (rainfall), uncertainties in the conceptual model, uncertainties in parameters, and uncertainties in measured data. This uncertainty is expressed as “p-factor” which is the percentage of measured data bracketed by the 95% prediction uncertainty (95PPU). The 95PPU is at the 2.5% and 97.5% levels of the cumulative distribution of an output variable obtained through Latin hypercube sampling. The “r-factor” measures the average thickness of the 95PPU band. During SUFI-2 calibration, one must first assume a large parameter uncertainty within a physically meaningful range, allowing measured data to fall within the 95PPU, and then run one iteration with 1000 simulations. After the first iteration, the parameter range is updated while monitoring the p-factor and r-factor. The updated parameter range will be centered around the best simulation and the updated range will be smaller than the previous iteration. This process is repeated and several iterations are run until desirable p-factor and r-factors along with other model efficiency criteria are satisfied. Ideally, the p-factor will be close to 100% and the r-factor will be close to 0. For stream discharge calibration, a p-factor > 70% and an r-factor of around 1 is considered acceptable (Abbaspour, 2007).

2.5 Estimation of Irrigation system reliability

Before implementing a water harvesting system one must assess the level of risk that the water harvesting system may not be able to supply sufficient water to meet demand in the command area. The reliability of a water harvesting scheme is required to understand this risk. Andersson et al. (2009) state that explicitly accounting for the risk of failure of a water harvesting system can make the ‘water harvesting suitability more transparent’ and therefore allows for ‘effective and flexible decision making.'

In other cases, the system reliability serves as a design target for water harvesting systems. For example, Hanson, Vogel, Kirshen, Shanahan, and Starrett (2009) used the system reliability estimation to predict the required water storage area for a given water yield.

The reliability of a water harvesting system is defined by the following equation:

$$P_r(\%) = 1 - \frac{d_f}{n}$$

Equation 2-15 Equation to calculate the reliability of a harvesting scheme

Where d_f is defined as the number of days when irrigation demand is not satisfied by the water harvesting scheme and n is the total number of days, P_r is the reliability of the scheme.

Baek (2011) further suggested that the reliability can also be calculated for weekly, monthly, and yearly time scales. These methods are called "period based estimation" or PE. The equation was generalized as:

$$P_f(\%) = \frac{(N_t - N_f)}{N_t}$$

Equation 2-16 Period based failure rate calculation

Where $\boldsymbol{N_t}$ is the total number of periods and $\boldsymbol{N_f}$ is the total number of periods where the water harvesting scheme fails to meet water demand, and $\boldsymbol{P_f}$ is the failure rate

Alternatively, the reliability can be estimated with the volume based method (VE), defined as:

$$P_f(\%) = \frac{\sum(V_t - VD_t)}{\sum(V_t)}$$

Equation 2-17 Volume based failure rate calculation

Where V_t is the total water demand in the command area over a given period of time (t) and VD_t is the total water demand that cannot be meet and P_f is the failure rate

There are drawbacks associated with all estimation methods/calculations/intervals within particular methods. When calculating the reliability of a water harvesting scheme using the annual PE method, the length of water deficit days cannot affect reliability estimation. For example, an estimate of the annual PE of 3 days of continuous failure (to meet demand) will have the same effect on the reliability calculation as 100 days continuous failure. On the other hand, calculating the reliability of water harvesting scheme using daily PE, weekly PE, or the VE method may lead to an overestimation of reliability due to the random nature of rainfall patterns. The understanding of the local seasonal rainfall distribution and water

demand of the farm command area can be used to select the best reliability estimation method.

Chapter 3 Methods Development

As mentioned previously in Chapter 1, there are three research questions this thesis aims to address. 1) How much water can be harvested, stored and irrigated on the case study farm and what is the reliability of this water harvesting and irrigation scheme? 2) What is the pasture response to irrigation water on the case study farm? 3) What is the cost to supply irrigation water and therefore the cost of extra pasture production on the case study farm?

3.1 How much water can be harvested and stored?

A SWAT model was first set up for the gauged catchment which the water harvesting catchment (WHC) is nested within: this gauged catchment is called the CVC. The model hydrologic parameters for the CVC were calibrated and validated using daily river flow data collected at the Te Mara and Mikimiki sites. SWAT-CUP was used to conduct the calibration and validation. These parameters were then transferred to a SWAT model established for the WHC so as to answer the first question asked i.e.'how much water can be harvested'? Due to the complexity of the development and application of SWAT, a detailed description of the setup, calibration, validation, and application of the SWAT model is presented in Chapter 4 and the results of the SWAT application are presented in Chapter 5.

Surplus water from the WHC is captured and stored behind a dam. ArcGIS was also employed to help in the modelling of the water harvesting capacity of the WHC. First of all, the relationship between the surface area of the water storage site and the water storage volume was identified. This provides the necessary data to model the water balance within the water storage site.

The topographical characteristics of the WHC basin outlet were studied (i.e. the dam), to estimate the maximum dam height and earth works required to construct the dam. The estimation of the earth works are a key component of the cost-benefit analysis as described in Chapter 6. Finally, a dynamic water balance for the command area and the water storage site is carried out in Chapter 6 and the "Optimal" dam size and water storage volume is determined.

Volume and Area of the water storage

The area where water is stored is called a “pond”. The surface area of the pond depends on the volume of water and the topography of the water storage site. A preliminary study was conducted to determine the pond surface area in relation to the stored water volume using ArcMap. The “Surface Volume” function was used to estimate the maximum water storage volume and surface area of the pond for a given height of the proposed dam wall. This process was repeated 14 times and the results are shown in Table 3-1

A nonlinear regression was performed using data in Table 3-1 to express the relationship between pond volume and pond surface area. The relationship between the volume of water in the pond and the surface area is expressed with a radial function:

$$SA = \beta * V^{(\frac{1}{\alpha})}$$

Equation 3-1 The relationship between the pond 2D surface area and Volume.

Where β is a coefficient, α is also a coefficient, SA is the 2D surface area, and V is the pond volume.

A least squares nonlinear regression was conducted in Excel using the method described by A. M. Brown (2001). Manual modification was made to find the best fit graphically. This regression resulted in the following equation that relates the pond surface area to the pond volume.

$$SA = 350 * V^{\left(\frac{1}{2.31}\right)}$$

Equation 3-2 Equation for calculating the surface area of the pond

This function simulates the relationship between pond water storage volume and pond surface area reasonably well, with an R2 of 0.91. In other words, this equation provides a good approximation for the surface area of the water stored behind the dam wall.

Maximum Dam height and Earthwork estimation

The design and configuration of the water harvesting dam is determined by the topography of the basin outlet. This section analyses the maximum embankment size and earthwork required for an embankment of any given height.

The maximum height of the embankment is limited by the height of banks on either side of the valley. For the WHC, a cross-sectional view of the valley at the basin outlet was taken using ArcGIS (see Figure 3-1).

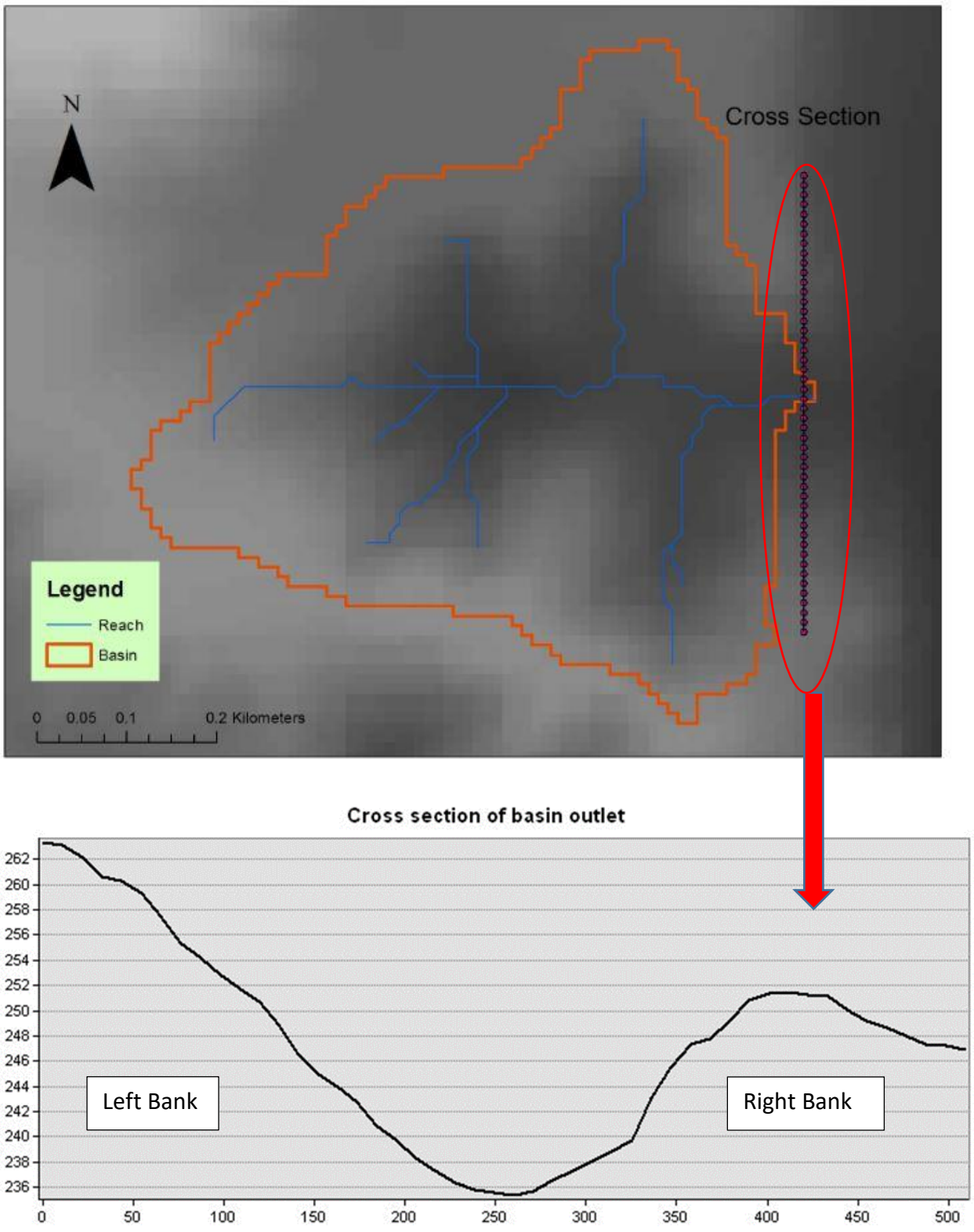

Figure 3-1 The cross section of the topography at the basin outlet of the water harvesting catchment (WHC).

From Figure 3-1, the maximum height for the proposed dam is limited by the right bank, which limits the height of the dam embankment to 14 meters above the lowest point of the cross section. The minimum freeboard, which measures the maximum water storage level

below the embankment height (crest level), is 0.5 meters (with 0.75 meters to 1.0 meters preferred) according to the FAO64. Therefore, the water level in this WHC should not exceed 13 meters. The New Zealand government requires a minimum freeboard of 0.6 meters.

In addition to specifying freeboard heights, FAO64 provides a guideline for the design of dams. This guideline was used as the basis for the calculations of the necessary earthworks required for an embankment of any given height.

Embankment and slopes

There are two types of embankment. The first type is called the homogenous embankment and the second type is called the zoned embankment. A homogenous embankment is essentially a wall of compacted soil that stops water from flowing out of the catchment. This type of embankment has the advantage of being relatively cheap to build and being easily maintained. A well designed homogenous embankment is also reliable. However, a homogenous embankment requires more earthworks and seepage can be a problem. Generally speaking, homogenous embankments should have relatively flat slopes (1:3 upstream and 1:2 downstream) according to the FAO64 guideline.

A zoned embankment is divided into three parts; the upstream side of the embankment which is made with relatively impervious material, an impervious clay core, and a pervious downstream slope. This design offers more stability and requires less earthworks because steeper slopes can be adopted (1:2 upstream and 1:1.75 downstream). However, the construction of such a structure may be more expensive.

The term crest width describes the width of the top of the embankment. The minimum crest width is 3 meters and the required crest width increases with dam height. Hawke's Bay Regional Council requires a crest width of at least 5 meters for dams over 8 meters in height (Shaver, 2009). The FAO64 manual provides an equation to calculate recommended crest width:

$$CW\ (in\ m) = 0.4H + 1$$

Equation 3-3 Equation for calculating the optimal crest width

Where H is the maximum height for the embankment and Cw is the crest width 1

The quantity of earthworks was estimated using the method suggested by FAO64. An illustrative figure is shown below to demonstrate the estimation process. First of all, the cross section of the proposed dam is squared off to allow an accurate calculation of the earthworks volume. Each of the rectangles are 1 meter in height. When the proposed dam is 14 metres high, the dam will be divided into 14 parts for calculation. The crest width at each embankment height is determined by Equation 3-3. The minimum crest width required at each maximum embankment height is shown in Table 3-1 Minimum Crest width required for each embankment height.

Once the crest width has been determined, as demonstrated in Table 3-1, the total area for the top 1 meter of the dam is the area in the rectangle and the area of both triangles upstream and downstream.

Embankment Height	Crest width	Distance between left and right bank at given embankment height (m) (LD)
14	6.6	249
13	6.2	235
12	5.8	217
11	5.4	208
10	5	192
9	4.6	178
8	4.2	164
7	3.8	155
6	3.4	147
5	3	130
4	3	120
3	3	98
2	3	70
1	3	7

Table 3-1 Minimum Crest width required for each embankment height

[1] This equation is in compliance with the requirement from the Hawke's Bay Regional Council. The greater Wellington regional council does not have its own set of guidelines for designing small scale earth dam structure

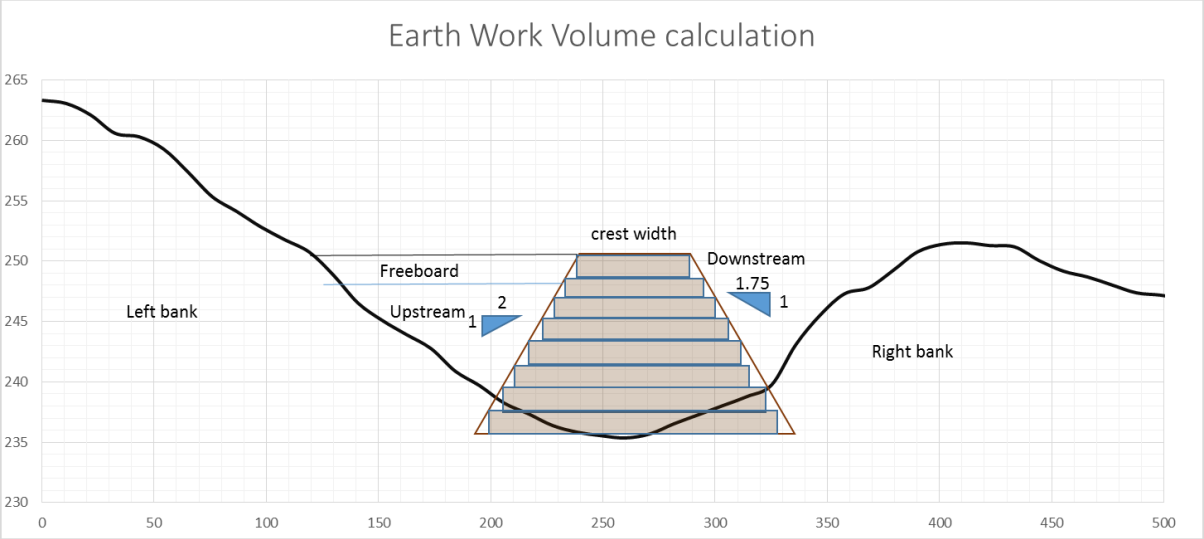

Figure 3-2 A cross-sectional view of the embankment

The following equation describes the cross sectional area of the top 1 meter of the dam:

$$CA_1 = (CW * 1) + \frac{1 * 2}{2} + \frac{1 * 1.75}{2}$$

Equation 3-4 Cross Sectional area of the top 1 meter of the dam calculation

Where CA_1 is the cross sectional area of the top 1 metre of the dam, and CW is the crest width

The cross sectional area of the section i meters of the dam crest is expressed as

$$CA_i = \big(CW + (2 + 1.7) * (i - 1)\big) * 1 + \frac{1 * 2}{2} + \frac{1 * 1.75}{2}$$

Equation 3-5 Cross sectional area of the i meters of the dam

Where CA_i is the cross sectional area of the i meters of the dam crest and CW is the crest width

Finally, the distance between the left bank and the right bank at each dam height i (LD_i) is measured using the cross sectional view of the basin outlet, as presented in Figure 3-2. The earthwork volume of the dam can be calculated with the following equation:

$$DV_i = CA_1 * LD_1 + CA_2 * LD_2 + \cdots + CA_i * LD_i$$

Equation 3-6 *the earth work volume of i meters height dam is equivalent to the sum of earth work volume of each section*

Where DV is the earth work volume needed for building a dam i meters height

The total earthworks required for a dam height ranging from 1 metre to 14 metres was calculated, considering both the homogenous embankment and the zone embankment methods. The result of these calculations are shown in Table 6-2 in Chapter 6.
The quantity of earthworks required by the homogenous embankment is much greater than a zoned embankment due to the gentler slope on both upstream and downstream sides of the dam.

3.2 What is the pasture's response to irrigated water?

Irrigation of the command area is scheduled according to the interaction between water supply and water demand. Irrigation water supply is the quantity of water the WHC can capture and store. A spreadsheet has been designed by Horne (2016) that calculates the water balance of the pond and the command area. This study adopted and modified the spreadsheet Horne made to model the performance of the water harvesting scheme. Specifically, the pasture response to irrigation. The key development of the original modelling exercise was the use of SWAT to more accurately estimate the water harvested from the WHC and the more rigorous treatment of the pond volume and surface area and the embankment profile.

Data input

Data input for this spreadsheet is relatively simple. Basic soil properties for the command area are required to determine the irrigation requirement. These include soil field capacity (FC) and permanent wilting point (PWP). Available water content (AWC) is calculated as the difference between FC and PWP. Daily rainfall and potential evapotranspiration (PET) is also required. PET is estimated with FAO56 using VCS data from Riverside farm. The SWAT daily basin outlet stream flow is used to calculate the pond water balance.

Pond Water balance

The water balance of the pond is defined as the difference between water harvested from the WHC and the water loss through evaporation and irrigation of the command area. When the pond is lined, drainage from the pond is assumed be zero; otherwise, drainage from the

pond is calculated as a function of the saturated hydraulic conductivity of the soil. The pond water balance is expressed as:

$$PondV_n = PondV_{n-1} + Flowin_n - E_n - I_n - Vseep_n$$

Equation 3-7 Equation for calculating the pond water balance

$PondV_n$ is the volume of water in the pond on day n.It is important to note that $PondV$ should not exceed the maximum pond volume which was determined by the height of the embankment. Any surplus water in the pond is assumed to flow out of the pond via the spillway.

$Flowin_n$ is the quantity of water that enters the pond from the catchment on day n. This value is modelled using SWAT as introduced previously. Several scenarios were considered for this value to consider uncertainty within the program.

E_n is the evaporation from the pond on day n, actual evaporation from a water surface such as that of a pond is often expressed as:

$$E = SA * \theta * PET$$

Equation 3-8 Equation for calculating actual evaporation from pond surface

Where SA is the surface volume of the pond and θ is the evaporative coefficient of the pond water surface. The coefficient θ is determined by the local climate. Jensen et al. (2010) discussed the factors influencing this coefficient in detail. This coefficient is assumed to be 0.6 in SWAT. This assumption is supported by Jensen. PET is calculated with FAO 56 method.

I_n is the quantity of water withdrawn from the pond for irrigation purposes. I_n is determined by the irrigation demand in the command area. The next section will provide greater detail on this variable.

The seepage is the amount of water lost from the bottom of the pond, this quantity of seepage from the pond on any given day is calculated as:

$$Vseep = Seepage\ Rate * Pond$$

Equation 3-9 General equation for calculating seepage from the bottom of the pond

$Vseep$ is the volume of seepage, $Seepage\ rate$ is a constant given to describe the speed of which water stored in the pond is leaving the pond through seepage and this value corresponds to the saturated hydraulic conductivity of the soil.

The bottom of the pond consists of mainly Otukura Soil series, which has a silty loam to silty clay loam texture which changes to silty clay texture with increasing depth. The soil is

mudstone based and tends to be wet and sticky with very low infiltration rate (A. Palmer, personal communication, 2016). In the SWAT model, water seepage from the bottom of the pond is calculated using the equation:

$$Vseep = 240 * Ksat * SA$$

Equation 3-10 Calculating seepage using saturated hydraulic conductivity of the lowest soil profile.

Where: $Ksat$ is the saturated hydraulic conductivity.

However, because exact saturated hydraulic conductivity of the lower soil profile and bed rock is unknown, we opted for the simpler modelling method by assuming a fixed percentage of water is lost on any given day.

Otherwise, seepage from the pond is minimized when an impervious layer is laid down to prevent loss of water. However, the impervious lining will be very expensive to construct and it is unlikely to be economically.

During the initial phase before irrigation water has been taken out of the pond system, the water balance of the pond is

$$PondV_n = PondV_{n-1} + Flowin_n - E_n - Vseep_n$$

Equation 3-11 Water balance of the pond during the initial water harvesting period.

Command Area Water balance

The soil water balance in the command area is modelled using a soil water balance, this irrigation system is assumed to be well managed.

$$Sw_t = Sw_0 + R_{day} + I - ET$$

Equation 3-12 Command area water balance

SW_t is the soil water content on day i (mm), the value of SW_t is assumed to be below or at field capacity. Any excess in soil water will leave the soil profile as drainage. Sw_0 (mm) is the soil water content on the previous day (day $i-1$). R_{day} is the precipitation on that day i (in mm). I is the irrigation water applied to the command area on day i. Finally ET is the actual evapotranspiration of the command area.

The actual ET is expected to be equal to PET when plants are drawing water from the readily available water pool, which is assumed to be 0.5 AWC. Once all of the readily

available water has been used, actual ET is assumed to decrease linearly until the soil water deficit reaches AWC. At this point, no more water can be drawn from the soil profile and actual ET equals 0. However, if the quantity of rain or irrigation to the command area is larger than evaporative demand on the day when soil water deficit is larger than $0.5AWC$, the actual evapotranspiration will also be equal to PET. This relationship is expressed mathematically below in Equation 3-13

$$\mathrm{ET} = \mathrm{PET}$$

$$\text{if } \mathrm{FC} - \mathrm{SW}_0 \geq 0.5\mathrm{AWC}$$

$$OR\ if\ I + R_{day} >= PET$$

$$\text{else } \mathrm{ET} = \ (\mathrm{AWC} - (\mathrm{FC} - \mathrm{SW}_0))/0.5\mathrm{AWC} * \mathrm{PET}$$

Equation 3-13 Calculation of the actual evapotranspiration in the command area.

Where: FC is the soil field capacity of the soil.

Therefore, when soil water deficit is greater or equal to a threshold value, an irrigation event will be triggered providing that the pond has sufficient water to irrigate the command area. If the water storage in the pond is insufficient for an irrigation event when soil water content drops below 0.5 AWC, a system failure is said to have occurred and is noted. This is a measure of system reliability.

The soil types at the command area are from the Kohinui and Tauherenikau series. For this study, an AWC of 50mm was selected for the modelling purposes.

Pasture biomass response to irrigation

The potential impact irrigation has on pasture production can be modelled simply. For example, Moir, Scotter, Hedley, and Mackay (2000) proposed that the pasture growth is proportional to the actual ET. The equation they use is:

$$G = kET$$

Equation 3-14 Total pasture growth is a function of actual evapotranspiration at a given Olsen P level.

G is the total pasture growth, and k (kg DM /ha/ mm) is a constant determined by the soil Olsen P level. and ET is the actual ET.

Moir, Scotter, Hedley, and Mackay (2000) explored the relationship between k and Olsen P and they estimated that for a mid-range Olsen P level (25 ug P/g), the k value is likely to be approximately 15 kg DM/ ha/mm/ day.

Therefore, pasture growth on any given day can be expressed as:

$$G = 15 * ET\ kg\ DM/ha$$

Equation 3-15 Pasture growth model for Riverside farm assuming a mid-range soil Olsen P level.

In order to calculate the potential increase in biomass production under irrigation allowed by the water harvesting scheme, an alternative water balance model was executed for the command area without irrigation (i.e. to predict pasture growth in the dryland situation). This water balance calculates actual ET for the unirrigated land is calculated (ETu), which in turn is to model the pasture production under the original dryland system. Finally, the difference in biomass production between both systems (irrigated verse non-irrigated) are calculated.

In addition to the pasture production for the non-irrigated and irrigated command area, the maximum potential pasture yield is also calculated- the maximum potential pasture yield is calculated assuming that the pasture can always access readily available water and therefore there is no limitation to growth i.e. soil water deficit is maintained above the 0.5 AWC point. In other words, the maximum potential pasture yield is calculated assuming PET=ET throughout the year. This allows an estimation of potential "loss" of pasture yield from irrigation system failure.

Pasture biomass is only calculated during the irrigation season because during the winter season pasture growth is more sensitive to other climatic variables and simple relationships with ET are less accurate. Also, due to the relatively wet climate and lower evaporative demand, pasture growth during the winter season is very rarely limited by soil water deficit and therefore it is likely to be identical for all three scenarios (irrigated, non-irrigated and potential).

The estimation of the increase in pasture production allows assessment of the economic viability of the water harvesting system.

System Reliability:

The command area water balance is calculated using a daily time step and system failures were counted on the same basis. As discussed in the literature review section, the calculation of system reliability is greatly influenced by the method selected for such calculation. A PE (period based reliability estimation) would probably produce different result than a VE (volume based reliability estimation). The time period selected for PE can also influence the estimation of system reliability.

In this study, daily PE will be carried out for the daily SWAT simulation using VCS data between 2002 and 2014 to calculate the reliability of the water harvesting system. A failure is counted when the soil water deficit is greater or equal to 0.5 AWC but the pond water storage is insufficient to meet irrigation demand. Three methods are used; the first method counts each day of insufficient water supply during irrigation season as one failure. The second method counts several consecutive system failures as "one" failure. For example, should the pond fail to supply water to the command area between January 1st and January 3rd, the first method would count 3 system failure events but the second method would consider this as one event. The third method is a period based method that calculates the percentage of irrigation season weeks when failure occurs. Using all three methods provides better insight into the distribution of system failure and thus allows for better assessment of the water harvesting scheme.

Suitable command area:

A farmer selects the size of the command area according to the level of risk that she thinks is appropriate. The risk is expressed as the chance of system failure, which was explained in detailed in the literature review. At any given level of risk, the suitable command area can be calculated according to the water harvesting and storage capacity of the WHC. An Excel spreadsheet was set up to automatically compute command area water balances, count system failure and calculate system reliability. The spreadsheet contains input cells which allows the user to change the size of the command area and variables related to irrigation management. Since the quantity of water required for any given irrigation event is determined by the size of the command area and the irrigation depth, changing either of these variables will have a direct effect on system failure or reliability rate. Different sized

command areas will be tested to find the command area size that maximizes the potential benefit from irrigation while limiting the system failure rate within the acceptable level. The cells in the Excel spreadsheet used for the command area water balance are shown in Appendix 1.

3.3 What's the cost to apply irrigation water and the cost of pasture

The cost of the embankment structure.

An approximate estimation of the cost of the embankment structure is required for a cost and benefit analysis of a water harvesting scheme. An approximate of the cost of construction of the earth embankment was obtained from a local contractor. The estimated unit cost for construction is $6.50/m3. This estimation includes the labour, equipment, material cost of excavation, transportation, placement, and compaction of the raw material; however, it does not include the expenses associated with resource consent, design, and other administrative activities. An estimation of the pond lining was also obtained, it is estimated that lining of the pond cost roughly $20/m2. Table 3 in Chapter 6 provides the estimation for the total cost of a zoned embankment at any given embankment height. The cost of lining the pond is disproportionally large when compared to the cost of constructing the embankment.

The topography at the study site allows a maximum embankment height of 14 metres, however, pond and command area water balances will be run to determine the maximum embankment height given the water harvesting catchment and designed risk acceptance.

Economic analysis of the WHC:

In order to test the economic viability of the small scale water harvesting system, it is also important to calculate the cost and benefit of the extra dry matter produced by the water harvesting scheme. it was assumed that a K-line system would apply irrigation water to the command area. A major benefit of a K-line system is that it is relatively cheap.

The economic cost for each extra kilogram of pasture produced is calculated by dividing the annual cost for installing and running the irrigation by annual extra production. Such calculations were performed by modifying an Excel template provided by (Howes, Horne, & Shadbolt, 2014). The template has been modified so that when entering the embankment

height and command area size, the cost of per kilogram pasture produced will be automatically calculated and presented.

The capital expenses include the costs associated with the embankment, irrigation system and the resource consent. The quotes for earth dam were obtained from contractor as described in the previous section. The dam is assumed to have a linear depreciation schedule of 70 years with a salvage value of $0. The earth dam requires little repair and maintenance for the first 30 years. The annual cost of R&M including desilting (Goel & Kumar, 2005) is set at 5% of the orignal construction cost. The estimated cost for resource consent application was obtained from the Greater Wellington Regional Council. The resource consent is considered to be an intangible asset and the cost for resource consent application is considered as a "capital expenses". K-line irrigation material, water pump, and installation cost were estimated from quotes from a local engineering firm. The K-line irrigation system material is assumed to have a depreciation schedule of 25 years with salvage value of $0. The pump has a linear depreciation schedule of 10 years with salvage value of $0. A power line was necessary to bring electricity of the WHC site, the cost for such operation is assumed to be $5000.

The default opportunity cost of capital must also be accounted for. This cost was set at 8% in the model set up by Howes et al. (2014). However, due to the low recent interest rate, the opportunity cost for capital is now estimated to be 6% (Waugh, 2015). Depreciation costs for the tangible asset are included in the calculation. R&M for the dam is estimated at 5% of the total construction cost, and R&M for the K-line is $30/ha. The costs of moving the K-line irrigator and electricity cost associated with pumping are calculated according to the volume of irrigation water and the command area size. Annual insurance cost for the K-line irrigation system are estimated at $500 (pers com FMG insurance agent).

After the scenarios were modelled and the economic analysis conducted, a matrix of cost of producing per kilogram of dry matter is constructed for each dam height and command area size.

The cost of a cubic meter of water supplied is also calculated. This calculation is conducted in the same spreadsheet, however, as it is the cost of supplied water (i.e. stored water) none of the costs associated with irrigation are included. The aim of this calculation is to provide a comparison of the cost for water from small scale (i.e. on-farm) water harvesting

system with the large scale (i.e. community) schemes. Because large scale schemes deliver water to farms with pressure, the cost of pumping water needs to be accounted for.

Chapter 4 SWAT Application

4.1 Application of SWAT

Data Collection

SWAT requires a large quantity of data. In this study, GIS data has been collected from Land Information New Zealand (LINZ) and the Land Resource Information Systems Portal (LRIS). The soil map and soil description of the small basin were collected from "The Soils and Geology of Riverside Farm" book ((Pollok, Neall, & DeRose, 1994). New Zealand Soil spatial information system (S-Map) soil reports were also used to construct the user soil database. Virtual climate data (VCD) were downloaded from National Institute of Water and Atmospheric Research (NIWA). Stream flow and rain gauge data for the parameterization basin were requested from Greater Wellington Regional Council.

Digital Elevation Model (DEM)

Digital elevations are one of the major inputs to the SWAT model. The DEM is used in delineating the watershed. The DEM directly affects stream network, sub-basin, hydrologic response units (HRU) classification and the model prediction. Numerous research groups have studied the effect of DEM resolution on SWAT model predictions. Lin et al. (2010) showed that although runoff prediction is not very sensitive to DEM resolution, total phosphorous and total nitrogen predictions benefit greatly from increases in spatial resolution. This finding was reiterated by (Chaplot, 2005), who stated that a DEM mesh size of 50 meters or lower is necessary for accurate watershed modelling. (Bosch, Sheridan, Batten, & Arnold, 2004) found that stream flow prediction improves with higher spatial resolution DEM. (Tan, Ficklin, Dixon, Yusop, & Chaplot, 2015) showed that stream flow simulation in SWAT is more sensitive to DEM resolution than DEM source and DEM resampling technique. Therefore, the DEM with the highest resolution available was selected for this study. The NZ 8 metre Digital Elevation Model was downloaded from LINZ and the raw data was re-projected into the New Zealand Geodetic Datum (NZGD) 2000 Wairarapa Circuit. The NZGD 2000 Wairarapa Circuit is the projection that allows the most accurate representation of the site of interest.

Soil Data

The SWAT model is extremely sensitive to the quality of soil data (Romanowicz, Vanclooster, Rounsevell, & La Junesse, 2005). Two default soil databases are built into SWAT; State Soil Geographic database (STATSGO) and the Soil Survey Geographic database (SSURGO). Geza and McCray (2008) found that when comparing the use of STATSGO and SSURGO in the same region, the higher spatial resolution soil data of SSURGO resulted in higher numbers of HRUs and a better prediction after calibration. Therefore, in an attempt to use the data of highest quality, two sources of soil data were used in this study to construct the user soil database. Fundamental Soil Layers database (FSL) was used to construct the soil map for the CVC. Ideally, S-Map would have been been used, however S-Map is not yet available for the area of interest. For the WHC, more detailed soil data is available from Soil Map of Riverside Farm, Wairapapa. The physical map was an attachment to 'A field descriptions of The Soils and Geology of Riverside Farm (Pollok, Neall, & DeRose, 1994)' document.

In addition to FSL and the field description of soils and geology of riverside farm, S-Map soil reports were downloaded for soil series within the CVC.

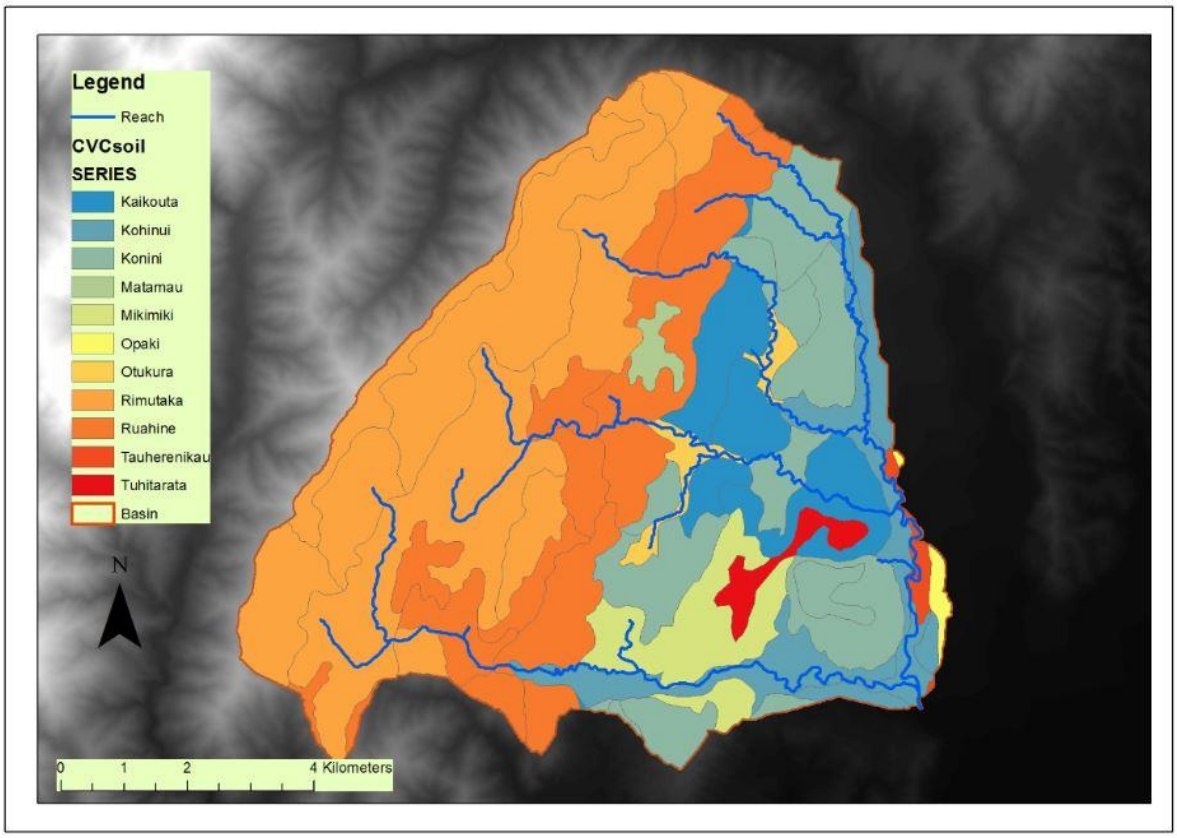

Figure 4-1 Map of soil types within the calibration/validation catchment (CVC)

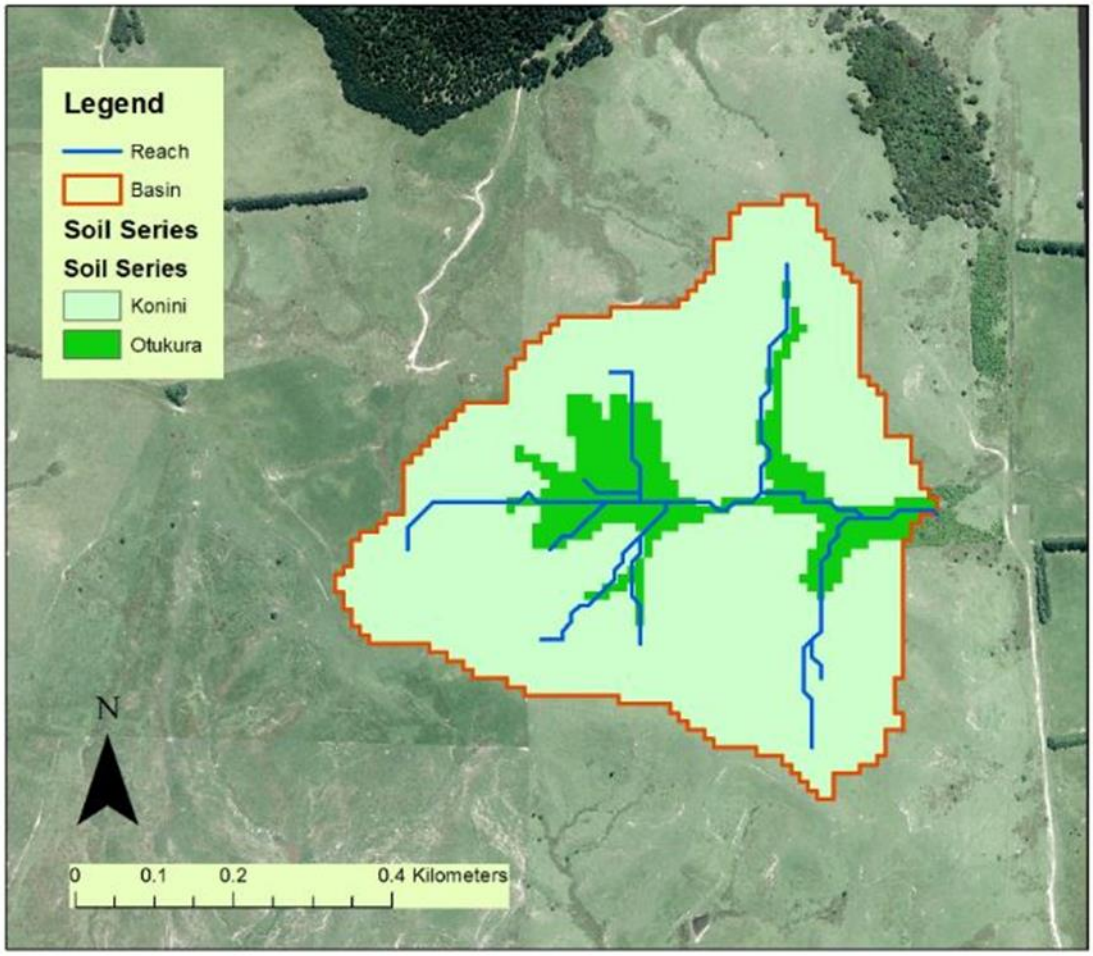

Figure 4-2 Soil map of the water harvesting catchment

Landuse

The entire WHC is covered by perennial ryegrass. However, the land use of the CVC is more complex. Therefore, Land Cover Database version 4.1 Mainland New Zealand (LCDB) was used to identify land use. LCDB is a multi-temporal, thematic classification of land use in New Zealand. It contains 33 classes of land use and the geographic boundaries of each land use. LCDB was created by Landcare Research New Zealand Ltd (LCR) from satellite imagery. The latest update of the LCDB map was on 16th July 2015.

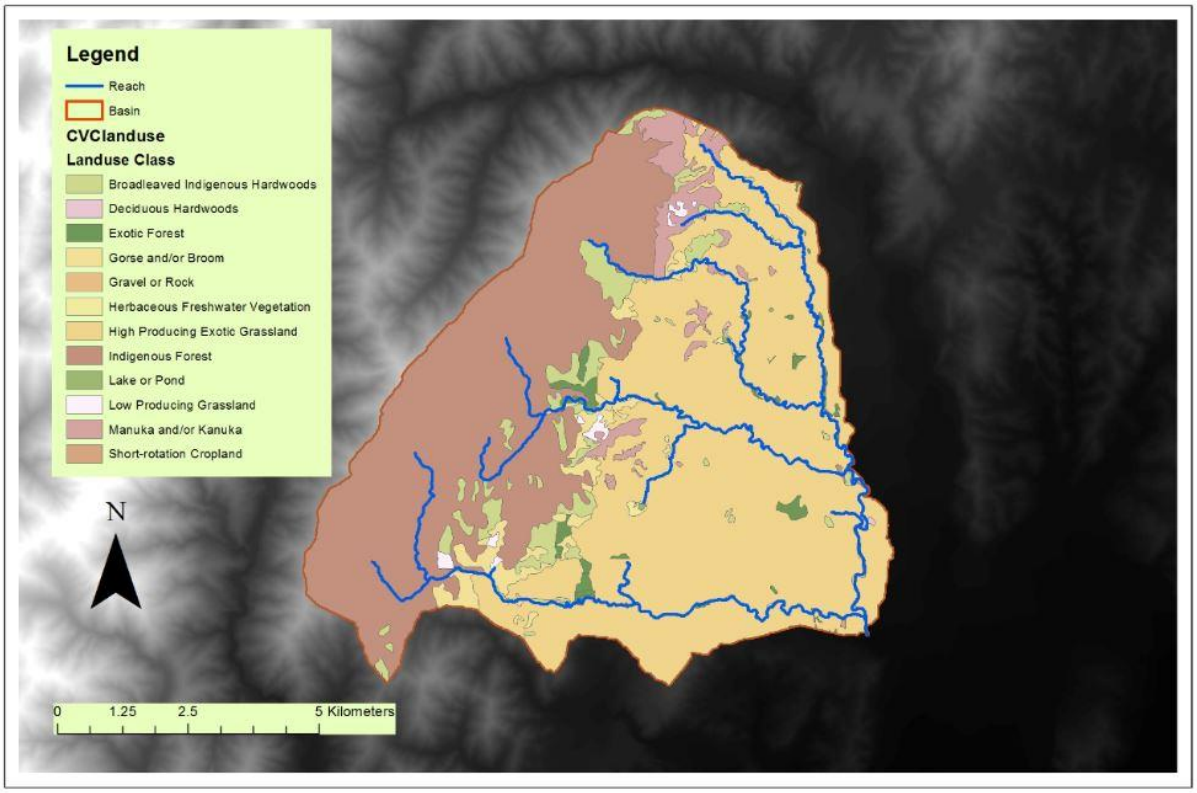

Figure 4-3 Landuse map of the CVC

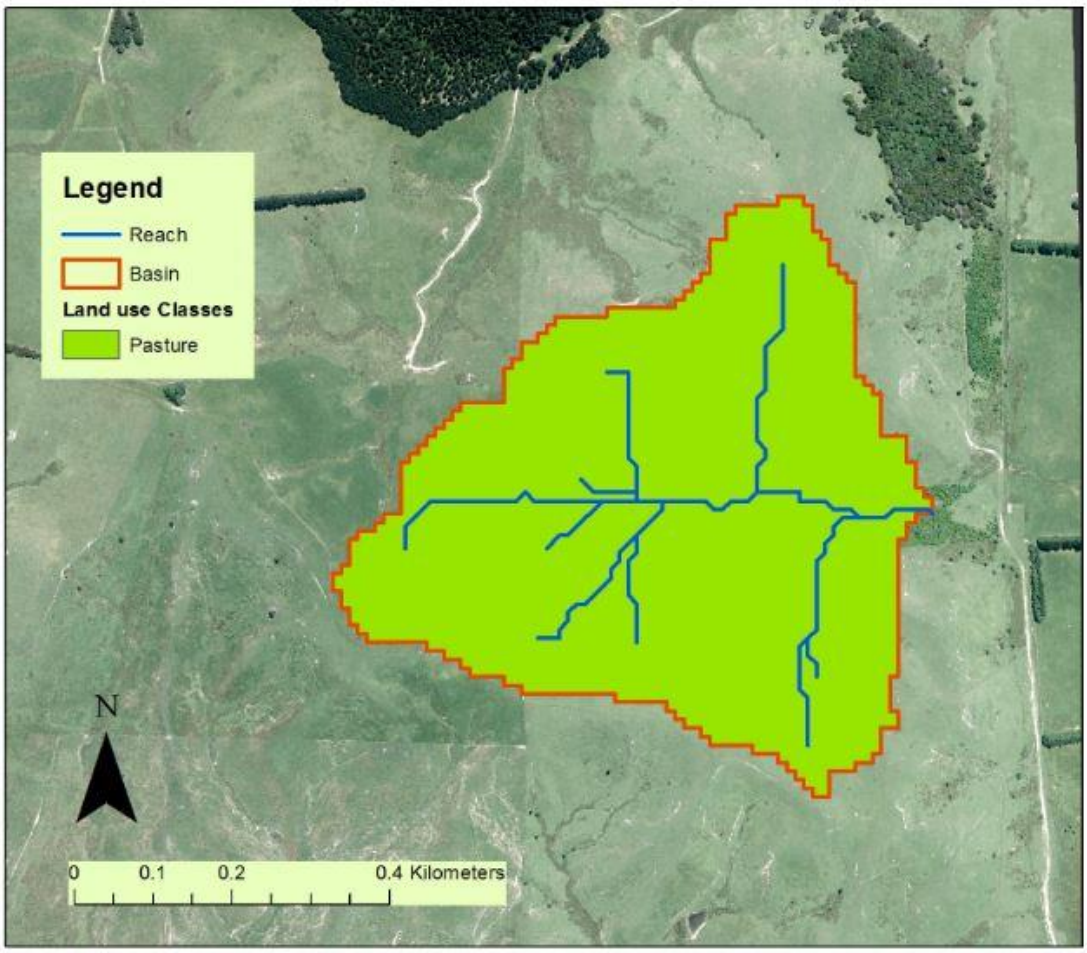

Figure 4-4 Landuse Map of the WHC

Rivers and Streams

New Zealand river centrelines, and New Zealand river polygon were used to improve the accuracy of watershed delineation. Both maps were part of the Topo50 map series, which contains topographic mapping for mainland New Zealand and New Zealand's offshore islands. These map series were created by LINZ in the late 1980s and early 1990s by scanning 1:50K maps. The map has since been updated by aerial photos, orthophotos, and satellite imagery.

Basin Outlet Point

The basin outlet point defines the location where the dam for water harvesting is proposed. This point was manually recorded with a handheld Garmin® GPSMAP. Data was originally

recorded in a .gpx file. The file has been converted to a shapefile and was projected onto NZGD 2000 Wairarapa Circuit.

Climate Data

Since the CVC covers a geographically diverse area, multiple climate data sources were used. Virtual Climate Data (VCD) was acquired from the National Institute of Water and Atmospheric Research (NIWA). The dataset contains daily estimation of; rainfall, potential evapotranspiration, air and vapour pressure, maximum and minimum air temperature, soil temperature, relative humidity, solar radiation, wind speed and soil moisture. This information is available on a 5 km grid covering New Zealand (NIWA, 2016). The dataset is created by interpolation from actual data observations. Data from Four VCD sites were downloaded and processed. In addition to VCD, one rainfall record was acquired from the Greater Wellington Regional Council. This dataset contains daily rainfall data at Westons on Waipoua River starting from November of 2007. Table 4-4-1 details the location, elevation, data source, and data type of all the climate information. Figure 4-5 shows the mean monthly precipitation with February being the driest month in a year. Site003 (rain gauge) recorded higher precipitation during the winter months than the VCDs surrounding it. Figure 6 shows the relative frequency of rainfall at the four VCD points: Site003 was omitted from this exercise because only 6 years of data was available. Figure 4-6 Shows the frequency distribution of rainfall which highlights the occurrence of extreme events.

Site ID	Source	Latitude,Longitude	Elevation (meters)	Data Type
001	VCS	-40.775,175.575	397	Rainfall, Windspeed,Radiation, Maximum and Minimum Temperature, Relative Humidity
002	VCS	-40.825,175.625	219	Rainfall, Windspeed,Radiation, Maximum and Minimum Temperature, Relative Humidity
003	Rain Gauge	-40.794,175.567	464	Rainfall
004	VCS	-40.825,175.525	586	Rainfall, Windspeed,Radiation, Maximum and Minimum Temperature, Relative Humidity
005	VCS	-40.825,175.575	400	Rainfall, Windspeed,Radiation, Maximum and Minimum Temperature, Relative Humidity

Table 4-4-1 Climate data used in this study and their source, geographic location, elevation.

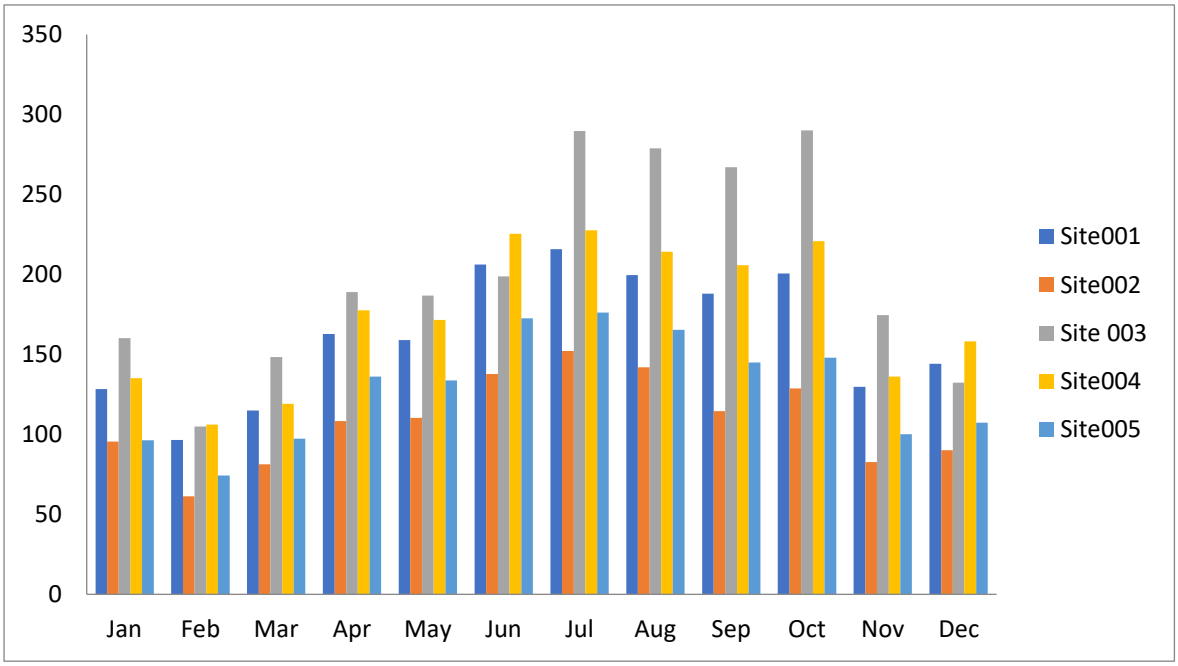

Figure 4-5 Six years average Monthly precipitation from each climate station between 2008 and 2014

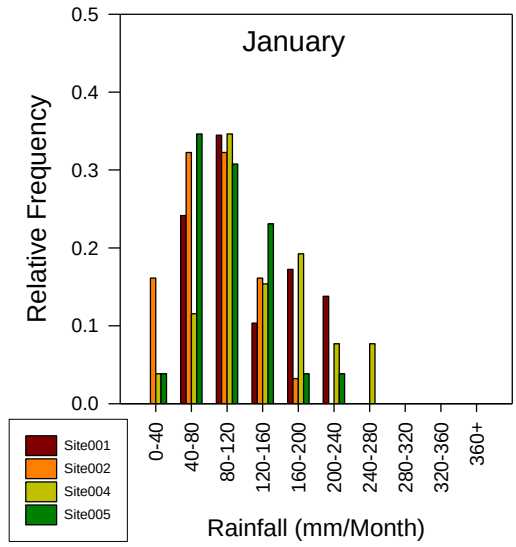
January
Relative Frequency
0.0
0.1
0.2
0.3
0.4
0.5
0-40
40-80
80-120
120-160
160-200
200-240
240-280
280-320
320-360
360+
Rainfall (mm/Month)
Site001
Site002
Site004
Site005

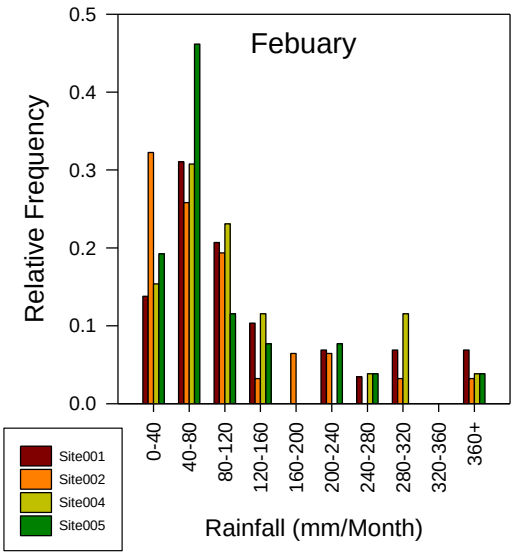
Febuary
Relative Frequency
0.0
0.1
0.2
0.3
0.4
0.5
0-40
40-80
80-120
120-160
160-200
200-240
240-280
280-320
320-360
360+
Rainfall (mm/Month)
Site001
Site002
Site004
Site005

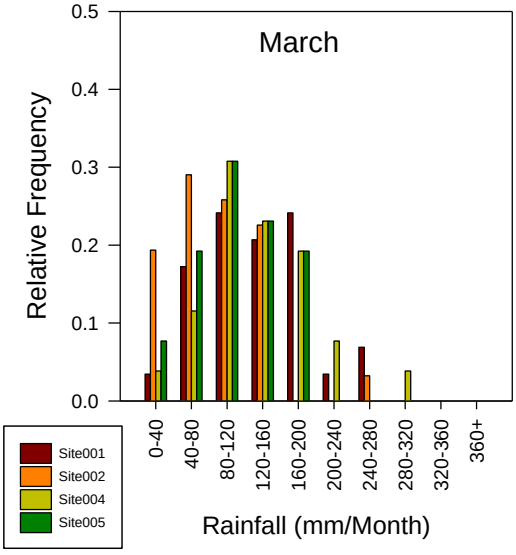
March
Relative Frequency
0.0
0.1
0.2
0.3
0.4
0.5
0-40
40-80
80-120
120-160
160-200
200-240
240-280
280-320
320-360
360+
Rainfall (mm/Month)
Site001
Site002
Site004
Site005

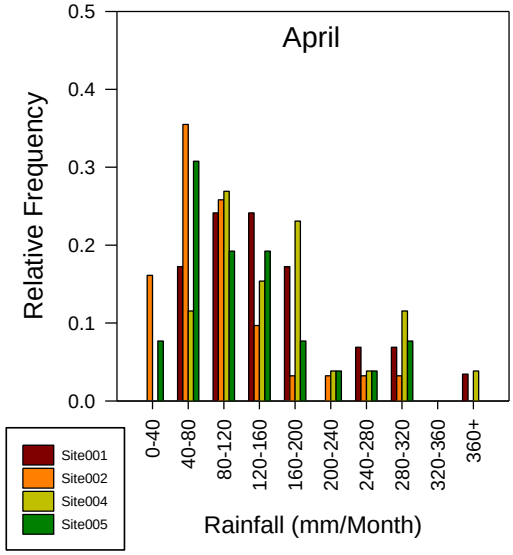
April
Relative Frequency
0.0
0.1
0.2
0.3
0.4
0.5
0-40
40-80
80-120
120-160
160-200
200-240
240-280
280-320
320-360
360+
Rainfall (mm/Month)
Site001
Site002
Site004
Site005

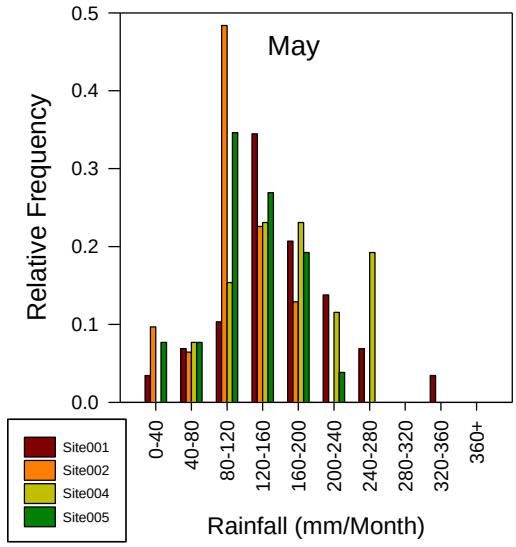
May
Relative Frequency
0.0
0.1
0.2
0.3
0.4
0.5
0-40
40-80
80-120
120-160
160-200
200-240
240-280
280-320
320-360
360+
Rainfall (mm/Month)
Site001
Site002
Site004
Site005

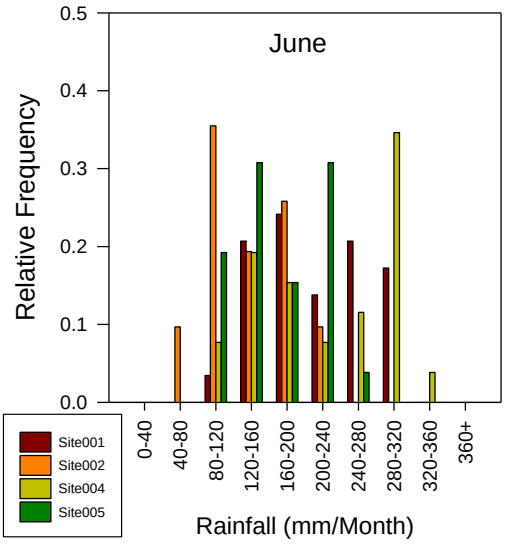
June
Relative Frequency
0.0
0.1
0.2
0.3
0.4
0.5
0-40
40-80
80-120
120-160
160-200
200-240
240-280
280-320
320-360
360+
Rainfall (mm/Month)
Site001
Site002
Site004
Site005

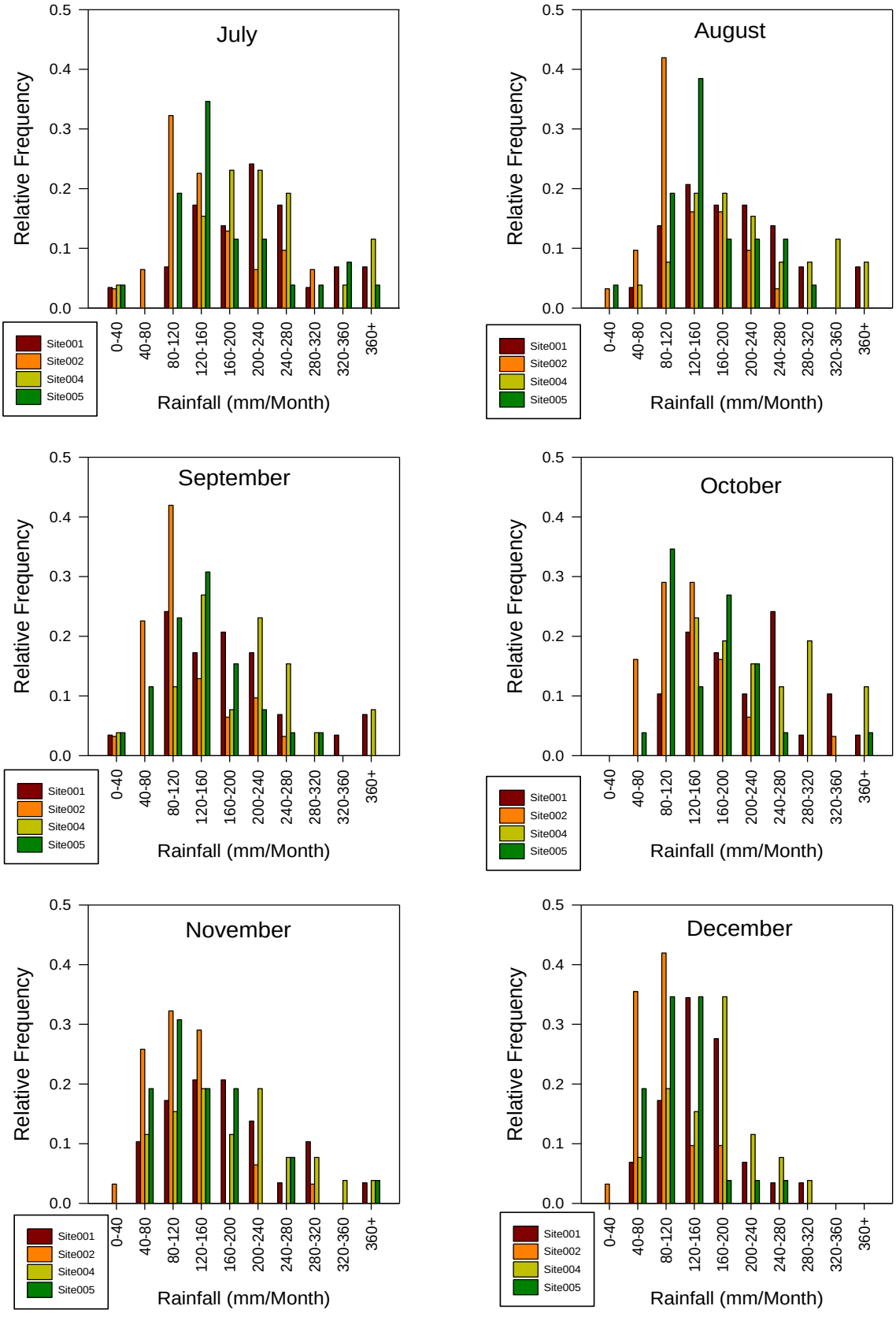

Figure 4-6 Frequency distribution of monthly rainfall from VCD (Site 001, Site 002, Site 004, Site 005) between year 1985-2014 over the CVC.

Flow Data

Flow data were acquired from the Greater Wellington Regional Council. Two flow gauges are located within the CVC. One of the flow gauges is located at the CVC outlet at Mikimiki Bridge, while the other is located on Te Mara stream at Kiriwhakapapa. Te Mara stream flow records are taken every 15 minutes starting from November 2008 while Mikimiki Bridge flow records are made every 15 minutes starting from February 2007. Both datasets were processed in Excel to obtain daily average flow rate.

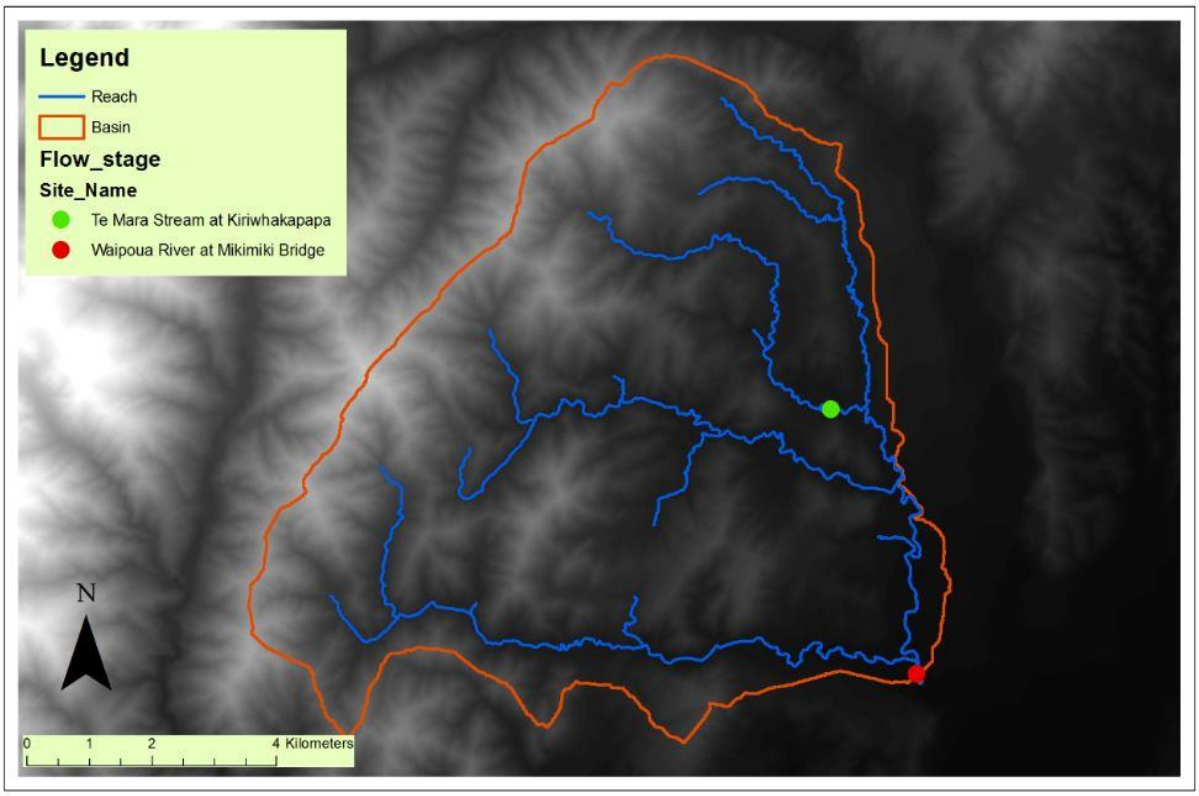

Figure 4-7 Reach within the CVC basin and Greater Wellington Regional Council Flow Rate Monitoring points

Data Processing

User Soil Database

SWAT requires a detailed soil database. This database characterizes soil physical and chemical properties. Soil physical properties govern the movement of air and water within the soil profile and between the soil and the atmosphere, and thus have a major impact on the modelling of the water cycle. Chemical properties characterize the initial level of

different chemicals in soil. Chemical properties are not required to run SWAT. The following table provides details of the variables within the soil database.

Variables	Definition and Description
SNAM	Soil Name
HYDGRP	Soil Hydraulic Group
SOL_ZMX	Maximum rooting depth of soil profile (mm).
ANION_EXCL	Fraction of Porosity (void space) from which anions are excluded. (Optional)
SOL_CRK	Potential or maximum crack volume of soil profile expressed as a fraction of the total soil volume. (Optional)
TEXTURE	Texture or soil layer (Optional)
SOL_Z(layer #)	Depth from soil surface to bottom of layer (mm)
SOL_BD(layer #)	Moist bulk density (g/cm^3)
SOL_AWC(layer #)	Available water capcity of the soil layer (mm H_2O/mm soil)
SOL_K(layer #)	Saturated Hydraulic conductivity (mm/hr)
SOL_CBN(layer #)	Organic carbon content (% soil weight)
SOL_CLAY(layer #)	Clay content (% soil weight)
SOL_SILT(layer #)	Silt content (% soil weight)
SOL_SAND(layer #)	Sand content (% soil weight)
SOL_ROCK(layer #)	Rock fragment content (% total weight)
SOL_ALB(top layer)	Moist soil albedo
USLE_K(top layer)	USLE equation soil erodibility (K) factor (units: 0.013 (metric ton m^2 hr)/(m^3-metric ton cm)
SOL_EC(layer #)	Electrical conductivity (dS/m) (Not currently active)
SOL_CAL(layer#)	Soil $CaCO_3$ (%) (Not currently active)
SOL_PH(layer #)	Soil pH (Not currently active)

Table 4-4-2 Definition and Descriptions of the variables within the SWAT soil database

As mentioned above, when applying SWAT to watersheds within the United States, there are readily available soil databases from the United States Department of Agriculture-Natural Resources Conservation Services (USDA-NRCS) such as SURRGO and STATGO. However, when applying SWAT in regions outside the United States, users must construct the soil database from available sources. Within New Zealand there are two main soil databases – FSL and S-maps.

FSL contains GIS layers with a range of soil data including chemical and physical attributes such as minimum pH, maximum salinity, cation exchange capacity (CEC), total carbon, phosphate retention, topsoil gravel content, particle size, potential rooting depth, soil permeability, depth to a slowly permeable horizon, and so on. FSL is derived from either

analytical result stored in the National Soil Database or as professional estimates by pedologists. However, FSL is patchy in scale and does not provide the detailed soil layer information that is required by SWAT.

S-Map was created as a replacement for FSL for New Zealand soil. The goal of S-map is to provide comprehensive, quantitative soil information to support sustainable development and scientific modelling. Although it is still under development and the current coverage is poor, S-map provides much higher quality soil data than FSL. Landcare Research New Zealand produces soil series factsheets for different regional councils. Detailed descriptions of the soil are given in these factsheets. In addition to FSL and S-maps, the aforementioned "A field descriptions of the soils and geology of riverside farm" (Pollok, Neall, & DeRose, 1994) has also been used to provide details of soil properties.

The User soil database was created using information from FSL, S-maps, and the field descriptions of the Riverside Farm.

SNAM

SNAM is the name to be used to define a particular type of soil. In this case, the abbreviation of soil series name was used to annotate soil name.

HYDGRP

HYDGRP defines the hydrologic soil group. For soil series with a corresponding S-Map factsheet, HYDGRP was taken directly from the factsheet. For soil series without a corresponding S-map factsheet, HYDGRP was determined using the identification criteria from the National Engineering Handbook Chapter 7 (Mockus et al., 2009) Table 7-1. This table contain rules for assigning hydrologic soil groups using saturated hydraulic conductivity.

Group	Characteristics
A	Soil having high infiltration rates when thoroughly wetted, consisting chiefly of sands or gravel that are deep and well-to-excessively drained. These soils have a high rate of water transmission (low runoff potential).
B	Soil having moderate infiltration rates when thoroughly wetted, chiefly moderately deep to deep, moderately well to well drained, with moderately fine to moderately coarse textures. These soils have a moderate rate of water transmission.
C	Soils having slow infiltration rates when thoroughly wetted. Chiefly with a layer that impedes the downward movement of water or of moderately fine

	to fine texture and a slow infiltration rate. These soils have a low rate of water transmission (high runoff potential).
D	Soils have very slow infiltration rate when thoroughly wetted, chiefly clay soils with a high swelling potential; soils with a high permanent water table; soil with a clay pan or clay layer at or near the surface; and shallow soils over nearly impervious materials. These soils have a very slow rate of water transmission.

Table 4-4-3 Soil Hydrologic Soil Group Definition used in SWAT (Neitsch et al., 2011)

SOL_ZMX

SOL_ZMX is the maximum soil rooting depth of a soil type. This value is given in S-map factsheets as "potential rooting depth" and "rooting barrier". For soil series without corresponding S-map factsheets, this value is determined by the soil description found on the field descriptions in "The soils and geology of Riverside farm".

ANION_EXCL, SOL_CRK, TEXTURE

ANION_EXCL is the faction of porosity from which anions are excluded by the net negative charge possessed by most soil minerals. This parameter was set to default of 0.5. SOL_CRK is the maximum potential crack volume of the soil profile. This parameter was also set to the default value of 0.5. TEXTURE describes the texture of soil in each layer. This parameter is inactive and does not affect SWAT calculation, therefore it was left blank.

SOL_Z (layer #)

SOL_Z (layer#) is the soil layer depth. This parameter is available both from S-maps factsheets and the field descriptions of "The soils and geology of Riverside farm". SOL_Z measures the cumulative depth from soil surface to the bottom of each layer.

SOL_BD (layer #)

SOL_BD is the soil bulk density. According to the SWAT input-ouput document it is expressed as the oven dried soil weight divided by the volume of the soil at or near field capacity. S-Map factsheets provide bulk density for the topsoil (0-20cm) and for the subsoil (20cm+). For soil series without a corresponding S-Map factsheet, bulk density was estimated from its texture class using the soil water characteristics hydraulic properties calculator (Saxton, Rawls, Romberger, & Papendick, 1986).

SOL_AWC (layer #)

Available water capacity is the difference between field capacity and wilting point (AWC = FC - WP). Both field capacity and wilting point can be found from S-Map factsheets. For soil series without a corresponding S-Map factsheet, AWC is estimated from its texture class using the Soil Water Characteristics Hydraulic Properties Calculator (Saxton, Rawls, Romberger, & Papendick, 1986).

SOL_K (layer #)

Saturated Hydraulic conductivity is estimated with Soil Water Characteristics Hydraulic Properties Calculator using soil particle size composition (Saxton, Rawls, Romberger, & Papendick, 1986).

SOL_CBN (layer #)

Organic carbon content is only available from the FSL map attribute table as "Carbon Class". The value for "Carbon Class" is for the top 20 cm of soil, and ranges from 1-5, which represents soil carbon content in a descending order as shown in Table 4-4-4.

CARBON_CLASS	CARBON_MIN (%)	CARBON_MAX (%)
1	20	60
2	10	19.9
3	4	9.9
4	2	3.9
5	0	1.9

Table 4-4-4 Soil Carbon Content for each Soil Carbon Class in the FSL

The soil series was used to find its corresponding carbon class. The maximum or medium value of the carbon min and carbon max are taken for the top layer. The lower layer was estimated to be 33%, 42% , and 50% of the carbon content of the first layer depending on whether the landuse were dominated by shrubland, grassland or forest, respectively (Jobbágy & Jackson, 2000). SOL_CBN is assumed to be 0 for layers below 1 metre.

SOL_CLAY (layer #), SOL_SILT (layer #), SOL_SAND (layer #)

Clay, silt, and sand contents for each layers are available from S-Map factsheets. For soil series for which corresponding S-map factsheet is not available, clay, silt, and sand content was estimated from the soil texture class using the soil texture triangle (USDA-NRCS).

SOL_ROCK (layer#)

Rock fragment content is available from S-Map factsheets. For soil series which S-map factsheet is not available, soil descriptions were used to estimate rock content.

SOL_ALB (Top layer)

The S-map factsheet does not contain information on soil albedo. Therefore, moist soil albedo was estimated from the description of soil colour. The description of soil colour (i.e. "light brown") was entered into the Munsell colour chart. After the matching colour name was found, colour values were taken (in the case of "light brown", colour value = 6) (Munsell Colour).

Soil albedo is calculated as:

$$Albedo = 0.069 * (Colour\ Value) - 0.114$$

Equation 4-1 Equation for calculating the albedo of the soil from the soil colour

For soil series without a description of colour, the default value of 0.13 was taken (classify as brown) (Gies & Merwade)

USLE_K (top layer)

USLE equation soil erodibility factor (K) is defined as the soil loss rate per erosion index unit for a specified soil as measured on a unit plot. A unit plot is defined as ; 22.1 meters long, with a uniform length-wise slope of 9%, is kept continuously fallow, and is tilled up and down the slope. The soil is tilled and kept free of vegetation for at least two years.

Since direct measures of USLE_K are very time consuming, expensive, and unrealistic, alternative methods were proposed. Wischmeier and Smith (1978) proposed a method that calculates USLE_K using particle size parameters, organic matter percentage, profile permeability class and soil structure. Again, this method requires too many variables that may be difficult to obtain, and so an alternative that was proposed by Williams and Singh (1995) was used instead.

This alternative equation (see below) does not require description of soil structure and permeability class;

$$K_{USLE} = f_{csand} \cdot f_{cl-si} \cdot f_{orgc} \cdot f_{hisand}$$

Equation 4-2 formula for calculating the K_{USLE}

$$f_{csand} = \left\{0.2 + 0.3 \cdot \exp\left[-0.256 \cdot m_s \cdot \left(1 - \frac{m_{silt}}{100}\right)\right]\right\}$$

Equation 4-3 Formula for calculating f_{csand}

$$f_{ci-si} = \left(\frac{m_{silt}}{m_c + m_{silt}}\right)^{0.3}$$

Equation 4-4 Formula for calculating f_{ci-si}

$$f_{orgc} = \left(1 - \frac{0.0256 \cdot orgC}{orgC + exp(3.72 - 2.95 \cdot orgC)}\right)$$

Equation 4-5 Formula for calculating f_{orgc}

$$f_{hisand} = \{1 - \frac{0.7 * \left(1 - \frac{m_s}{100}\right)}{\left(1 - \frac{m_s}{100}\right) + \exp\left[-5.51 + 22.9 \cdot \left(1 - \frac{m_s}{100}\right)\right]}\}$$

Equation 4-6 formula for calculating f_{hisand}

Where ms is the percent sand content, msilt is the percent silt content, mc is the percent clay content and orgC is the percent organic carbon content of the soil layer.

WGEN_user

In order to run SWAT, climatic data such as daily precipitation, maximum air temperature, minimum air temperature, wind speed, solar radiation, and relative humidity are required. When certain data are missing, or when predicting future scenarios, SWAT uses statistical records of historical climate data to generate climatic inputs. The first step of the weather generator is to generate precipitation for the day. After the total rainfall has been generated, rainfall distribution within a day is then computed for the calculation of Green & Ampt infiltration. When the SCS runoff curve method has been selected, this step is skipped. Maximum and minimum temperature, solar radiation and relative humidity are generated based on the presence or absence of rain. Lastly, wind speed is generated independently. WXGEN simulates precipitation of the local area using the Markov chain-gamma model. The model first generates the occurrence of wet or dry days. Then, the quantity of precipitation is determined by the second part of the model.

WGEN_user contains statistical data needed to generate daily climatic data for SWAT. It is recommended that at least 20 years of records are used to calculate these parameters.

All the variables used in WGEN_user are enlisted below in

Table 4-4-5 with a definition and brief description;

Variable Name	Definition and Descriptions
WLATITUDE	Latitude of the weather stations used

WLONGITUDE	Longitude of weather stations used
WELEV	Elevation of weather stations Note; NIWA does not provide elevations of the VCS sites. Elevations were estimated by entering the Latitude and Longitude of the VCS site into Google Earth Pro
RAIN_YRS	Number of years of maximum monthly 0.5h rainfall data used to define values for RAIN_HHMX(mon)
TMPMX(mon)	Average or mean daily maximum air temperature for a month
TMPMN(mon)	Average or mean daily minimum air temperature for a month
TMPSTDMX(mon)	Standard deviation for daily maximum air temperature in a month
TMPSTDMN(mon)	Standard minimum for daily maximum air temperature in a month
PCPMM(mon)	Average or mean total monthly precipitation in a month This parameter was calculated with pcpSTAT.exe software
PCPSTD(mon)	Standard Deviation for daily precipitation in a month This parameter was calculated with pcpSTAT.exe software
PCPSKW(mon)	Skew coefficient for daily precipitation in a month This parameter was calculated with pcpSTAT.exe software
PR_W(1,mon)	Probability of a wet day following a dry day in a month This parameter was calculated with pcpSTAT.exe software
PR_W(2,mon)	Probability of a wet day following a wet day in a month This parameter was calculated with pcpSTAT.exe software
PCPD(mon)	Average number of days of precipitation in a month This parameter was calculated with pcpSTAT.exe software
RAINHHMX(mon)	Maximum 0.5 hour rainfall in entire period of record for a month
SOLARAV(mon)	Average daily solar radiation for month
DEWPT(mon)	Average daily dew point temperature for a month or relative humidity can be input This parameter was calculated with dew02.exe software
WNDAV(mon)	Average daily wind speed in a month measured at 10 meters

Table 4-4-5 Definition and Descriptions of parameters within SWAT WGEN database

Two sets of data were used to construct WGEN_user. For Riverside farm site, VCD from 1981 to 2015 were used. However, wind speed was not recorded until 1997. Riverside Hill (Site 001) represents the area 5km North East of Riverside farm. This site was taken to account for the climate variability of hill country. Data from 1986 to 2015 were used to generate WGEN for both sites. However, the wind speed record is not available for period prior to 1997.

Data Processing: The majority of the parameters were processed using Excel with the exception of PCP and DEWPT. Specific software was designed for calculating these parameters. It is worth noting that the 0.5 hourly rainfall records are not available for the site of interest, and RAINHHMX was estimated by taking 1/3 of maximum daily rainfall for the month. This method was recommended by R. Srinivasan, (personal communication, 2016) and the result was visually validated by comparing with the NIWA High intensity Rainfall System V3. No statistical test was performed for this comparison.
WGEN was tested for its ability to generate long term precipitation. This test is described in Appendix II. The validation test shows that WGEN is able to generate precipitation data that is statistically similar to the actual precipitation record. Although there are problems with the variance in certain months, the WXGEN model has demonstrated its strength in predicting the quantity and seasonal variation of precipitation.

Land Cover / Plant Growth Database and management database

Land Cover Classification

The LCDB is modified to match a land cover type in SWAT. Some land use classes were grouped together due to their similarities.

SWAT Landuse Class and Abbreviations	LCDB land use class
FRSD Forest Deciduous	Broadleaved indigenous hardwood deciduous hardwood
FRSE Forest, evergreen	Exotic forest (softwood coniferous)
RNGB Range bush	Gorse and broom Manuka/Kanuka
BARR Barren	Gravel or Rock landslides, surface mine or dump
WETN wetland, not forested	Herbaceous freshwater vegetation
WPAS winter pasture, model based on tall fescue	High producing exotic grassland low producing grassland
FRST forest, mixed	Indigenous forest
WATR water	Lakes,ponds,rivers
AGRR agriculture, Row Crops	Short rotation cropland

Table 4-4-6 Corresponding SWAT landuse class and New Zealand landuse classification

Plant growth and management database

Default plant growth and management parameters result in an unrealistic simulation of plant leaf area index (LAI), which significantly affects the water balance of the model. LAI plays an important role in calculating the actual ET and thus affects water balance directly. Therefore, the correct LAI value is necessary for a successful SWAT model. As mentioned previously, actual ET is calculated as the total of three main parts; evaporation from canopy storage, transpiration from plant, and evaporation from soil. Plant transpiration is directly affected by LAI. For example, Almeida, Chambel-Leitao, and Jauch (2011) calibrated LAI in the SWAT model and discovered that the maximum actual LAI in a corn plantation was half of what was predicted by the model; and that the reduction in LAI at the end of the growing season was much slower than the default model prediction. Subsequent calibration resulted in 9% reduction in ET predictions.

Fortunately, the LAI for pasture is less variable then for crops and so issues associated with LAI values should be less of a problem in the current exercise where perennial pasture is the main landcover. In New Zealand, the best grazing practice will leave at least 3-4 cm pasture cover to ensure maximum regrowth. This translates to a LAI of 4 (Wall, Stevens, Thompson, & Goulter, 2012). In reality, the pasture is often grazed down to LAI of 2. On average, the whole farm LAI is estimated to be around 3 (C. Matthews, personal communication, 2006) All of the plant LAI values in the model are manually manipulated to keep the LAI above 3 the whole year round. However, during the winter, LAI drops to 0.9 when daylight hours fall below a certain threshold. The SWAT plant growth model imposes a dormancy period for trees, perennials, and cool season annual plants.

Despite the best efforts to carefully manipulate LAI values in this study, there is room for improvement of this feature of the exercise in the future . Ideally, calibration should be carried out using local measured LAI data to improve LAI simulation. Alternatively, source code could be modified to allow more precise control over the change of LAI.

SWAT model Set Up

SWAT models were established for both the CVC and WHC following the ArcSWAT interface user's manual (Arnold et al., 2012). Two blank SWAT projects (CVC and WHC) were set up and the SWAT2012 database was updated with new usersoil and WGEN_user databases.

Watershed Delineation

Firstly, two 8 meter projected DEMs of different sizes were loaded into the corresponding SWAT project. Both maps were clipped picture areas slightly larger than the catchment of interest to reduce processing time. Secondly, the projected stream centrelines were loaded on to each project interface to ensure that delineated streams were located on the actual streams. Next, the WHC basin outlet was set to the location of the proposed water harvesting dam and the CVC basin outlet was set to be at the Mikimiki bridge flow gauge. Finally, the sub-basin parameters were calculated.

HRU Analysis

HRU analysis includes two steps. The first step defines land use, soil type, and slope classification. The second step is called the HRU definitions, and allows the user to choose the intensity of land use, soil type, and slope classes in HRU definition. Pasture is assumed to cover the entirety of the WHC, and the land use map used for the CVC is the LCDB described in the previous section. Land use polygons were matched with their corresponding land use database. For the WHC, soil data was loaded using the map attached to "A field descriptions of The Soils and Geology of Riverside Farm" (Pollok et al., 1994). For the CVC, the FSL was used to define the geographic boundary of each of the soil type polygons. After the geographic boundary was defined, each soil polygon was matched with the corresponding soil description from the user soil database. Under the slope classification tab, 'multiple slope' was selected. Four slope classes were defined, and the natural Jenk method was used to minimize variance within group and maximize difference between groups.

This process was done independently, prior to SWAT set up. DEM was extracted with the mask which ensured the DEM only covered the area of interest. The slope was taken for the DEM, and classification was calculated with ArcGIS.

The slope classifications were defined as:

Class	Slopes
Class 1	0-7.07
Class 2	7.07-16.21
Class 3	16.21-34.41
Class 4	34.41-9999

Table 4-4-7 Slope steepness classification

Using the HRU definition, multiple HRUs were selected for the CVC due to its complexity, land use percentage over sub basin area is set to be 20%, Soil class percentage over the land use area is set to be 10%, and slope class percentage over the soil area is set to be 20%. For WHC, the dominant land use, soils and slope was chosen.

Climate Data and Write input tables

First, processed climate data was organized into folders that SWAT could process. For the CVC, all five climate data points were used. For the WHC, only the local VCD was used. WGEN_user was selected to fill in the missing data. Next, under 'write input tables', the 'all of the options and create tables' was selected; this process writes input files for default SWAT simulations.

SWAT run and data extraction

After SWAT has been properly set up. SWAT can be run under the "run SWAT" tab. The starting date and the ending date of the simulation can be chosen, depending on the dataset given. NYSKIP is the warm up period. This value is set to 1 for all of the simulations. Daily simulations were selected for the CVC calibration and validation as well as WHC water partitioning analysis. Monthly was selected to calculate the cumulative probability of water harvesting potential distribution. Unselect "limit HRU Output" and set all parameters on this page as default. Setup SWAT run and run SWAT.

After SWAT has been ran successfully, save the SWAT simulation under the SWAT output tab. The save SWAT simulations can be used for model calibration.

Extraction of data is conducted with SWAT-CUP. The "no-observation" function of SWAT-CUP software allows extraction of model output with any given parameter set. This method

is used in favour of extracting the results directly from SWAT output table due to its superior user experience.

4.2 SWAT Calibration, Validation, and Sensitivity Analysis

The default run of SWAT simulation of CVC was saved. SWAT-CUP is then used to calibrate and validate the SWAT model. The new set of improved parameters is transferred to the WHC to model the water harvesting potential.

Parameter Selected for Calibration

Arnold et al. (2012) discussed the importance and methods of the calibration parameters selection. Parameter selection should be guided by processes, however, since SWAT is a comprehensive model, one parameter may affect many different processes. For example, as Arnold et al. (2012) noted, CN affects runoff directly but changes in runoff also modify all aspects of the hydrological balance, soil erosion, and nutrient transport. Therefore, calibration should start with hydrological processes.

A literature review has been conducted to determine parameters used for model calibration (Refer to Table 4-4-8). Douglas-Mankin, Srinivasan, and Arnold (2010) summarized parameters used in 64 selected SWAT studies: 12 parameters were used for calibrating for surface runoff and baseflow. These parameters are CN2, SOL_AWC, ESCO, EPCO, SURLAG, OV_N, ALPHA_BF, GW_REVAP, GW_DELAY, GWQWN, REVAPMN, and RCHARG_DP. In addition, LAT_TTIME was added due to the role it plays in the modelling of quick flow. EVRCH was also added due to its potential importance to hydrology processes(Me et al., 2015a).

SOL_AWC is the available water capacity of the soil layer (mm/H2O/mm soil). It is widely used in SWAT calibration and it has been shown to be a sensitive parameter for hydrology processes. (Arnold et al., 2012; S. C. Brown, Versace, Lester, & Walter, 2015; Cibin, Sudheer, & Chaubey, 2010). However, this parameter has been excluded from the list of parameters for calibration in this study because SOL_AWC can be derived from inferences of the physical reality.

Thirteen parameters were selected for calibration. The same sets of parameter are also used to conduct global sensitivity analysis. Parameters selected for calibration are listed below in Table 4-4-8.

	Parameter	Default Range	Default Value	Parameter description and specifications
1	ESCO.hru	0-1	0.95	Soil evaporation compensation factor
2	SURLAG.bsn	0.05-24	4	Surface runoff lag coefficient
3	EVRCH.bsn	0.5-1	1	Reach evaporation adjustment factor
4	ALPHA_BF.gw	0-1	0.048	Baseflow alpha factor (1/days) It is a direct index of ground water flow response to changes in recharge A value vary from 0.1-0.3 indicates slow response to recharge. 0.9-1 indicates rapid response.
5	GW_DELAY.gw	0-500	31	Ground water delay time Depend on the hydraulic properties of the geologic formation in the vadose and ground water zone. How long it takes for water to enter ground water
6	GW_REVAP.gw	0.02-0.2	0.02	Groundwater “revap” coefficient As this value approaches 0, movement from aquifer to the soil above is restricted.
7	GWQMN.gw	0-5000	1000	Threshold depth of water in the shallow aquifer required for return flow to occur (mm H2O)
8	RCHRG_DP.gw	0-1	0.05	Deep aquifer percolation fraction
9	EPCO.bsn	0-1	1	Plant uptake compensation factor
10	REVAPMN.hru	0-500	750	Threshold depth of water in the shallow aquifer for revap or percolation to the deep aquifer to occur
11	LAT_TTIME.hru	0-180	0	Lateral Flow travel time
12	CN2.mgt	35-98	80,79,69	Initial SCS runoff curve number for moisture condition II
13	O_N.hru	0.01-30	0.15,0.1	Manning’s N value for overland flow

Table 4-4-8 Descriptions and specification, default range and values of the SWAT parameters used for calibration and validation.

SWAT-CUP set up for Calibration Validation and sensitivity analysis

The SWAT-CUP set up is straight forward. First of all, the selected parameters mentioned above were entered into the SWAT-CUP input table. Next, the recorded flow data from flow

gauges acquired from the Greater Wellington Regional council (recorded in 15 minutes interval) was entered. This information was processed and the average daily flow rate was calculated for both flow gauges. This information is then inputed into the SWAT-CUP under the 'observation and extraction' tab. SWAT-CUP is set up to run an iteration of 1000 simulations with parameter sets generated with the Latin Hypercube technique within the parameter limits and each result is compared with the observed data. The first iteration ran by SWAT-CUP uses the default maximum and minimum range of parameters with the exception of CN2 and OV_N. For CN2 and OV_N relative change was used within the given range for calibration purposes. The program then recommends another new set of parameter ranges around the best simulation parameter set. This new parameter set is then used to run the next iteration of 1000 simulation. Efficiency criteria are reviewed after each iteration and the calibration is completed when desirable results have been reached.

The process for validation is similar to that of calibration. The observed data was changed to the recorded data for the validation period. Only one iteration of 1000 simulations was run and the parameter set that produced the most desirable calibration output was used.

SWAT-CUP automatically conducts global sensitivity analysis after running an iteration of auto calibration which contains 1000 simulations. Parameter sets generated using Latin Hypercube sampling technique were regressed against the objective function values. The multiple regression analysis provides statistics of parameter sensitivity. The higher the absolute value of t-stats and te lower the p-value signals the more sensitive the parameter. After each iteration, the t-stats and p-value of each of the parameters are recorded. The parameter's range is then narrowed and updated, followed by running another iteration of 1000 simulations. This process is repeated until the p-factor, which measures the percentage of observed values which are enveloped by the 95% prediction uncertainty band, is larger or equal to 0.7; and the r-factor, which measures the thickness of the 95% prediction uncertainty band, is less than 1 and as close to 0 as possible (Abbaspour, 2007). After each iteration, the parameters with the top five largest absolute value of t-stats or the lowest p-value is recorded; a score between 1-5 is assigned to each parameter, with 1 given to the least sensitive parameter of the five and 5 to the most sensitive of the five. When calibration is completed, the sum of the scores of each parameter is calculated and ranked. The parameter with the highest cumulative score is the most sensitive parameter.

4.3 Parameter regionalization

Parameter regionalization refers to the process of transferring model parameters from a calibrated catchment to a hydrologically similar ungauged catchment. After the CVC has been calibrated and the optimal parameter set has been obtained, this parameter set was transferred to the WHC.

The WHC model was set up under the ArcSWAT interface and a simulation was saved. A SWAT-CUP SUFI-2 calibration was set up for this simulation. The observation tab was set to default and no observation tab was filled out according to the SWAT-CUP user manual's instructions to extract results from simulations. Two simulations were run, the first with default SWAT parameters, the second one with the medium value of the optimal parameter set. Flow rate from the basin outlet, surface runoff, lateral flow, and ground water contribution to each parameter before and after parameter regionalization were extracted for analysing.

4.4 Sensitivity of water harvesting potential to water partitioning

As mentioned above, the first stage of the Pond-Command Area water balance is constructed using the average stream flow at the basin outlet. Such stream flow is close to the SWAT catchment water yield with minor differences. The minor differences include in-stream processes such as evaporation from water surface, rainfall onto the stream, and transmission losses. However, such differences between reach output and water yield is low and negligible for the WHC. Water yield is the net amount of water that leaves each sub-basin and contributes to stream flow in the reach:

$$WLYD = SURQ + LATQ + GWQ - TLOSS - pond\ abstraction$$

Equation 4-7 Composition of the water yield in SWAT.

WLYD is the water yield, SURQ is the surface runoff, LATQ is the quantity of lateral flow, GWQ is the ground water contribution to steam flow., and finally TLOSS is the water loss from reach by transmission at every time step. The value of TLOSS is 0 across all sub-basins i.e. due to the small size of the WHC basin, transmission loss is assumed to be minimized. In this simulation the pond abstraction is equal to 0.

A sensitivity analysis was carried out to examine the effect each component has on the basin water harvesting potential. This analysis is necessary because the WHC is relatively

small and SWAT consider the system as a “closed” system. Water yield is nearly equal to the difference between rainfall and evapotranspiration with the difference being the water that drains to the deep aquifer which is assumed to be “lost”. This assumption is usually valid for large to medium scale catchments but it is less certain in smaller scale catchments. Ground water and lateral flow may leave the system, by-passing the water harvesting dam, resulting in an over prediction of the water yield . Despite whether the partitioned water will leave the system is uncertain, the anlysis presented here allows for a better understanding of the fate of the water then a simple soil water balance. Three water harvesting scenarios were studied:

- Water yield
- Only SURQ is harvested
- 80% of water yield is harvested

The first scenario assumed all of the water yields are harvested. This is the assumption made by SWAT: this scenario is considered to correspond closely to reality. However, as stated above, this model can overestimate the quantity of harvested water because not all of the water will resurface at the basin outlet. LATQ and GWQ may by-pass the hypothetical gauging station at the basin outlet and leave the WHC before it can be stored and harvested for irrigation purposes. This scenario represents the most optimistic estimation of the water harvesting ability of the WHC.

The second scenario assumes only surface runoff is harvested. This is the assumptions made in the modelling of other water harvesting schemes particularly in urban or roof top settings. This is the worst-case scenario and predicts the least amount of water the WHC is able to capture. However, this scenario is unlikely to be valid due to the bowl-shaped basin, which means that lateral flow and return flow are likely to contribute to the ephemeral stream and the water harvesting system.

The third scenarios assume that 80% of the water yield is collected in the basin: 80% is an arbitrary number. However, the 20% reduction from scenario 1 represents a “leaky” catchment and allows an exploration of the challenge to the assumption that all water yield surface at the basin outlet. The reduction in water yield is water “lost” from the WHC to GWQ and LATQ as it by passed the basin outlet. This approach gives a conservative estimation of the quantity of water WHC is able to harvest and store, and the result is in line with the experiment conducted by (Lambert, Devantler, Nes, & Penny, 1985)

Finally, the quantity of water that can be harvested under each scenario is fed into the command area water balance model. A pivot table is made to analyse the scenarios.
A matrix for each scenario is set up to obtain the optimal embankment height and command area size by comparing the daily and weekly irrigation failure rate as well as the increase in per hectare biomass production.

Chapter 5 Results of SWAT Analysis

5.1 Results

Calibration and validation of CVC

The calibration was completed after 6 iterations of 1000 rounds Latin Hypercube Sampling and both p-factor and r-factor had reached the optimal range. The calibrated parameter set is summarized in Table 5-5-2. The statistics for calibration and validation of the CVC is summarized below in Table 5-5-1. Calibration used the flow data recorded between 2009 and 2011 at Mikimiki Bridge. The calibrated R2, NSE and PBIAS are considered "satisfactory" by Moriasi et al. (2007). During the validation period (2012-2014), the model performance slightly decreased when compared to the calibration period but most are still considered "satisfactory". Figure 5-1 shows the 1:1 plot of observed and simulated flow rate at Mikimiki bridge and Te Mara site during calibration and validation period. This figure shows that the model systematically under predicts flow rate and the under prediction bias is particularly large during low and high flow events.

	Gauge	p-factor	r-factor	R^2	NSE	PBAIS
Calibration	Mikimiki	0.72	0.35	0.59	0.58	14.1
	Te Mara	0.71	0.32	0.59	0.58	14.2
Validation	Mikimiki	-	-	0.54	0.53	21.5
	TeMara	-	-	0.57	0.54	24.9

Table 5-5-1 calibration and validation efficiency of the CVC

Parameter Abbreviation	Parameter Name	Calibration fitted value
v__ESCO.hru	Soil evaporation compensation factor	0.783353
v__SURLAG.bsn	Surface runoff lag coefficient	9.660118
v__EVRCH.bsn	Reach evaporation adjustment factor	0.999667
v__ALPHA_BF.gw	Baseflow alpha factor	0.726982
v__GW_DELAY.gw	Ground water delay time	0.424046
v__GW_REVAP.gw	Groundwater “revap” coefficient	0.021916
v__GWQMN.gw	Threshold depth of water in the shallow aquifer required for return flow to occur (mm H2O)	1182.858521
v__RCHRG_DP.gw	Deep aquifer percolation fraction	0.015647
v__EPCO.bsn	Plant uptake compensation factor	0.455900
v__REVAPMN.gw	Threshold depth of water in the shallow aquifer for revap or percolation to the deep aquifer to occur	595.104736
v__LAT_TTIME.hru	Lateral Flow travel time	8.913342
r__CN2.mgt	Initial SCS runoff curve number for moisture condition II	-0.197804
r__OV_N.hru	Manning’s N value for overland flow	0.702814

Table 5-5-2 Parameter set that produced the optimal calibration and validation results

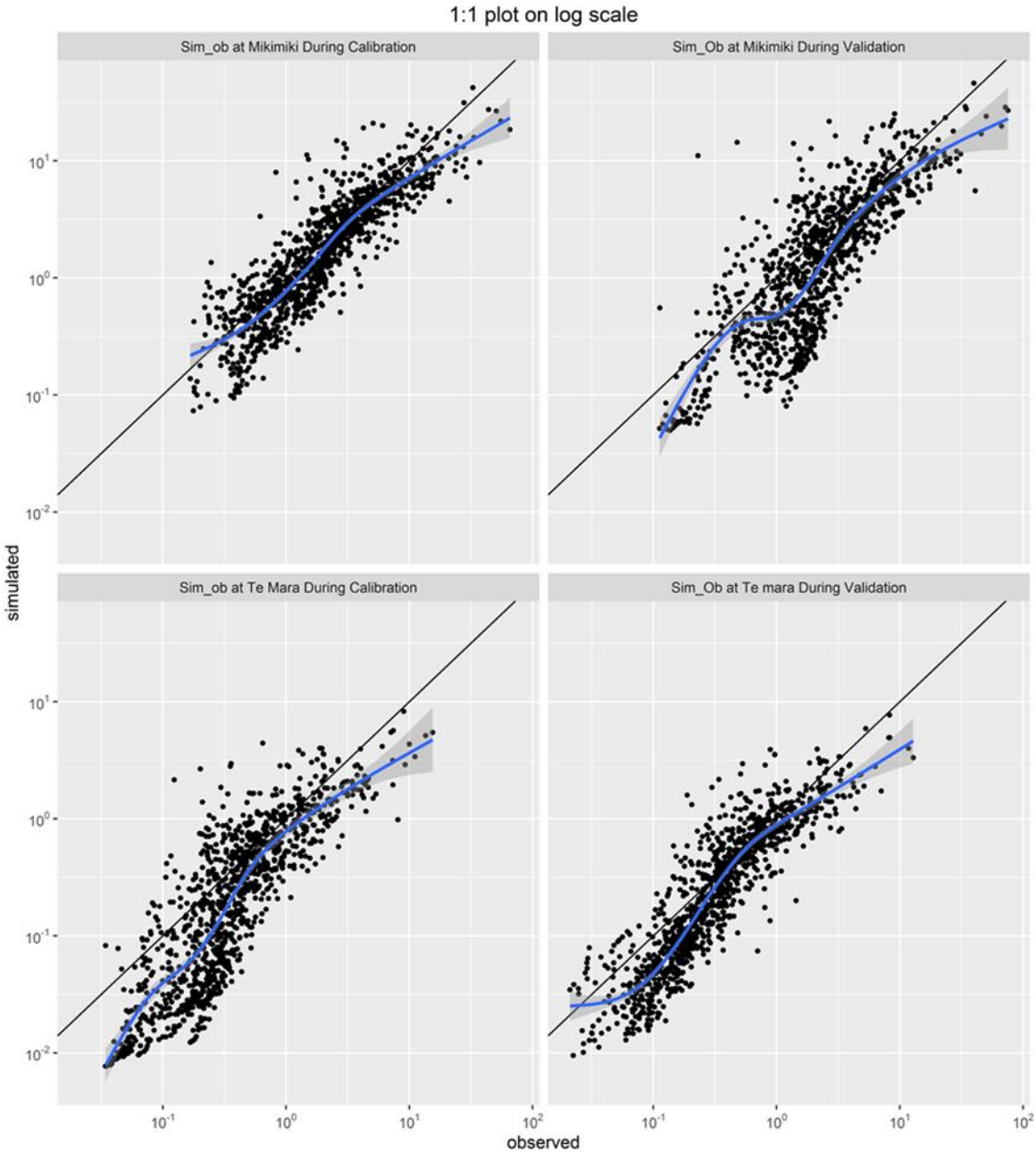

Figure 5-1 Simulated and observed flow events plotted against one another in log scale for Mikimiki and Te Mara site

Parameter Sensitivity analysis for the CVC calibration

The calibration reached a desirable result on the 6th iteration. The five most sensitive parameters during each iteration are listed in Table 5-5-3 with the score of 5 representing the highest sensitivity and score of 1 representing the lowest sensitivity. The scoring of sensitivity given in Table 5-5-3 is summarized and presented in Table 5-5-4. CN2 is the most sensitive parameters of all, while GW_DELAY and LAT_TTIME are the second and third most sensitive parameters.

In terms identifiability of parameters, Figure 5-2 shows the likelihood of NSE as a function of the variation of 13 parameters used for calibration during the first iteration. CN2 is the parameters that is immediately identifiable. Increases in CN2 decrease model efficiency and the model predictability is very sensitive to changes in CN2. GW_DELAY, GWQMN, RCHRG_DP, and LAT_TTIME may also be considered to be identifiable but they are less identifiable compared to CN2. The rest of the parameters are not identifiable. However, as (Cibin et al., 2010) points out, it is important to note that the non-identifiability of parameters does not indicate lack of parameter sensitivity. For the non-identifiable parameters, the final calibrated parameters must be checked and validated against physical reality in order to reduce the problem of equifinality.

Score	Iteration 1	Iteration2	Iteration3	Iteration4	Iteration5	Iteration 6
1	7:V__GWQMN.gw	1:V__ESCO.hru	11:V__LAT_TTIME.hru	1:V__ESCO.hru	13:R__OV_N.hru	13:R__OV_N.hru
2	11:V__LAT_TTIME.hru	11:V__LAT_TTIME.hru	1:V__ESCO.hru	8:V__RCHRG_DP.gw	8:V__RCHRG_DP.gw	8:V__RCHRG_DP.gw
3	8:V__RCHRG_DP.gw	5:V__GW_DELAY.gw	8:V__RCHRG_DP.gw	12:R__CN2.mgt	11:V__LAT_TTIME.hru	11:V__LAT_TTIME.hru
4	1:V__ESCO.hru	7:V__GWQMN.gw	12:R__CN2.mgt	11:V__LAT_TTIME.hru	5:V__GW_DELAY.gw	12:R__CN2.mgt
5	12:R__CN2.mgt	12:R__CN2.mgt	5:V__GW_DELAY.gw	5:V__GW_DELAY.gw	12:R__CN2.mgt	5:V__GW_DELAY.gw

Table 5-5-3 The 5 most sensitive parameters in each iteration

Ranking	Parameter	Total Score
1	CN	26
2	GW_DELAY	22
3	LAT_TTIME	15
4	RCHRG_DP	12
5	ESCO	8
6	GWQMN	5
7	OV_N	2

Table 5-5-4 Total Parameter Sensitivity Ranking

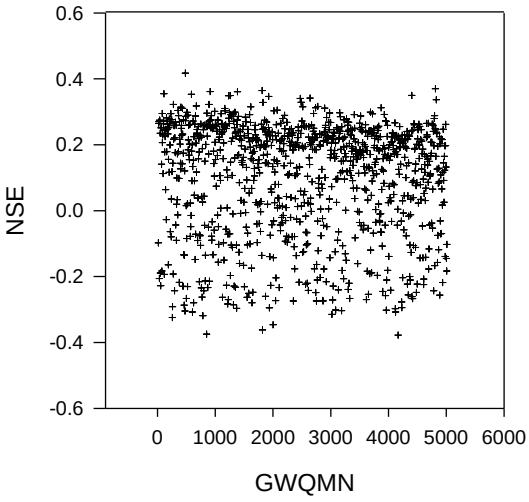
NSE
0.6
0.4
0.2
0.0
-0.2
-0.4
-0.6
0
1000
2000
3000
4000
5000
6000
GWQMN

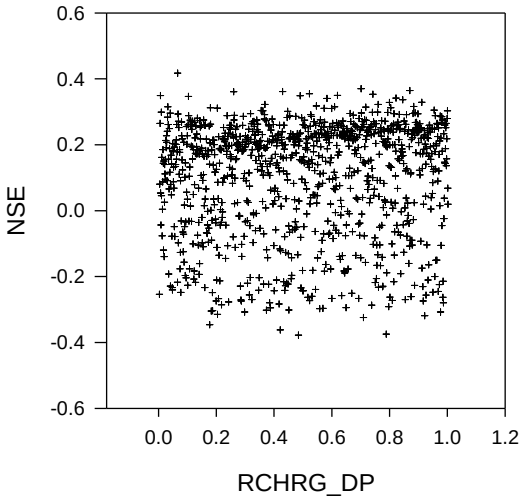
NSE
0.6
0.4
0.2
0.0
-0.2
-0.4
-0.6
0.0
0.2
0.4
0.6
0.8
1.0
1.2
RCHRG_DP

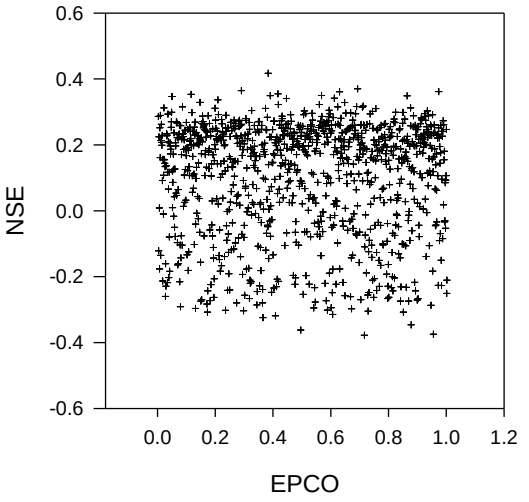
NSE
0.6
0.4
0.2
0.0
-0.2
-0.4
-0.6
0.0
0.2
0.4
0.6
0.8
1.0
1.2
EPCO

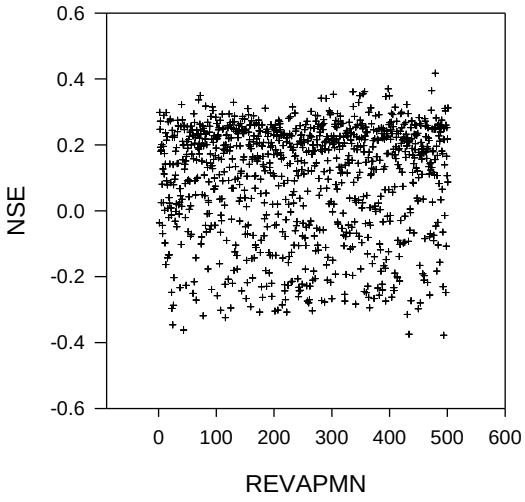
NSE
0.6
0.4
0.2
0.0
-0.2
-0.4
-0.6
0
100
200
300
400
500
600
REVAPMN

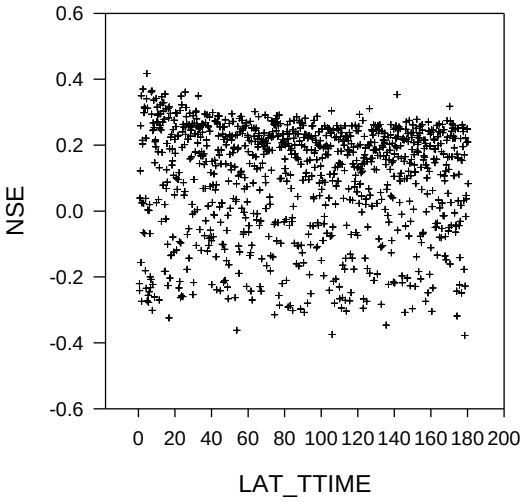
NSE
0.6
0.4
0.2
0.0
-0.2
-0.4
-0.6
0
20
40
60
80
100
120
140
160
180
200
LAT_TTIME

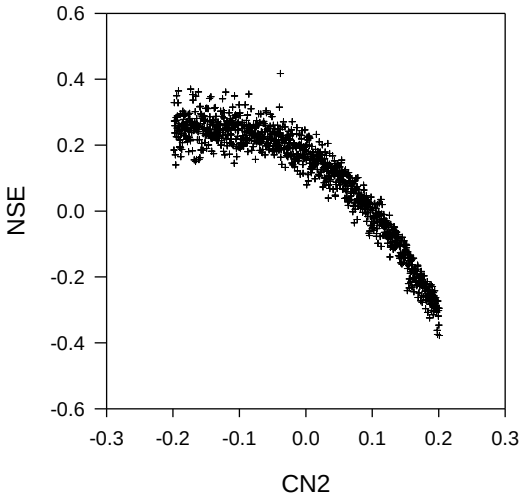
NSE
0.6
0.4
0.2
0.0
-0.2
-0.4
-0.6
-0.3
-0.2
-0.1
0.0
0.1
0.2
0.3
CN2

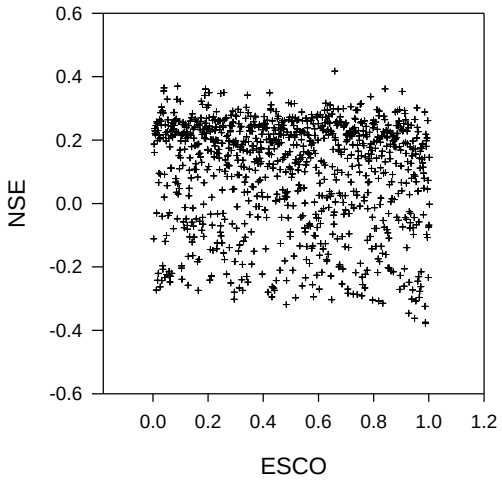
NSE
0.6
0.4
0.2
0.0
-0.2
-0.4
-0.6
0.0 0.2 0.4 0.6 0.8 1.0 1.2
ESCO

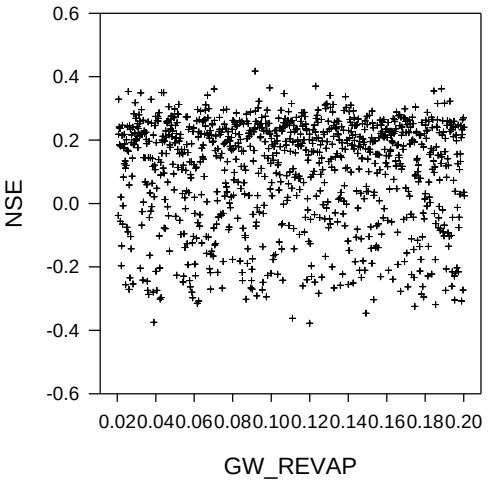
NSE
0.6
0.4
0.2
0.0
-0.2
-0.4
-0.6
0.020.040.060.080.100.120.140.160.180.20
GW_REVAP

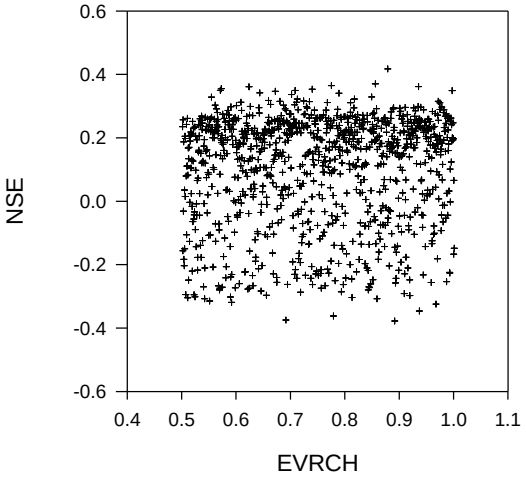
NSE
0.6
0.4
0.2
0.0
-0.2
-0.4
-0.6
0.4 0.5 0.6 0.7 0.8 0.9 1.0 1.1
EVRCH

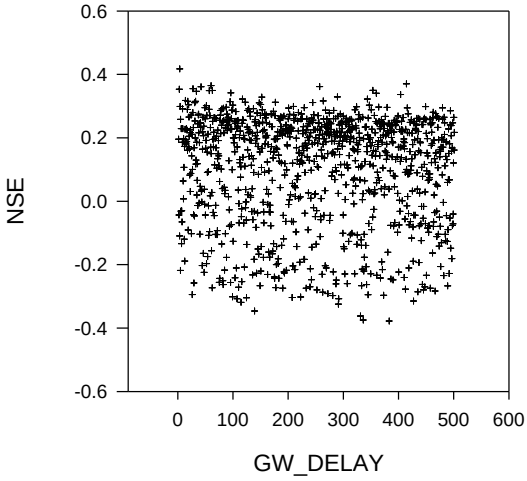
NSE
0.6
0.4
0.2
0.0
-0.2
-0.4
-0.6
0 100 200 300 400 500 600
GW_DELAY

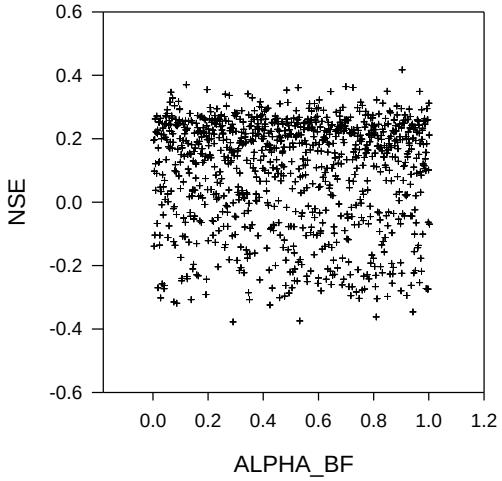
NSE
0.6
0.4
0.2
0.0
-0.2
-0.4
-0.6
0.0 0.2 0.4 0.6 0.8 1.0 1.2
ALPHA_BF

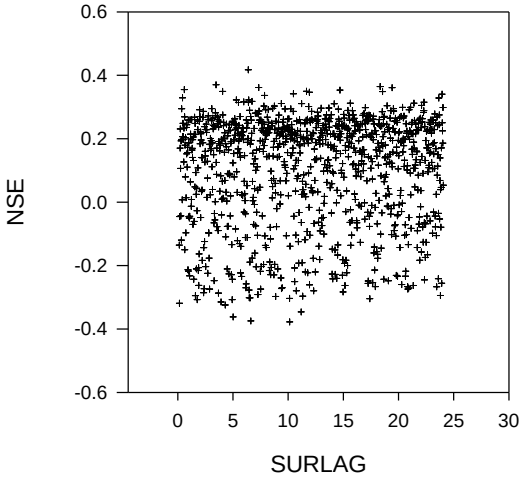
NSE
0.6
0.4
0.2
0.0
-0.2
-0.4
-0.6
0 5 10 15 20 25 30
SURLAG

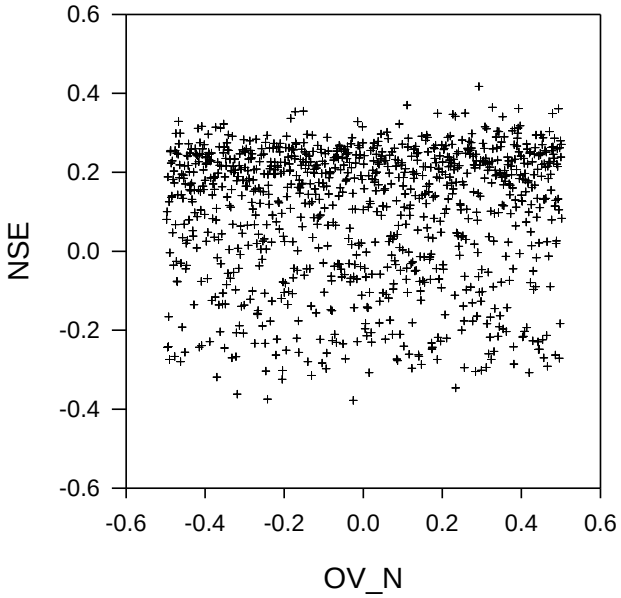

Figure 5-2 The relationship between parameters and the corresponding Nash-Sutcliff efficiency in the full parameter space using Latin Hypercube sampling technique.

Parameter regionalization

WHC simulation was ran twice, the first time with a default parameter set, and the second time with the regionalized parameter set. The regionalized parameter set resulted in a much lower predicted flow. Figure 5-3 illustrated the changes in water yield/ rainfall ratio (W/R ratio) for the whole basin from 1992 to 2015. For both the default and regionalized parameter sets, W/R ratio decreases during the years of low rainfall. For example, 2005 and 2007 are two of the driest years within this period and their W/R ratios were lower than an average year. However, it appears that the regionalized parameters predict an even lower W/R ratio than the default parameter set.

In addition to changes in the quantity of water yield, changes also have been observed in the distribution of flow. W/R ratio decreased during the summer months. Figure 5-4 ranks monthly W/R ratio for each year between 1992 and 2015. The top three W/R ratios from each year were counted, and the frequency of the month when W/R is the top three in that given year is plotted. Regionalized parameters predict that the highest W/R occur more frequently during the winter months. The result is consistent with the observation that the highest flow occurs during the winter months.

Another change is observed in the composition of water yield. On one hand, surface runoff predicted by the regionalized parameter set dramatically reduced. First of all, this is due to

the lowering of the CN value during calibration as, less surface runoff has been generated than what the default model has predicted. Greater surface roughness and better infiltration than the default assumptions may explain this. The second explanation is that surface runoff typically subsides as soon as the precipitation event stops in a small catchment (Moldan, Hultberg, Nyström, & Wright, 1995). The reduction in predicted SURQ in the regionalized model mostly occurs on days with 0 mm precipitation. This indicates an improvement in the model compared to the default parameter set. On the other hand, predicted lateral flow increased in the regionalized model when compared with the default model. On average, the regionalized ground water recharge prediction is also higher than the default and the distribution of the GWQ has changed. However, there is a seasonal pattern to be observed: during the summer, the regionalized prediction for GWQ is generally smaller than for the default case. In the winter months, GWQ increased under the regionalized prediction compared to the default. This indicates a relatively small catchment storage, and water entering the ground water return flow happens at a rather rapid rate.

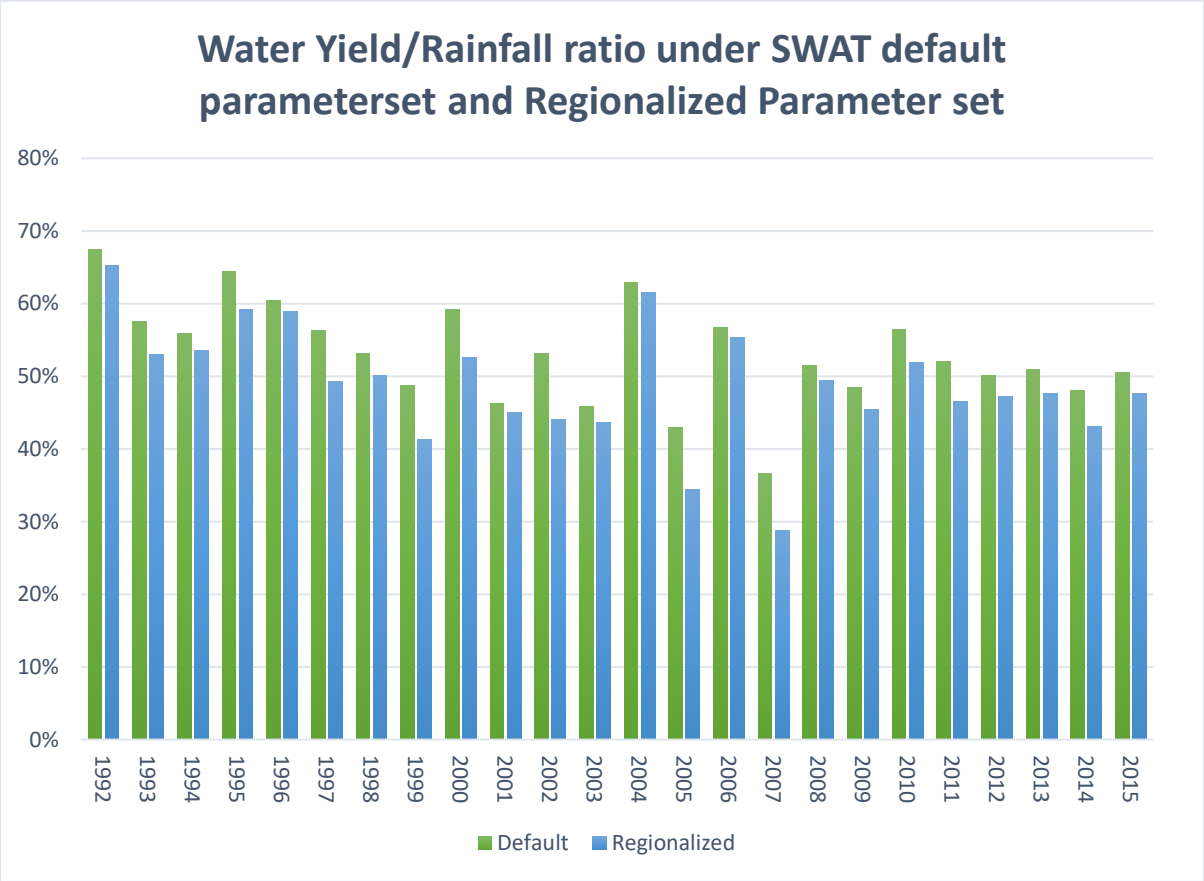

Figure 5-3 The ratio between water yield and rainfall under both the default parameter sets and the regionalized parameter sets.

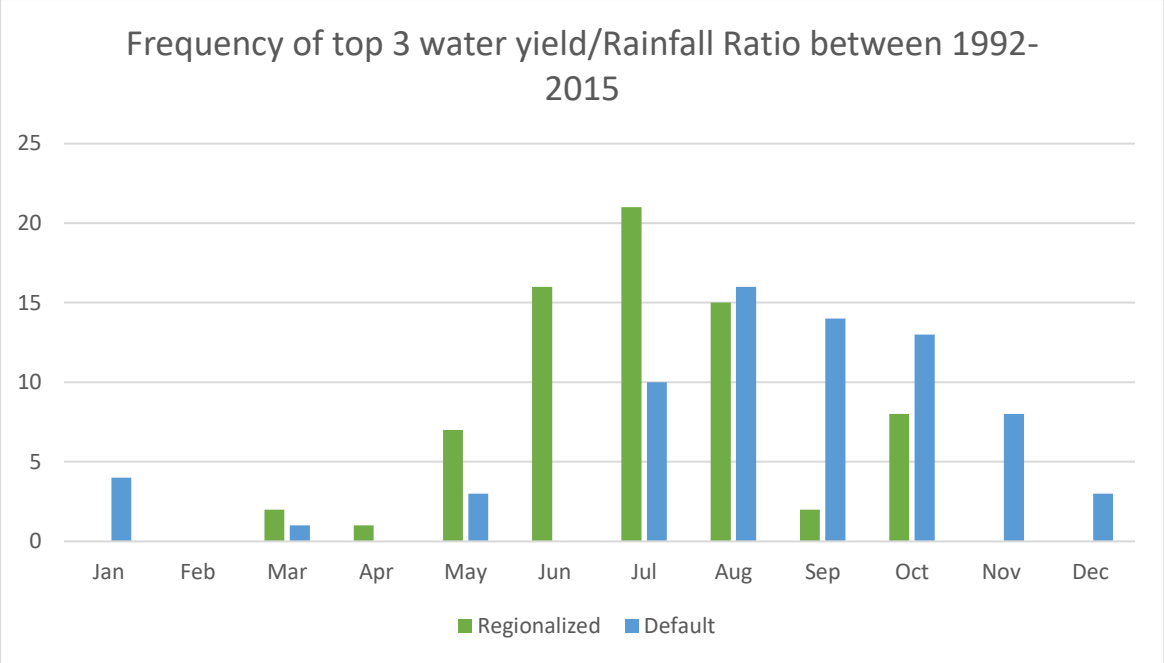

Figure 5-4 The frequency of the top three water yield to rainfall ratio under both parameter sets

5.2 Discussion:

CVC Calibration and Validation

As Figure 5-2 indicates, as CN2 decreases, there is a clear trend of improvement in model efficiency. This indicates that less runoff is generated than with the default setting. OV_N is the Manning's roughness for overland flow: this parameter describes the characteristics of the land surface that help to determine the velocity of overland flow. The value of this parameter increases when the roughness of the soil surface increases. The calibrated result suggests that the surface roughness is higher than the default value indicates. The decrease in both EPCO and ESCO in the calibrated parameter allows more plant water and evaporative water demand to be met from deeper in the soil profile (S.L. Neitsch, Arnold, Kiniry, & Williams, 2005). The high value of ALPHA_BF and low value of GW_DELAY indicates the catchment cannot hold much water, thereby generating rapid response to changes in recharge.

Although the SWAT calibration result for CVC is considered "satisfactory" there are many studies that were able to achieve much better modelling efficiency through calibration. For instance, Me et al. (2015a) achieved a R2 of 0.77, a NSE of 0.73, and a PBIAS of 7.8 during the calibration period and a R2 of 0.68, a NSE of 0.62 and a PBIAS of 8.8 during the validation period for simulation of discharge. Cao et al. (2006) achieved a R2 of 0.82 and a

NSE of 0.78 during calibration and a R2 of 0.75 and a NSE of 0.72 during the validation period for daily discharge simulation. (Behera & Panda, 2006)modelled a small catchment (9.73 km2) and achieved a R2 of 0.94 and a NSE of 0.88 during calibration and a R2 of 0.91 and a NSE of 0.85 during the validation period for daily runoff simulation. Meanwhile, there are many studies that resulted in worse daily R2 and NSE than the result obtained here. For example, the study conducted by Coffey, Workman, Taraba, and Fogle (2004) (daily stream flow with a R2=0.26, a NSE=0.09 during calibration) or (El-Nasr, Arnold, Feyen, & Berlamont, 2005) (daily stream flow with a R2= 0.45, a NSE= 0.39 during calibration and a R2=0.55, a NSE=0.60 during validation). Comparatively speaking, the calibrated model efficiency of this study is mediocre but acceptable. Many reasons might contribute to this apparent mediocre model efficiency.

One of the many reasons is that the climate data used for this study is mostly collected from VCS. VCS uses thin-plate smoothing spline modelling to spatially interpolate the latest observed data, and then the post interpolated data are adjusted to ensure the long term average annual rainfall is consistent with the independently derived climatology. (Cichota, Snow, & Tait, 2008) showed that the difference between recorded rainfall and VCS derived rainfall in New Zealand is generally acceptable with an index of agreement of over 0.8 for most sites. However, the VCS tends to under represent large rainfall events and over represent rainy days and these differences are larger in more complex terrain such as the CVC. The disparity of rainfall intensity between VCS and recorded rainfall may explain the high PBIAS during both the calibration and validation periods as the model systematically underestimates peak flow. Figure 5-5 Figure 5-6 plotted the observed daily flow, calibrated daily flow, and the nearest climate station for both the Mikimiki Bridge and Te Mara sites. Recorded rainfall data is used for the Te Mara site and VCS rainfall data is used for the Mikimiki Bridge site. As observed in the graphs, SWAT consistently underestimates the peak flow rate at both site. However, when comparing the Mikimiki site to the Te Mara site, the match between peak rainfall and peak streamflow is better for recorded rainfall than for VCS rainfall. In addition, the monthly average rainfall at the recorded rainfall site is higher than the monthly rainfall of the VCS surrounding it. There are 4 VCS within the CVC and only 1 recorded data site, and the weight of VCS in this model is able to reduce the model performance. When better data is available or monthly instead of daily simulation is

conducted, a better match between observed and simulated flow rate can be expected during both the calibration and validation periods.

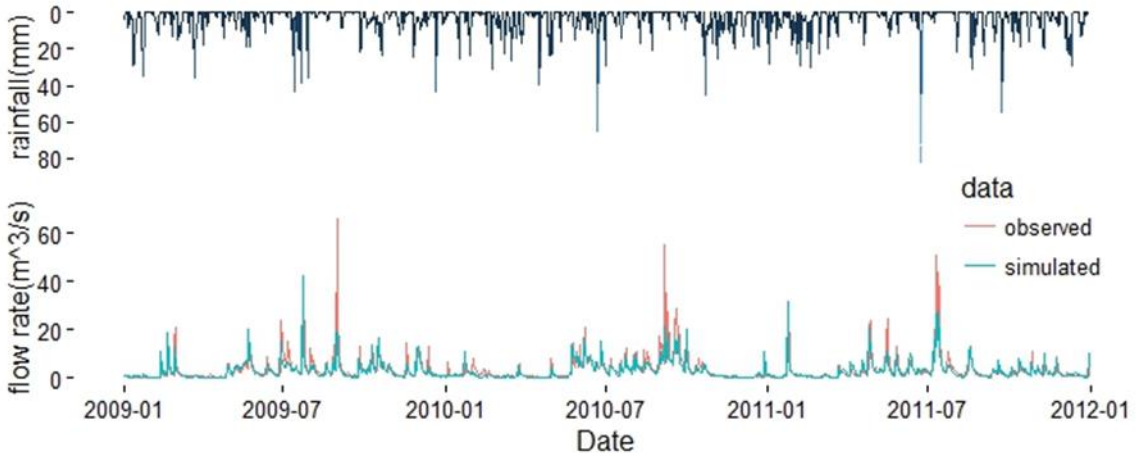

Figure 5-5 Simulated and observed flow rate during calibration period and the daily rainfall data for the period from the nearest climate record point at Mikimiki bridge.

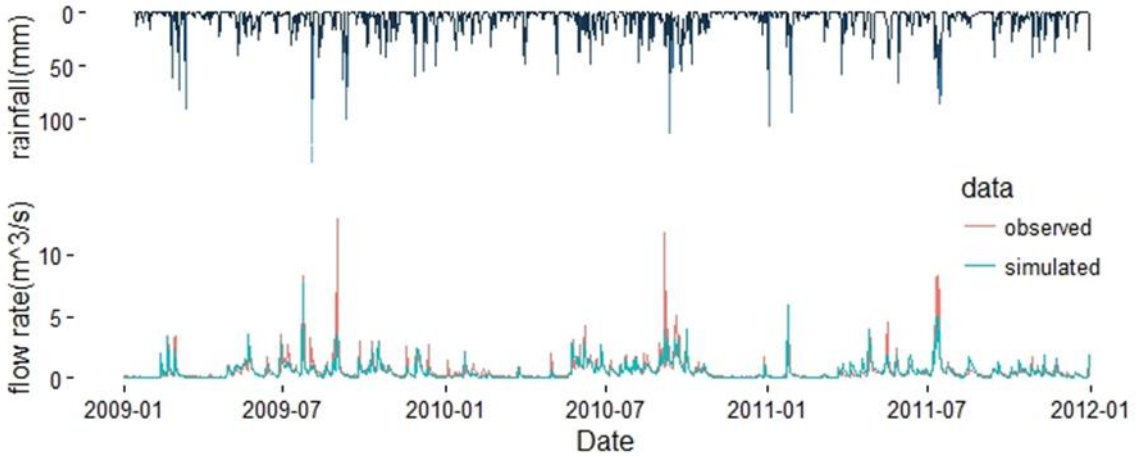

Figure 5-6 Simulated and observed flow rate during calibration period and the daily rainfall for the period from the nearest climate record point at Te Mara site.

Furthermore, as mentioned in the literature review, SWAT is a physical model and the modelling accuracy and efficiency depends on the availability of quality data. In the case of this study, the soil data is less than ideal: the spatial resolution of the soil data is low and some of the important soil parameters are derived from pedo-transfer functions. However, the pedo-transferred soil parameter is the bets option available to this study. Alternative options- such as deriving soil hydraulic parameters from auto-calibration using stream flow has been shown to be ineffective (Sun, Yao, Cao, Xu, & Yu, 2016)

Also, only three years of data were used for calibration and another three years were used for validation. Ideally, as Her and Chaubey (2015) point out, as the number of observation increase, the model performance improves as well.

Many calibrations separate the flow regime into base flow and quick flow before conducting calibration of the SWAT model. This is because the mechanisms controlling base flow and quick flow are different. Calibrating for base flow and quick flow separately can allow for a higher degree of calibration and better model efficiency. However, this process is very complex and the improvement in model efficiency may not be justifiable.

CVC Sensitivity Analysis

It is not surprising the CN2 is the most sensitive parameter of all since it controls the first step of water diversion (Arabi, Frankenberger, Engel, & Arnold, 2008; S. C. Brown et al., 2015; Cibin et al., 2010; Saha, Zeleke, & Hafeez, 2014; Ullrich & Volk, 2009). Numerous studies found that stream flow and surface runoff are very sensitive to CN2. For example, Conan, de Marsily, Bouraoui, and Bidoglio (2003) studied the effect of long term land use in the upper Gaudiana river basin and found that water yield and stream flow are sensitive to CN2, SOL_AWC, Ksoil (soil hydraulic conductivity) and aquifer properties. Ouessar et al. (2009) who modelled a water harvesting system with SWAT also found that the water balance part of the SWAT model is most sensitive to CN. Several studies found insensitive CN2 such as that of (Me et al., 2015a). and (Shen, Chen, & Chen, 2012) : this is because these two study used the Green and Ampt runoff calculation methodh instead of the CN curve number method.

GW_DELAY, RCHRGH_DP, and GWQMN, these three parameters which control ground water movement are all found to be sensitive. GW_DELAY is a parameter that reflects the time lag of soil water entry to the shallow aquifers. RCHRGH_DP which is the deep aquifer percolation fraction controls the proportion of ground water loss to deep aquifers. SWAT consider water lost to the deep aquifer as a system loss. GWQMN is the threshold value of shallow aquifer depth for return flow to occur. The sensitivity of stream flow to ground water parameters may be due to the high variation in seasonal rainfall, particularly the drier summer months when the evaporative demand is high (C. Zhang, Chu, & Fu, 2013).

LAT_TTIME is the lateral flow travel time. The relatively high sensitivity of this parameter can be attibuted to the controlling effect LAT_TTIME has on the quantity of lateral flow contributing to stream flow.

ESCO controls upward movement of water from lower soil horizons to upper soil horizons: as this value decreases, the model allows soil to extract more water to meet evaporative demand from lower in the soil profile. The high sensitivity to ESCO is contrasted with the result of Me et al.,(2015) who found low sensitivity to ESCO. Guse, Reusser, and Fohrer (2014) found that ESCO is less sensitive during high flow events. This high sensitivity to ESCO can be attributed to the low rainfall and increased evaporative demand during the summer period (Cibin et al., 2014). Although OV_N contributes to surface runoff, the sensitivity results show that stream flow is relatively insensitive to OV_N. Ullrich and Volk (2009) show that OV_N only has a moderate effect on the water balance components of the SWAT model but it can significantly affect organic nitrogen and sediment loading and therefore, this parameter plays a more important role in the modelling of nutrient and sediment loads. ALPHA_BF determines the rate of ground water returning to the stream; it is often found to be sensitive due to the effect it has on the base flow recession curve(Spruill, Workman, & Taraba, 2000). Many studies have found ALPHA_BF to be a sensitive parameter for stream flow prediction e.g. Saha et al. (2014) an S. C. Brown et al. (2015). However, this study found ALPHA_BF to be insensitive, echoing the finding of Van Griensven et al. (2006) whose result indicate ALPHA_BF is more important for sediment and nutrient estimation than it is for stream flow.

The surface lag runoff coefficient (SURLAG), which controls the fractions of total water allowed to enter the reach on any given day, was not found to be a sensitive parameter in this study. As SURLAG decrease in value more water is stored in off channel storage site. This lack of sensitivity, is contrary to the finding of Brown et al. (2015), where the surface lag runoff coefficient (SURLAG) was the most sensitive parameter for the Hopkins sub-catchment in south-eastern Australia The lack of sensitivity of SURLAG reflects the fact that the CVC is relatively small (77 km2) compared to the Hopkins sub-catchment (407 km2). Larger catchments are more sensitive to SURLAG due to the longer time of concentration (SWAT input/output). Me et al., (2015) also find low sensitivity in SURLAG and attributed the insensitivity of SURLAG to the short distance from runoff site to main channels and less potential for attenuation of surface runoff in off channel storage sites. Soil texture may also contribute to the low sensitivity of SURLAG.

Parameter Regionalization

The predicted water yield was reduced under the regionalized parameter set. This is most likely because the reduced ESCO in the regionalized parameter set allows the model to extract more water from lower in the profile to satisfy evaporative demand (SWAT user manual) , and therefore, in a dry year, a greater percentage of rainfall will be lost through evaporation compared to predictions made with the default parameter set. The reduction of W/R during the summer in the regionalized model reflects the higher evaporative demand in this season (Blöschl, 2013), The change in the composition of the water yield is the result of the new parameter set. A lower CN2 in the regionalization parameter set will reduce the quantity of surface runoff predicted as expected. The reduction in SURQ and increase in prediction for LATQ after parameterization indicates a relatively permeable surface layer and a relatively impermeable layer at shallow depth. The distribution of GWQ changed to better reflect the catchment reality. In this case, it shows that the ability of the WHC to store water is limited, and water entering the shallow ground water system is quickly returned to the stream, reflecting a system with rapid lateral flow. Nevertheless, there are great uncertainties regarding the partitioning of water within the small ungauged catchment. Further studies are needed to validate the calibration result.

(Lambert et al., 1985) conducted research on several small catchments with ephemeral flow similar to the WHC and showed that on average the runoff to rainfall ratio is around 45%. However, the “runoff” was collected behind a backfilled trench with polythene sheeting extended down to bed rock up to 3 meters deep. The purpose of the polythene sheeting was to force subsurface flow to the surface. This means that the “runoff” is actually water yield. This result is generally consistent with the output of the model developed here.

The fact that a polythene sheet was required to force all of the subsurface flow up to the surface in (Lambert et al., 1985) study, may mean that not all of the modelled water yield will naturally surface at the basin outlet. However, the relatively impervious upstream side of the embankment and the impervious core serves a similar function as the polythene sheet and allows more subsurface water to surface. Therefore, the actual water harvesting potential should be close to the SWAT modelled water yield.

Chapter 6 Results and Discussion on Water Balance

6.1 Results

Preliminary results, study of the water storage characteristics

The relationship between water surface height and the 2D and 3D surface area, as well as pond volume is given in Table 6-1. The 2D surface area represents the area of the water surface while the 3D area represents the area covered by water in the bottom of the pond. The earthwork volume estimated for each embankment height is listed in Table 6-2: due to superior design, the earthwork volume required for zoned embankments is much lower than for homogenous embankments. Table 6-3 describes the cost of constructing a zoned embankment with or without lining. As we can see here, lining the pond bottom increases the cost of construction dramatically, thus rendering construction of a lined dam uneconomical. Therefore, lining will not be considered in further analysis.

Plane height m	Water surface height m	2D m^2	3D m^2	Volume m^3
233	1	753	758	320
234	2	2348	2348	1607
235	3	5891	5918	5554
236	4	10914	10962	13794
237	5	17734	17811	27719
238	6	29808	29923	50739
239	7	47624	47793	89520
240	8	63004	63248	144635
241	9	75614	75960	214019
242	10	86429	86907	294639
243	11	95809	96445	385531
244	12	103215	104037	485040
245	13	109742	110766	590916
246	14	116527	117757	703632

Table 6-1 The height of the dam, and the potential water storage volume and the corresponding surface areas. 2D surface area is the surface area on the top of the water surface and 3D surface area is the surface area covered by water at the bottom of the dam

Embankment Height(m)	Earthwork Volume for Zoned Embankment (m^3)	Earthwork Volume for homogenous embankment (m^3)
14	58047	72622
13	47964	59982
12	39070	48833
11	31308	39100
10	24561	30647
9	18805	23434
8	13955	17359
7	9941	12335
6	6688	8269
5	4149	5107
4	2409	2917
3	1168	1382
2	401	458
1	34	38

Table 6-2 The volume of earthworks needed for two different types of embankments at each embankment height.

Emankment Height(m)	Cost of Zoned Embankment ($)	Cost of Lining ($)	Total Cost ($)
14	377306	2215334	2592640
13	311770	2080754	2392524
12	253955	1928908	2182863
11	203503	1738156	1941659
10	159652	1519208	1678860
9	122236	1264960	1387196
8	90710	955870	1046580
7	64623	598468	663091
6	43476	356226	399702
5	26971	219248	246219
4	15661	118376	134037
3	7593	46970	54564
2	2611	15164	17775

Table 6-3 The cost of constructing zoned embankments and lining at ponds with a range of given embankment heights. The total cost is the cost of constructing the embankment and the cost of lining combined.

WHC and command area water balance

The WHC and command area water balance depends on the definition of “harvestable” water. Several alternative scenarios are tested to study the ability of the WHC to supply irrigation water to the command area. The first scenario allows all of the water yield to be collected for irrigation purposes. SWAT-CUP was used to calculates and extract daily SURQ,

LATQ, and GWQ for each of the 19 sub-basins within the WHC using the regionalized parameter set. The results were exported to Microsoft excel and the total volume of SURQ, LATQ, and GWQ at the basin outlet were calculated. TLOSS, precipitation onto the stream surface, and ET from the stream surface is discounted due to its minimal effect on the overall modelling. Several scenarios were tested:

Scenario 1- "Harvestable" water = Water yield

When the first scenario is selected, the water that can be harvested by the earth dam is the water yield predicted by the regionalized SWAT model. As mentioned previously, the water yield is likely to be excessive because not all of GWQ and LATQ ends up in the stream Table details all the assumptions made in this water balance model: these values are chosen as the baseline scenario. This dam height, command area size in the baseline scenario were chosen because as shown in Table 6-5, this combination results in the optimal increase in farm pasture production while maintaining a 'very low' risk level.

Soil Properties		Dam Properties		Irrigation Scheduling	
FC	100mm/m	**Dam Height**	10 meters	**Trigger Deficit**	15 mm
PWP	50mm/m	**Maximum storage volume**	294639 m^3	**Irrigation Depth**	10 mm
AWC	50mm/m	**Seepage Rate**	0.2%/day	**Command Area Size**	40 ha
RAWC	25mm/m				

Table 6-4 Assumptions made for soil properties, dam properties, and irrigation scheduling made for Scenario 1

Under the assumptions stated above, irrigation failure was observed once: there was a 51 day period in 2008 when irrigation failed (Show in Figure 6-2). The cumulative frequency of annual pasture production under the baseline irrigation scenario and under no irrigation are depicted in Figure 6-1.

While keeping all other parameters fixed, various embankment heights and command areas were modelled to identify the increase in pasture production and the irrigation system failure rate. The results are shown in Table 6-5. An increase in embankment height up to 10 metres will decrease system failure for any given command area size. Increase in command area for any given embankment height will increase failure rate and reduce per unit additional pasture production.

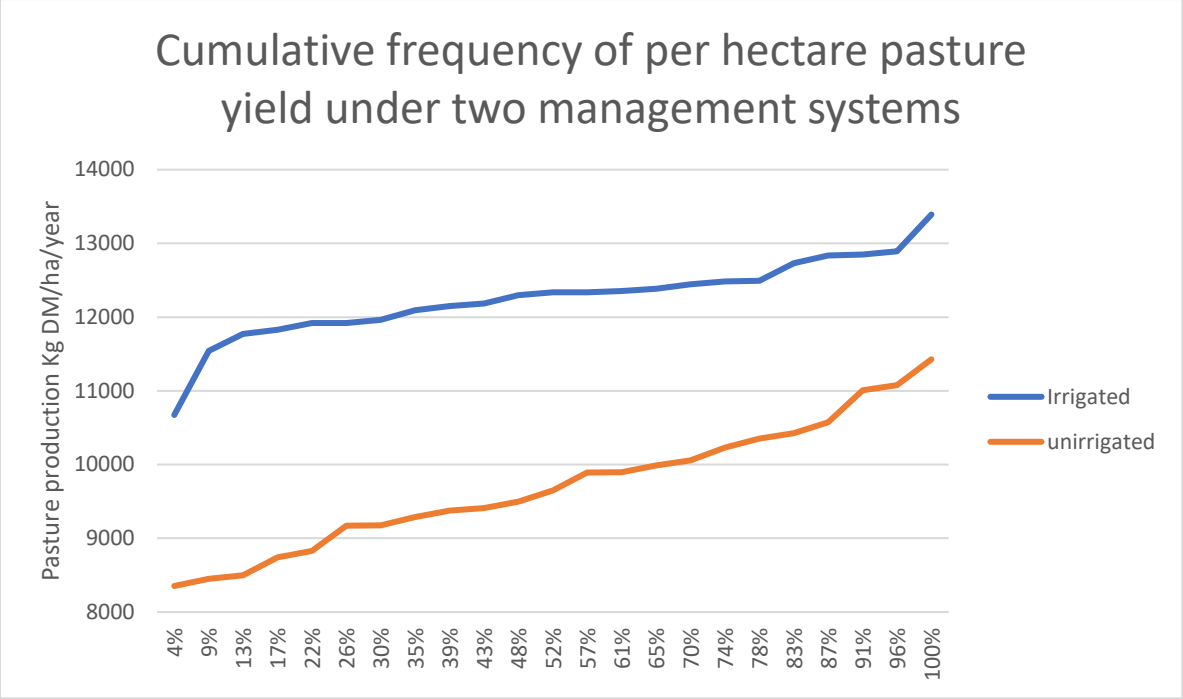

Figure 6-1 Cumulative frequency of annual per hectare pasture yield (kg/ha) under irrigated and unirrigated systems

Table 6-5 gives the increase in pasture production. For example, when the embankment is assumed to be 10 m tall, the maximum pasture production per unit is achieved when the command area is 35 ha. In order to maximize per unit production under irrigation, the command area ought to be kept under 40 hectare. However, this is not a viable option when the goal of the farm is to maximize profit. Therefore, Table 6-6 calculates the difference in total yield for the whole farm between irrigated and unirrigated land per year under various combination of embankment heights and command areas. The maximum increase in pasture production for embankment heights of 8 metres and above occurs when the command area is 85 ha.

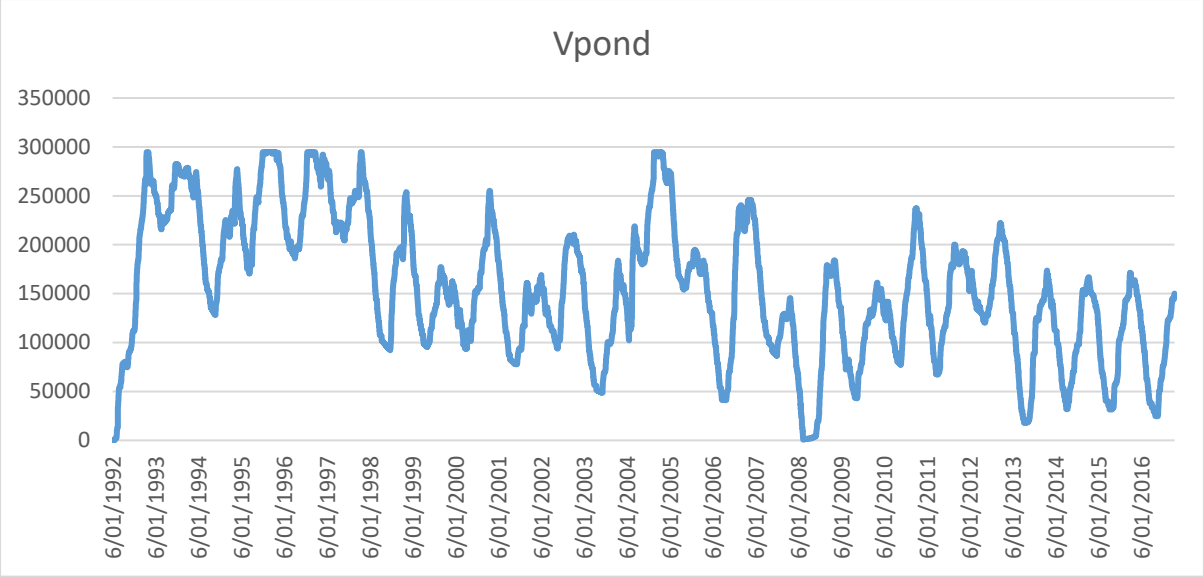

Figure 6-2 Volume of the pond during a typical simulation under the assumption made in table 6-4.

CA	7 metres			8 metres			9 metres			10 metres			11 metres			12 metres			13 metres		
	FRD	FRW	APG	FRD	FRW	APG	FRD	FRW	APG	FRD	FRW	APG	FRD	FRW	APG	FRD	FRW	APG	FRD	FRW	APG
15 ha	0%	0%	2555	0%	0%	2555	0%	0%	2555	0%	0%	2555	0%	0%	2555	0%	0%	2555	0%	0%	2555
20 ha	0%	0%	2554	0%	0%	2555	0%	0%	2555	0%	0%	2555	0%	0%	2555	0%	0%	2555	0%	0%	2555
25 ha	1%	2%	2504	0%	0%	2555	0%	0%	2555	0%	0%	2555	0%	0%	2555	0%	0%	2555	0%	0%	2555
30 ha	5%	6%	2359	1%	1%	2529	0%	0%	2555	0%	0%	2555	0%	0%	2555	0%	0%	2555	0%	0%	2555
35 ha	9%	12%	2188	2%	2%	2476	1%	1%	2536	0%	0%	2555	0%	0%	2555	0%	0%	2555	0%	0%	2555
40 ha	12%	16%	2035	3%	3%	2395	1%	1%	2499	1%	1%	2524	1%	1%	2525	1%	1%	2524	1%	1%	2525
45 ha	15%	19%	1873	5%	7%	2308	2%	2%	2462	2%	2%	2472	2%	2%	2478	2%	2%	2478	2%	2%	2478
50 ha	17%	21%	1703	7%	10%	2217	4%	5%	2382	3%	4%	2412	3%	3%	2415	3%	3%	2415	3%	3%	2415
55 ha	19%	25%	1593	11%	14%	2081	6%	8%	2280	6%	7%	2307	5%	7%	2309	5%	7%	2309	5%	7%	2309
60 ha	22%	27%	1447	13%	17%	1967	9%	12%	2173	8%	11%	2210	8%	11%	2210	8%	11%	2210	8%	11%	2210
65 ha	23%	28%	1355	15%	20%	1869	11%	14%	2029	10%	13%	2078	11%	13%	2077	11%	13%	2077	11%	13%	2077
70 ha	24%	30%	1258	17%	22%	1765	13%	17%	1926	13%	16%	1956	13%	16%	1958	13%	16%	1958	13%	16%	1958

Table 6-5 The failure rate and additional pasture growth at each command area and embankment height combination. FRD= failure rate by day. FRW= failure rate by week. APG= additional pasture growth (kg/ha) for each hectare. CA= Command area size

EH / CA	7 metres	8 metres	9 metres	10 metres	11 metres	12 metres	13 metres
15 ha	38329	38329	38329	38329	38329	38329	38329
20 ha	51075	51106	51106	51106	51106	51106	51105
25 ha	62597	63882	63882	63882	63882	63882	63882
30 ha	70781	75883	76658	76658.	76658	76658	76658
35 ha	76570	86650	88773	89434	89435	89435	89435
40 ha	81396	95781	99959	100941	100992	100992	100992
45 ha	84265	103533	110771	111227	111508	111508	111508
50 ha	85151	110827	119114	120596	120728	120728	120728
55 ha	87615	114444	125426	126877	126997	126997	126997
60 ha	86809	118027	130402	132616	132625	132625	132625
65 ha	88084	121506	131905	135055	135031	135031	135031
70 ha	88074	123546	134834	136900	137062	137062	137062
75 ha	87218	123112	136345	138955	138955	138955	138955
80 ha	84983	123764	138503	141646	141646	141646	141646
85 ha	83715	123772	139957	141676	141676	141676	141676
90 ha	82627	121941	137758	140622	140622	140622	140622
95 ha	80460	122677	138565	141201	141201	141201	141201
100 ha	78056	120440	137126	140785	140785	140785	140785
105 ha	79712	118619	135096	138171	138171	138171	138171
110 ha	77135	117604	133348	136494	136494	136494	136494
115 ha	77561	114355	132167	136487	136487	136487	136487

Table 6-6 Additional pasture growth for the whole farm (kg/year). CA= command area size. EH= Embankment height

The maximum increase in pasture production to the farm occurs when the command area size is equal to 85 ha and the dam height is above 10 meters. An average of up to 141676 kg of additional dry matter per year can be produced under irrigation for the farm compared to a dry land system. This is larger than the low system failure scenario when 40 ha of land is under irrigation. However, when comparing the two command area scenario, it is important to acknowledge the difference in production size because an 85 ha farm area will produce more pasture than a 40 ha area when everything else is equal. Hence when comparing total impact of irrigation on either scenario, it is important to control for the production area. Therefore, the following comparison between two command area regimes, both of the same size (85 ha). A) the sum of pasture production on a 40 ha scenario and pasture production on 45 ha unirrigated land, and B) pasture production on 85 hectare scenario. Figure 6-3 illustrates the difference in pasture dry matter production on 85 ha under system A and system B. On average, the 85 hectare irrigated scenario produce 41661 kg more pasture per year compared to the 40 ha irrigated 45 ha dry land scenario, which equates to a difference of 490 kg/ha/year.

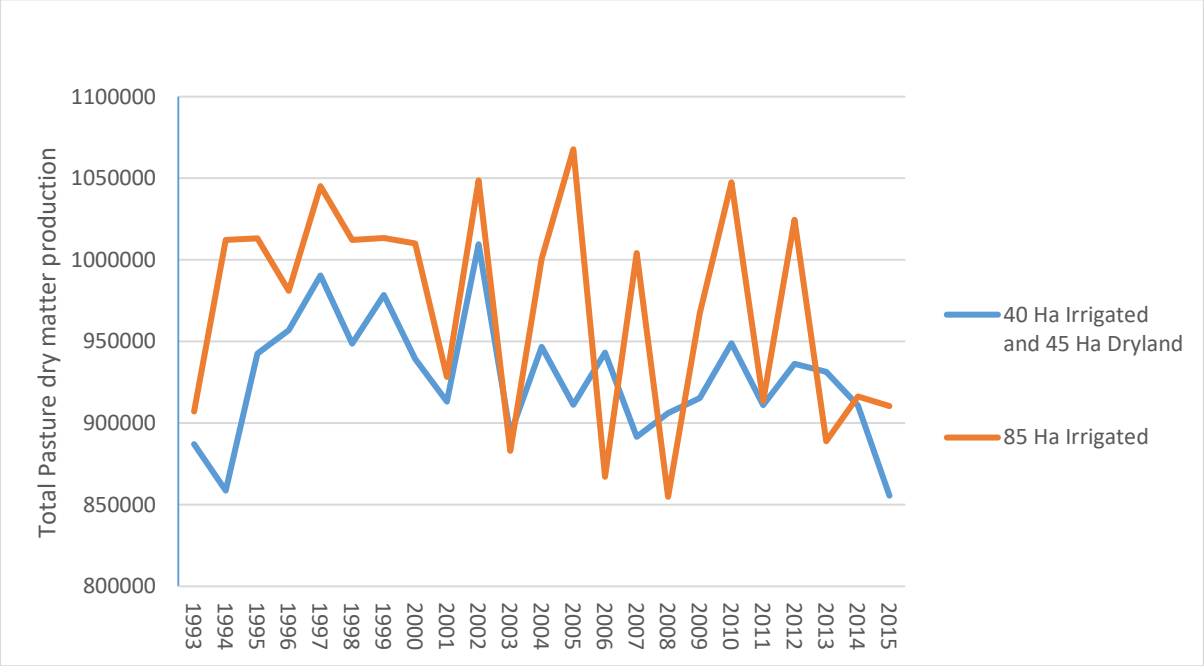

Figure 6-3 Total dry matter production in case study 1 under two circumstances. The first scenario irrigates 40 ha of land while leaving 45 unirrigated. The second one accepts risks and irrigates 85 ha of land.

Although irrigating 85 ha produces the highest average increase in pasture production on the whole farm basis. The system failure rate is very high (irrigation demand for 23% of the weeks during irrigation season will not be met) and may be considered unacceptable.

Irrigation under scenario 1 increases pasture production on the farm. The optimal dam height for the WHC assuming all of the water yield is harvested is 10 meters and irrigating 85 hectare allows the greatest average increase in dry matter production. Irrigating at 40 ha reduce will result in lower failure rate but on average 41661 kg less dry matter produce per year.

Scenario 2- Only SURQ were harvested

In scenario 2 it is assumed that only the surface runoff portion of the total water yield can be harvested and stored for irrigation purposes. This scenario represents the most conservative estimation of the water harvesting potential of the WHC and this scenario is likely to be an underrepresentation of the total water harvested.

The basic assumptions made in scenario 1 are kept constant such as the soil properties, seepage rate, irrigation trigger deficit depth. Some of the assumptions made for the analysis are stated here on Table 6-7. Various combinations of dam size and command area are tested in Table 6-8 . For a given command area size, the increase in dam height decrease the failure rate and increase per unit pasture yield. Meanwhile, for a given dam height, increase in command area size resulted in a higher failure rate and lower per unit (ha) production rate.

Less water is assumed to be “harvestable” in this scenario and this resulted in a reduction in the water volume in the dam. Therefore. The optimal dam height and command area size are reduced accordingly. The maximum dam height necessary for this scenario is 7 metres i.e. there is no production benefit from increasing the dam size to above 7 metres.

A system with a 7 metres high dam which is irrigating 10 ha of command area will have a reasonable failure rate while producing a reasonable increase in pasture production.

The difference in total yield for the whole farm between irrigated and unirrigated land per year is highest when the dam height is at 7 meters and the catchment size is at 20 ha (as seen in Table 6-9. However, a WHC with 6 metres high dam irrigating 20 ha of land can achieve a similar production gain with a similar failure rate. The marginal benefit from the additional metre of dam height maybe insufficient to justify the extra cost.

Even under the worst case scenario where the WHC is only able to capture and store runoff, the WHC is able to provide sufficient water to increase, on average, whole farm pasture dry

matter production by up to 22473 kg/year assuming the dam height is 7 metres and 20 ha of land is irrigated.

Soil Properties		Dam Properties		Irrigation Scheduling	
FC	100mm/m	**Dam Height**	N/A	**Trigger Deficit**	15 mm
PWP	50mm/m	**Maximum storage volume**	N/A	**Irrigation Depth**	10 mm
AWC	50mm/m	**Seepage Rate**	0.2%/day	**Command Area Size**	N/A
RAWC	25mm/m				

Table 6-7 Assumptions made for scenario 2

EH / CA	2 metres			3 metres			4 metres			5 metres			6 metres			7 metres			8 metres		
	FRD	FRW	APG	FRD	FRW	APG	FRD	FRW	APG	FRD	FRW	APG	FRD	FRW	APG	FRD	FRW	APG	FRD	FRW	APG
5 ha	33%	43%	675	19%	24%	1548	4%	4%	2344	1%	1%	2524	0%	0%	2555	0%	0%	2555	0%	0%	2555
10 ha	40%	52%	340	31%	40%	787	21%	25%	1471	11%	14%	1978	7%	9%	2176	6%	8%	2217	6%	8%	2217
15 ha	42%	55%	214	37%	46%	467	29%	36%	954	22%	28%	1404	18%	22%	1581	17%	21%	1645	17%	21%	1645
20 ha	46%	60%	0	39%	50%	332	33%	41%	639	28%	36%	1020	25%	32%	1216	25%	31%	1248	25%	31%	1248
25 ha	46%	60%	0	41%	52%	276	36%	46%	482	31%	40%	767	30%	38%	942	29%	36%	994	29%	36%	994
30 ha	46%	60%	0	42%	54%	218	37%	48%	392	34%	43%	595	33%	41%	716	32%	40%	768	32%	40%	768
35 ha	46%	60%	0	43%	55%	173	39%	49%	340	36%	45%	480	35%	44%	592	35%	44%	628	35%	44%	628
40 ha	46%	60%	0	43%	55%	159	40%	51%	281	37%	47%	388	36%	45%	493	36%	45%	513	36%	45%	513
45 ha	46%	60%	0	43%	56%	141	41%	53%	234	39%	49%	336	37%	47%	443	37%	47%	446	37%	47%	446
50 ha	46%	60%	0	44%	57%	98	41%	52%	216	39%	50%	300	38%	48%	372	38%	48%	357	38%	48%	357

Table 6-8 The failure rate and additional pasture growth at each command area and embankment height combination. FRD= Failure rate by day FRW= failure rate by week APG= additional pasture growth for each hectare (kKg/ha) CA= command area size, EH= Embankment height

CA \ EH	2 metres	3 metres	4 metres	5 metres	6 metres	7 metres	8 metres
5 ha	3375	7741	11722	12618	12776	12776	12776
10 ha	3395	7871	14712	19775	21757	22168	22168
15 ha	3205	7007	14316	21054	23717	24673	24673
20 ha	0	6633	12780	20402	24318	24952	24952
25 ha	0	6889	12073	19169	23560	24854	24854
30 ha	0	6530	11771	17845	21482	23046	23046
35 ha	0	6069	10834	16791	20735	21986	21986
40 ha	0	6351	11240	15535	19715	20505	20505

Table 6-9 Additional pasture growth (kg) for the whole farm at different combination of dam size and embankment height CA= command area, EH= embankment height

Scenario 3 - 80% Water yield

Scenario 3 assumes the WHC has the ability to harvest 80% of the water yield predicted by SWAT model. This assumption provides a conservative estimation of the water harvesting ability of the model. It provides a reasonable estimation of the total "harvestable water", or a middle ground between the extremes of scenario 1 and scenario 2.

Scenario 3 used the same assumptions for command area and irrigation scheduling stated in Table 6-4. As expected, under this scenario, less water can be harvested and stored in the WHC for irrigation purposes later in the year compared to scenario 1 and therefore the optimal dam height and command area size and the maximum additional pasture produced are smaller than those predicted for scenario 1. Here, the maximum increase in pasture production for the whole farm occurs when the dam height is equivalent to 10 metres and 75 ha of land are irrigated. However, a dam height of 9 meters and command area of 75 ha can produce only slightly less additional pasture. The maximum increase in pasture production is 114902 kg DM per year. This value is 19% less than the 141676 kg DM per year increase for the whole farm predicted for by scenario 1.

Alternatively, a 10 metres high dam and a 35 ha command area allows the optimal increase in farm pasture production while maintaining risk a very low level.

EH / CA	7 metres			8 metres			9 metres			10 metres			11 metres			12 metres			13 metres			14 metres		
	FRD	FRW	APG	FRD	FRW	APG	FRD	FRW	APG	FRD	FRW	APG	FRD	FRW	APG	FRD	FRW	APG	FRD	FRW	APG	FRD	FRW	APG
15 ha	0%	0%	2555	0%	0%	2555	0%	0%	2555	0%	0%	2555	0%	0%	2555	0%	0%	2555	0%	0%	2555	0%	0%	2555
20 ha	0%	1%	2541	0%	0%	2555	0%	0%	2555	0%	0%	2555	0%	0%	2555	0%	0%	2555	0%	0%	2555	0%	0%	2555
25 ha	2%	3%	2465	0%	1%	2546	0%	0%	2555	0%	0%	2555	0%	0%	2555	0%	0%	2555	0%	0%	2555	0%	0%	2555
30 ha	6%	7%	2306	1%	1%	2499	0%	1%	2541	0%	1%	2551	0%	1%	2551	0%	1%	2551	0%	1%	2551	0%	1%	2551
35 ha	10%	13%	2140	2%	3%	2440	1%	1%	2493	1%	1%	2490	1%	1%	2499	1%	1%	2499	1%	1%	2499	1%	1%	2499
40 ha	13%	17%	1979	4%	6%	2368	2%	3%	2418	2%	3%	2421	2%	3%	2421	2%	3%	2421	2%	3%	2421	2%	3%	2421
45 ha	16%	20%	1819	8%	10%	2232	6%	8%	2289	6%	8%	2310	6%	8%	2310	6%	8%	2310	6%	8%	2310	6%	8%	2310
50 ha	18%	23%	1655	10%	14%	2083	9%	12%	2160	9%	12%	2172	9%	12%	2172	9%	12%	2172	9%	12%	2172	9%	12%	2172
55 ha	21%	25%	1498	14%	18%	1942	12%	15%	1997	12%	15%	2006	12%	15%	2006	12%	15%	2006	12%	15%	2006	12%	15%	2006
60 ha	23%	28%	1401	16%	21%	1809	15%	19%	1868	15%	19%	1861	15%	19%	1861	15%	19%	1861	15%	19%	1861	15%	19%	1861
65 ha	24%	30%	1295	19%	23%	1699	17%	21%	1764	17%	20%	1764	17%	20%	1764	17%	20%	1764	17%	20%	1764	17%	20%	1764
70 ha	26%	32%	1194	21%	26%	1574	19%	24%	1637	19%	23%	1632	19%	23%	1632	19%	23%	1632	19%	23%	1632	19%	23%	1632
75 ha	27%	33%	1067	22%	28%	1458	21%	26%	1531	21%	26%	1532	21%	26%	1532	21%	26%	1532	21%	26%	1532	21%	26%	1532
80 ha	29%	35%	973	23%	29%	1344	22%	27%	1419	22%	28%	1429	22%	28%	1429	22%	28%	1429	22%	28%	1429	22%	28%	1429
85 ha	30%	36%	908	25%	31%	1259	24%	30%	1316	24%	30%	1323	24%	30%	1323	24%	30%	1323	24%	30%	1322	24%	30%	1323

Table 6-10 The failure rate and additional pasture growth at each command area and embankment height combination. FRD= Failure rate by day FRW= failure rate by week APG= additional pasture growth for each hectare (Kg/ah) CA= command area size, EH= Embankment height

CA \ EH	7 metres	8 metres	9 metres	10 metres	11 metres
15 ha	38329	38329	38329	38329	38329
20 ha	50829	51106	51106	51106	51106
25 ha	61615	63659	63882	63882	63882
30 ha	69184	74969	76244	76517	76517
35 ha	74889	85414	87241	87464	87464
40 ha	79178	94703	96731	96826	96826
45 ha	81838	100456	102987	103952	103952
50 ha	82743	104139	108017	108594	108594
55 ha	82395	106813	109852	110343	110343
60 ha	84066	108546	112049	111681	111681
65 ha	84159	110413	114631	114645	114645
70 ha	83579	110158	114620	114242	114242
75 ha	80043	109360	114822	114902	114902
80 ha	77824	107519	113504	114284	114284
85 ha	77197	107036	111885	112446	112446

Table 6-11 Additional pasture growth for the whole farm (kg) at different combination of dam size and embankment height CA= command area, EH= embankment height

Scenario 3 offers a compromise between Scenario 1 which assumes all water yield is harvested and stored and Scenario 3 which only allows the harvest and storage of surface runoff. Scenario 3 shows that irrigating 35 ha when the embankment height is 10 metres maximizes additional pasture growth while maintaining the daily failure rate at 1%. While irrigating 75 ha with an embankment height of 10 metres maximizes the total additional pasture growth without considering the system failure rate.

Economic Analysis

The economic performance of only scenarios 1 and 3 were analysed because scenario 2 is unlikely to be a realistic estimation of catchment performance. Table 6-14 to Table 6-17 give the cost per kilogram dry matter produced by irrigation for different combinations of command area size and embankment height. The opportunity cost of capital is assumed to be 8% or 6%. When the opportunity cost of capital is set at 8% the lowest cost per kg DM is observed when the command area is 45 ha and the dam height is at 9 metres in both scenario 1 and scenario 3 as seen in Table 6-14 and Table 6-16.

Capital Expenses				
	Dam Cost		$122,235.91	NZD
	K-Line Irrigation Material		$ 46,250.00	NZD
	K-line Installation		$ 9,000.00	NZD
	Powerline		$ 5,000.00	
	Pump		$ 7,650.00	NZD
	Consent Cost		$ 24,300.00	NZD
		Total	$214,435.91	NZD
		Per Ha	$ 4,765.24	NZD
Annual Cost				
	Long term Opportunity cost of Capital		$ 17,154.87	NZD
	Depreciation Cost		$ 4,361.23	NZD
	R&M K-Line		$ 1,350.00	NZD
	R&M Dam		$ 6,111.80	NZD
	Running Cost		$ 7,200.00	NZD
	Electricty		$ 8,000.00	NZD
	Insurance		$ 500.00	NZD
		Total	$ 44,677.90	NZD

Figure 6-4 Screenshot of the calculation for annual cost. Opportunity cost for capital is assumed to be 8%, embankment height is set to be 9 meters with a command area of 45 ha.

Figure 6-4 shows a screenshot of the financial analysis spreadsheet. The opportunity cost of capital represents 38% of the total annual cost. Due to the recent low interest rate, the opportunity cost of the capital is likely to be lower. When 6% opportunity cost for capital was assumed, the cost per kilogram dry matter produced under scenario 1 dropped from 43 c/kg to 39 c/kg. Similarly, reducing the cost of capital in scenario 3 sees a decrease cost per kg dry matter from 44 c/kg to 40 c/kg.

Cost per cubic meter of water under various combinations of embankment height and command area for scenario 1 are listed in in Table 6-12. Similarly, the cost per cubic meter of water under various combinations of embankment height and command area for scenario 3 are presented in Table 6-13. Unlike large scale schemes where farmers are charged by the unit, farmers with on-farm harvesting systems have complete control over the irrigation practices. Furthermore, the more water a farmer is able to use, the lower the per unit cost for water. However, increases in the command area increases the risk of system failure where the water harvesting scheme is unable to provide sufficient water to meet plant water needs during critical times. When a minimum reliability requirement of 95% is imposed, the minimum per unit cost of water is observed for scenario 1 when an

embankment height of 9 metres and a command area of 50 ha. The minimum per unit cost observed for scenario 3 is observed when the embankment height is 9 metres and the command area is 40 ha. The cost per cubic meter of water delivered with pressure and 95% reliability therefore costs either 19 cents or 20 cents depending on the scenario chosen.

CA \ EH	9 metres	10 metres	11 metres	12 metres
15 ha	$ 0.50	$ 0.60	$ 0.73	$ 0.87
20 ha	$ 0.39	$ 0.46	$ 0.56	$ 0.67
25 ha	$ 0.32	$ 0.38	$ 0.46	$ 0.55
30 ha	$ 0.28	$ 0.33	$ 0.39	$ 0.46
35 ha	$ 0.25	$ 0.29	$ 0.34	$ 0.41
40 ha	$ 0.22	$ 0.26	$ 0.31	$ 0.36
45 ha	$ 0.20	$ 0.24	$ 0.28	$ 0.33
50 ha	$ 0.19	$ 0.22	$ 0.26	$ 0.30
55 ha	$ 0.18	$ 0.20	$ 0.24	$ 0.28
60 ha	$ 0.17	$ 0.19	$ 0.22	$ 0.26

Table 6-12 Cost per cubic meter of water under different combinations of embankment height and command area size for scenario 1 when the opportunity cost for capital is 8%

CA \ EH	9 metres	10 metres	11 metres	12 metres
15 ha	$ 0.49	$ 0.61	$ 0.74	$ 0.89
20 ha	$ 0.38	$ 0.46	$ 0.56	$ 0.67
25 ha	$ 0.30	$ 0.37	$ 0.45	$ 0.54
30 ha	$ 0.25	$ 0.31	$ 0.37	$ 0.45
35 ha	$ 0.22	$ 0.27	$ 0.33	$ 0.39
40 ha	$ 0.20	$ 0.24	$ 0.30	$ 0.35
45 ha	$ 0.19	$ 0.23	$ 0.28	$ 0.33
50 ha	$ 0.18	$ 0.22	$ 0.27	$ 0.32
55 ha	$ 0.18	$ 0.22	$ 0.26	$ 0.31
60 ha	$ 0.17	$ 0.21	$ 0.26	$ 0.31

Table 6-13 Cost per cubic meter of water under different combination of embankment height and command area size for scenario 3 when the opportunity cost for capital is 8%

Embankment Height	Command Area size											
	15 ha	20 ha	25 ha	30 ha	35 ha	40 ha	45 ha	50 ha	55 ha	60 ha	65 ha	70 ha
12 meters	$ 1.27	$ 1.00	$ 0.84	$ 0.73	$ 0.66	$ 0.61	$ 0.57	$ 0.55	$ 0.54	$ 0.54	$ 0.55	$ 0.56
11 meters	$ 1.08	$ 0.86	$ 0.73	$ 0.64	$ 0.58	$ 0.53	$ 0.51	$ 0.49	$ 0.48	$ 0.48	$ 0.49	$ 0.50
10 meters	$ 0.92	$ 0.74	$ 0.63	$ 0.56	$ 0.51	$ 0.48	$ 0.45	$ 0.44	$ 0.44	$ 0.44	$ 0.46	$ 0.46
9 meters	$ 0.78	$ 0.63	$ 0.54	$ 0.49	$ 0.46	$ 0.44	$ 0.43	$ 0.43	$ 0.43	$ 0.44	$ 0.45	$ 0.46

Table 6-14 Cost of additional per kg pasture under each corresponding and command area size under scenario 1 assuming 8% opportunity cost for capital

Embankment height	Command Area size											
	15 ha	20 ha	25 ha	30 ha	35 ha	40 ha	45 ha	50 ha	55 ha	60 ha	65 ha	70 ha
12 meters	$ 1.11	$ 0.88	$ 0.74	$ 0.65	$ 0.58	$ 0.54	$ 0.51	$ 0.49	$ 0.48	$ 0.48	$ 0.49	$ 0.50
11 meters	$ 0.95	$ 0.76	$ 0.64	$ 0.57	$ 0.51	$ 0.48	$ 0.45	$ 0.44	$ 0.44	$ 0.43	$ 0.44	$ 0.46
10 meters	$ 0.80	$ 0.65	$ 0.56	$ 0.49	$ 0.45	$ 0.43	$ 0.41	$ 0.40	$ 0.40	$ 0.40	$ 0.41	$ 0.42
9 meters	$ 0.68	$ 0.56	$ 0.48	$ 0.44	$ 0.41	$ 0.40	$ 0.39	$ 0.39	$ 0.39	$ 0.40	$ 0.41	$ 0.42

Table 6-15 Cost of additional per kg pasture under each corresponding and command area size under scenario 1 assuming 6% opportunity cost for capital

	Command Area Size										
Embankment height	**15 ha**	**20 ha**	**25 ha**	**30 ha**	**35 ha**	**40 ha**	**45 ha**	**50 ha**	**55 ha**	**60 ha**	**65 ha**	**70 ha**
12 meters	$ 1.27	$ 1.00	$ 0.84	$ 0.73	$ 0.67	$ 0.63	$ 0.61	$ 0.61	$ 0.62	$ 0.64	$ 0.64	$ 0.67
11 meters	$ 1.08	$ 0.86	$ 0.73	$ 0.64	$ 0.59	$ 0.56	$ 0.54	$ 0.54	$ 0.56	$ 0.57	$ 0.58	$ 0.60
10 meters	$ 0.92	$ 0.74	$ 0.63	$ 0.56	$ 0.52	$ 0.49	$ 0.49	$ 0.49	$ 0.50	$ 0.51	$ 0.52	$ 0.55
9 meters	$ 0.78	$ 0.63	$ 0.55	$ 0.50	$ 0.46	$ 0.45	$ 0.44	$ 0.45	$ 0.46	$ 0.48	$ 0.49	$ 0.52

Table 6-16 Cost of additional per kg pasture under each corresponding and command area size under scenario 3 assuming 8% opportunity cost for capital

	Command Area Sze										
Embankment height	**15 ha**	**20 ha**	**25 ha**	**30 ha**	**35 ha**	**40 ha**	**45 ha**	**50 ha**	**55 ha**	**60 ha**	**65 ha**	**70 ha**
12 meters	$ 1.11	$ 0.88	$ 0.74	$ 0.65	$ 0.59	$ 0.56	$ 0.55	$ 0.54	$ 0.56	$ 0.57	$ 0.58	$ 0.60
11 meters	$ 0.95	$ 0.76	$ 0.64	$ 0.57	$ 0.52	$ 0.50	$ 0.49	$ 0.49	$ 0.50	$ 0.52	$ 0.52	$ 0.55
10 meters	$ 0.80	$ 0.65	$ 0.56	$ 0.50	$ 0.46	$ 0.44	$ 0.44	$ 0.44	$ 0.45	$ 0.47	$ 0.48	$ 0.50
9 meters	$ 0.68	$ 0.56	$ 0.49	$ 0.44	$ 0.42	$ 0.40	$ 0.40	$ 0.41	$ 0.42	$ 0.44	$ 0.45	$ 0.47

Table 6-17 17 Cost of additional per kg pasture under each corresponding and command area size under scenario 3 assuming 6% opportunity cost for capital

6.2 Discussion

Scenario 1

Before analysing the scenario results, it is important to first examine the rainfall data from the study period. As seen in Figure 6-5, annual rainfall from 1992- 2015 varies, the period average is 1347 mm/year, similar to the 30 years long term average for the region. Within the study period, the rainfall variation is large. 2005 and 2007 are the driest years with

annual precipitation equal to 914 mm/ year. 1992 and 2004 are two of the wettest years with precipitation reaching 1800 mm/ year and 1909 mm/ year, respectively. There has been an observed trend of decrease in annual rainfall from 1992 to 2015 (Fig 6.5). However, such observation may not be statistically meaningful.

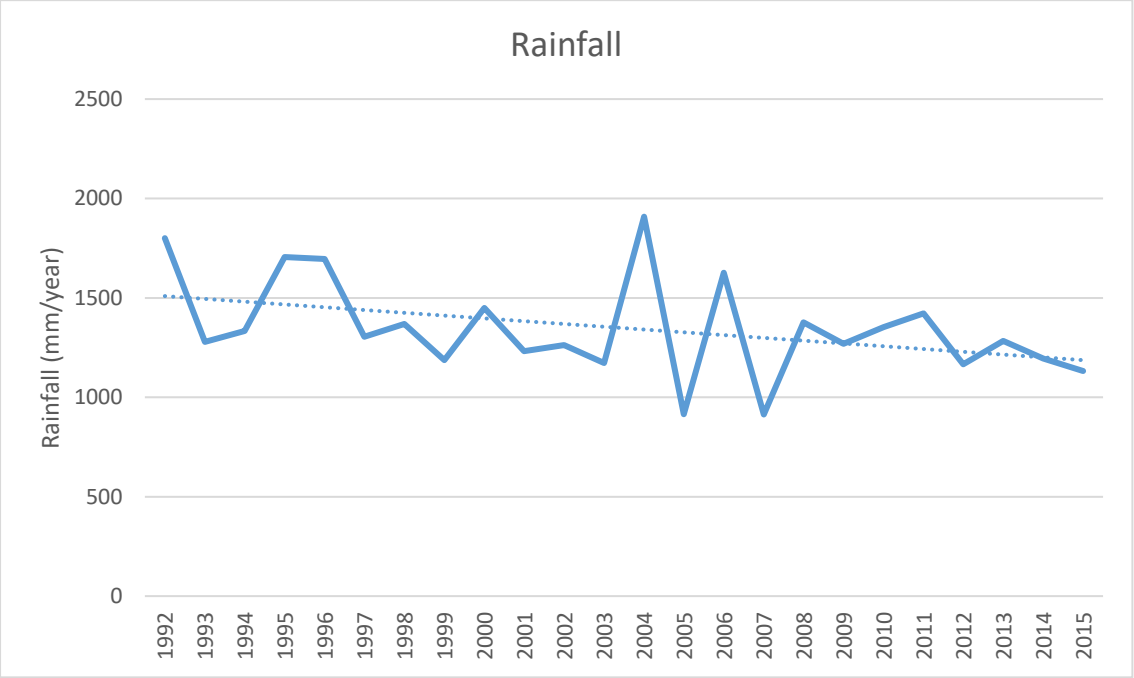

Figure 6-5 Yearly rainfall in the command area between 1992-2015

Irrigating with a low failure rate system increases per unit pasture dry matter production: such increases are more obvious at the low end of the cumulative frequency curve demonstrating the ability of such an irrigation system to relieve drought when rainfall is particularly low. Under the low failure rate system, the only failure occurred in 2008 which lasted for 51 days with temporary relief in March. Low pond storage was to blame for the failure and to see the beginnings of this failure, one needs to look back three years. 2005 was a particularly dry year with high irrigation demand. By the beginning of 2006, the pond level was very low. Despite higher than average rainfall in 2006, the pond was not recharged to its maximum water storage potential. The following year of 2007 was also particularly dry and the pond water level was drawn to an even lower level. The winter of 2007 was slightly dryer than average and the water harvested during this period were insufficient to help the pond fully recover from the series of lower levels begun in 2005. The combination of the above factors caused the system failure in 2008.

From Table 6-5, it is noted that embankment heights above 11 meters have no effect on system failure rate or per unit additional pasture production. This is because at embankment heights of 11 meters or above, the system becomes water yield limited and the embankment height no longer affects the irrigation system. Therefore, the maximum embankment height should be set at 10 metres.

The maximum increase in pasture production to the farm occurs when the command area size is equal to 85 ha. However, the reliability of the water harvesting scheme to supply water to an 85 ha command area is very low. High failure rate results in high year to year variability in pasture production. Table 6-18 shows the mean biomass production per hectare under stress-free (perfect irrigation), unirrigated, and irrigated conditions and the standard deviation between 1992 and 2015 assuming the embankment height to be 10 meters. Figure 6-3 also shows that the 40 ha irrigation plus 45 unirrigated land scenario is less productive, but the range in pasture yield are smaller than the 85 ha irrigation scenario. The 40 irrigated hectare plus 45 unirrigated hectare is more productive during the summer on a per hectare basis, as shown in Figure 6-7: the 40 ha irrigation regime produces more pasture per unit of irrigated land than the 85 ha irrigation system during the summer. On the whole farm basis, the 40 hectare irrigated plus 45 hectare unirrigated scenario produce more pasture in March, April and May compared to the scenario where the whole 85 ha were irrigated as shown in Figure 6-6.

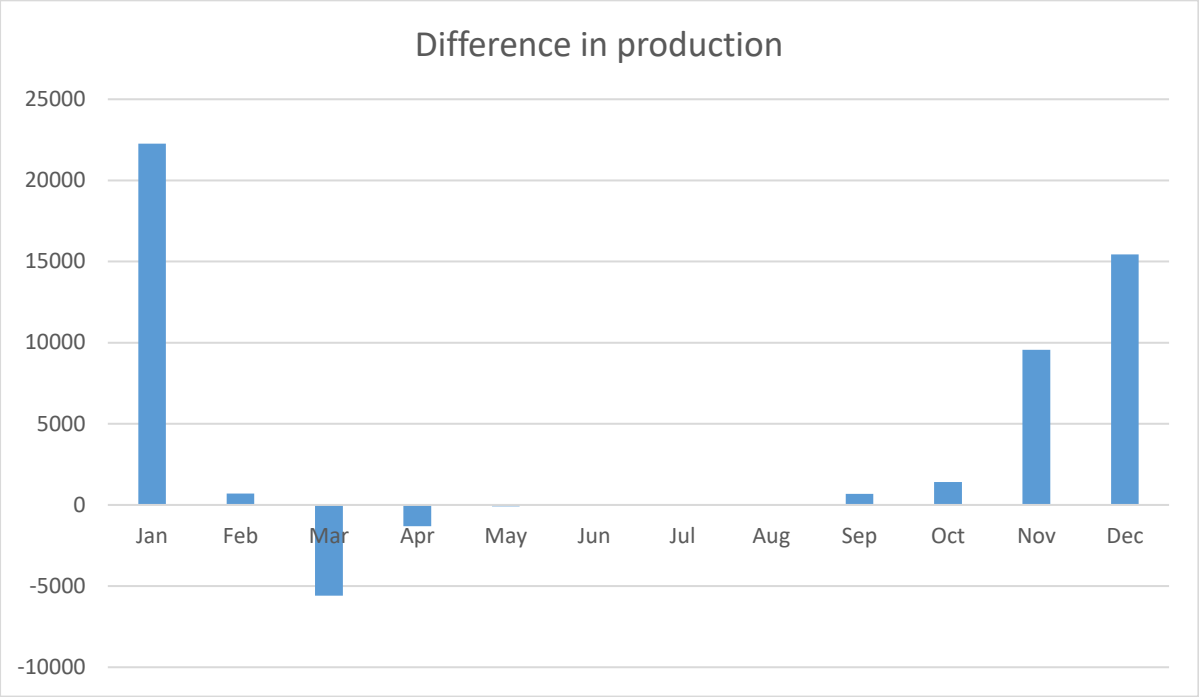

Figure 6-6 Plotted the difference in average total biomass production between the 85 ha irrigated and 40 ha irrigated plus 45 ha dryland system. On a whole farm basis, irrigating 85 ha of land resulted in higher production in January, February, September, October, November, and December, while the 40 ha irrigated + 45 ha dryland system produce more biomass in March and April.

However, the low reliability of the water harvesting system as a result of increased irrigation demand in the larger command area increases the seasonal variability in pasture production. Reduction in pasture growth compared to the low risk option is particularly obvious in the autumn months. (Barlow, 1985) found that sheep and beef farm stocking rate is more closely related to autumn pasture production than annual pasture production as autumn growth rate determines the pasture stored on the paddock for winter consumption. Autumn growth under irrigation may be a consideration for the planning and management of water harvesting schemes on sheep and beef farms. Having said this, it is important to note that although autumn production provides a better statistical estimation of stocking rate than annual production, it is by no mean the only factor determining stocking rate.

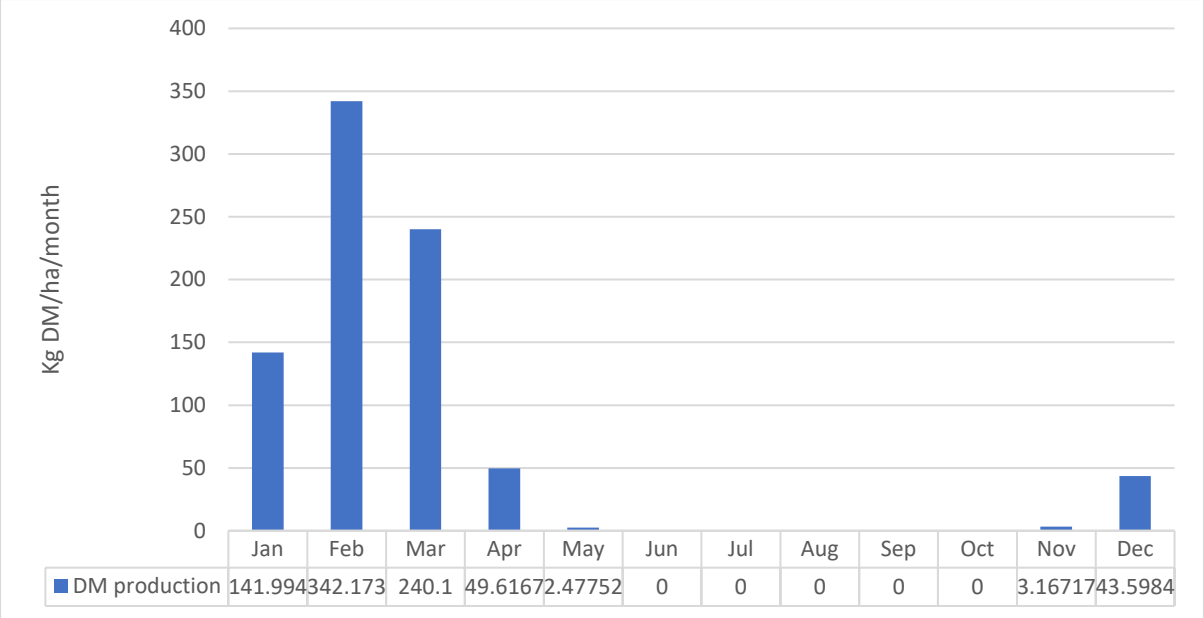

Figure 6-7 The difference between additional pasture growth per irrigated hectare under the high reliability scenario (40 ha irrigated) and additional pasture growth per irrigated hectare under the low reliability scenario (85 ha irrigated)

	40 Hectare			85 Hectare		
	Stressfree	**Unirrigated**	**Irrigated**	**Stressfree**	**Unirrigated**	**Irrigated**
Mean	12215.13	9698.049	12144.17	12215.13	9698.049	11339.3
Standard deviation	653.1593	827.6343	747.9146	653.1593	827.6343	825.2705

Table 6-18 Mean and standard deviation of per hectare biomass production of the low risk and high risk scenarios.

Scenario 2

Under the assumption that a 7 metres dam was constructed and a command area of 20 ha was irrigated, the water harvesting system in scenario 2 is able to produce, on average, 22,473 kg more pasture dry matter per year than the current unirrigated system. This increase in pasture production is considerably less than scenario 1 with a 10 metres dam and 85 ha command area (dry matter production 141,676 kg/year). It is important to remember that scenario 2 represents the "worst case scenario" i.e. it is the minimum the WHC is able to harvest and store. This scenario provides the most conservative measure of the economic benefit of the irrigation scheme.

Scenario 3

Scenario 3 is similar to scenario 1 with minor differences in pasture yield and optimal command area. Combination of the risk and additional pasture growth data in Table 6-10 and Table 6-11, cost of pasture dry matter in Table 6-14 and Table 6-15 reveals that a 9 meter embankment combined with 40 ha irrigated area allows the maximum increase in pasture growth while limiting the failure rate to under 5% for the lowest cost. As with scenario 1, scenario 3 faces the same dilemma in balancing the risks and benefits.

Economic Analysis

Irrigation v.s. fertilizer

The cost of producing one extra kilogram of pasture dry matter by irrigating the water harvested in the small scale water harvesting scheme is estimated at 39-44 cents/ kg DM. Given the current price for urea is $507/tonne (Ravensdown, 2017), the cost of growing one extra kilogram of pasture dry matter by adding nitrogen fertilizer as urea is estimated to be between 11-22 cents/ kg DM assuming a slow to moderate pasture response to N fertilizer. The application of nitrogen fertilizer is likely to increase pasture production rate during autumn, spring, and fall: the pasture response to nitrogen fertilizer applications are 4-8 Kg DM/kg N during the winter, 10-15kg DM/kg N during the early spring, 20 kg DM/kg N during late spring (NZ, 2012). Summer application is usually not recommended unless the pasture is irrigated. This is because in the absence of irrigation, summer pasture production is often limited by water, not nutrient avialability. It is important to note that the timing of pasture growth is often ignored in comparisons of irrigation and N fertiliser. If pasture cannot grow in summer or autumn due to a lack of moisture, then N fertiliser applications are likely to be very ineffective.

Irrigation v.s. buying feed

In contrast to the response to nitrogen fertiliser, the purchase of supplemental feed is not limited by the season. The cost of Palm kernel (PKE) is $235/ tonne which is equivalent to 26 cents/ kg DM (AgriHQ, 2016). The cost of feed barley is $256/ tonne, which equates to 30 cents/ kg DM. The cost of feed wheat is $274 /tonne, or 32 cents/ kg DM. The cost for maize grain is $335/ tonne, which equates to 41 cents/ kg DM. The prices quoted above include delivery fee to the nearest store or mill and so there is an additional cost associated with delivery to the farm and feeding it to animals. While feed prices fluctuate, and they

may well increase in the future, this very simple comparison tends to suggest that there may be some supplements that could be used more cost-effectively than the irrigation of harvested water on the case study farm. It is somewhat noteworthy that the irrigation system proposed here produces extra grass at a very similar cost to maize supplement. In the long run, the cost of producing additional dry matter on farm using an on-farm water harvesting system may be able to compete with buying in feed.

WHC v.s. large scale dam

The pasture response to irrigation is - in part – determined by, and to some extent limited by, the soil properties, and climate of the command area of the case study farm. The cost of a cubic meter of water supplied may be a better indication of the value of the water harvesting system. The cost of supplying one cubic meter of water to the Riverside farm with a reliability of 90% is 20 cents/ cubic meter. This value is the "farm gate value" of water which does not include the cost of irrigation application. This estimation indicates that the small scale water harvesting system is more expensive than the New Zealand average cost of supplying water to farm gate with a reliability of 95%, which is at 14 cent/ cubic meter (Curtis, 2016). When the irrigation reliability is increased to 95%, the cost of supplying water to farm gate rose to 22 cents/ cubic meter. The cost of per cubic meter water is 8 cents more than national average, but a fairer comparison is probably with other forms of harvested water particularly large scale schemes. Here the cost of on-farm harvested water compares favourably: it is lower than the Ruatuaniwha scheme which is being considered in the Hawkes Bay region. The cost of supplying one cubic meter of water for irrigation purpose in the Ruataniwha scheme is estimated to be 23.5-27 cents/ cubic meter (Osullivan, 2017).

Chapter 7 Conclusion

A small scale water harvesting and irrigation system was proposed as a solution to the shortage of pasture growth in summer and as a means to boost farm productivity in hill country New Zealand. It is also seen as an alternative to large scale irrigation schemes. Compared to large scale irrigation schemes that require the involvement of the whole community and large initial investment, these small on-farm schemes can be built relatively easily and cheaply. A case study was carried out to investigate the feasibility and viability of a small scale water harvesting scheme on a sheep and beef farm in the Wairarapa Region in New Zealand.

SWAT model was set up and calibrated to model the quantity of water that the proposed water harvesting catchment can harvest for irrigation purposes. This was the first time an attempt has been made to rigorously model the quantity of water that can be harvested from a catchment. Then a simple water balance was used to calculate the pasture response to water stored in the catchment. Finally, a financial analysis was carried out to model the additional pasture growth as result of irrigation.

According to the most conservative estimates (Scenario 3), 9 metre high on the case study farm can harvest and store enough water to irrigate 40 ha of command area with 95% reliability. This would allow 2.4 tonnes of pasture to be produced from each hectare irrigated. Alternatively, 114.8 tonnes extra pasture can be produced on a whole farm basis when 85 ha of land are being irrigated, although with a much lower reliability rate. The unit cost of the extra dry matter produced from irrigation is currently more expensive than buying supplementary feed such as PKE but this could change in the future. The cost per cubic meter of water from the small scale scheme is also higher than the national average, however, it seems to have a small advantage over the large scale water harvesting scheme proposed Ruatuaniwha region in the Hawkes Bay region.

Several problems have surfaced during this research. First of all, it has been discovered that SWAT may not be a practical candidate for hydrological modelling in New Zealand. SWAT requires large amounts of detailed data which is often unavailable in New Zealand. For example, compiling a suitable soil database requires expert knowledge of the local soils and this information is often unavailable. Pedotransfer functions can provide approximation to the variables needed however the accuracy of this approach is hard to quantify. Furthermore, the plant growth module built into SWAT has limitations when it comes to

modelling New Zealand pastoral system: the modelling of the LAI lacks the flexibility to adjust to southern hemisphere growth conditions. In addition, it was discovered that the virtual climate data provided by NIWA appears to give a “muted” record of daily rainfall resulting in low calibration efficiency on the daily time scale.

Second, despite years of research, the study of ungauged catchments is still in its infancy. The uncertainty in parameter regionalization has not been quantified. More research needs to be done to study the uncertainty caused by transferring model parameters from gauged catchments to an ungauged one.

Third, although a small scale water harvesting system is able to significantly improve farm pasture production, under current economic climate, such systems are uneconomical for hill country sheep and beef farmers. However, the analysis of the cost benefits presented here is necessarily rudimentary, it does not consider the additional pasture growth from a systems or feed budget stand point. In pastoral system the timing of the additional pasture growth matters as much as the quantity. A reliable additional source of pasture growth in summer/autumn may allow some change to stocking rate or animal performance at key times or the mix of enterprises on the farm that may well make irrigation of harvested water a much more attractive proposition. Therefore, further research is needed to identify whether any innovative alternative feeding regimes can justify the small scale water harvesting system.

Reference

Abbaspour, K. (2007). User manual for SWAT-CUP, SWAT calibration and uncertainty analysis programs. *Swiss Federal Institute of Aquatic Science and Technology, Eawag, Duebendorf, Switzerland*.

AgriHQ. (2016, October 24). Market Snapshot. *Farmers Weekly,* p. 36.

Al-Kaisi, M. M., Berrada, A., & Stack, M. (1997). Evaluation of irrigation scheduling program and spring wheat yield response in southwestern Colorado. *Agricultural Water Management, 34*(2), 137-148. doi:http://dx.doi.org/10.1016/S0378-3774(97)00010-3

Allen, R. G., Pereira, L. S., Raes, D., & Smith, M. (1998). Crop evapotranspiration-Guidelines for computing crop water requirements-FAO Irrigation and drainage paper 56. *FAO, Rome, 300*(9), D05109.

Almeida, C., Chambel-Leitao, P., & Jauch, E. (2011). *SWAT LAI calibration with local LAI measurements*. Paper presented at the SWAT Soil and Water assessment Tool.

Andersson, J., Zehnder, A., Jewitt, G., & Yang, H. (2009). Water availability, demand and reliability of in situ water harvesting in smallholder rain-fed agriculture in the Thukela River Basin, South Africa. *Hydrology and Earth System Sciences, 13*(12), 2329-2347.

Arabi, M., Frankenberger, J. R., Engel, B. A., & Arnold, J. G. (2008). Representation of agricultural conservation practices with SWAT. *Hydrological Processes, 22*(16), 3042-3055.

Arnold, J., Moriasi, D., Gassman, P., Abbaspour, K., White, M., Srinivasan, R., . . . Van Liew, M. (2012). SWAT: Model use, calibration, and validation. *Transactions of the ASABE, 55*(4), 1491-1508.

Baars, J., & Coulter, J. (1974). *Soil moisture and its influence on pasture production in the Waikato.* Paper presented at the Proceedings of the New Zealand Grassland Association.

Baek, C. W., Coles, N.A., . (2011). *Defining reliability for rainwater harvesting system*. Paper presented at the 19th International Congress on Modelling and Simulation, Perth, Australia.

Barlow, N. (1985). Value of sheep pasture, and the relationship between pasture production and stocking rate. *New Zealand journal of experimental agriculture, 13*(1), 5-12.

Behera, S., & Panda, R. K. (2006). Evaluation of management alternatives for an agricultural watershed in a sub-humid subtropical region using a physical process based model. *Agriculture, Ecosystems & Environment, 113*(1–4), 62-72. doi:http://dx.doi.org/10.1016/j.agee.2005.08.032

Black, A., & Murdoch, H. (2013). *Yield and water use of a ryegrass/white clover sward under different nitrogen and irrigation regimes.* Paper presented at the Proceedings of the New Zealand Grassland Association.

Blöschl, G. (2005). *Rainfall‐runoff modeling of ungauged catchments*: Wiley Online Library.

Blöschl, G. (2013). *Runoff prediction in ungauged basins: synthesis across processes, places and scales*: Cambridge University Press.

Bosch, D., Sheridan, J., Batten, H., & Arnold, J. (2004). Evaluation of the SWAT model on a coastal plain agricultural watershed. *Transactions of the ASAE, 47*(5), 1493.

Brown, A. M. (2001). A step-by-step guide to non-linear regression analysis of experimental data using a Microsoft Excel spreadsheet. *Computer methods and programs in biomedicine, 65*(3), 191-200.

Brown, S. C., Versace, V. L., Lester, R. E., & Walter, M. T. (2015). Assessing the impact of drought and forestry on streamflows in south-eastern Australia using a physically based hydrological model. *Environmental Earth Sciences, 74*(7), 6047-6063.

Caloiero, T. (2015). Analysis of rainfall trend in New Zealand. *Environmental Earth Sciences, 73*(10), 6297-6310.

Cameron, K., Di, H., & Moir, J. (2013). Nitrogen losses from the soil/plant system: a review. *Annals of Applied Biology, 162*(2), 145-173.

Cao, W., Bowden, W. B., Davie, T., & Fenemor, A. (2006). Multi‐variable and multi‐site calibration and validation of SWAT in a large mountainous catchment with high spatial variability. *Hydrological Processes, 20*(5), 1057-1073.

Cao, W., Bowden, W. B., Davie, T., & Fenemor, A. (2009). Modelling impacts of land cover change on critical water resources in the Motueka River catchment, New Zealand. *Water resources management, 23*(1), 137-151.

Chaplot, V. (2005). Impact of DEM mesh size and soil map scale on SWAT runoff, sediment, and NO3–N loads predictions. *Journal of Hydrology, 312*(1–4), 207-222. doi:http://dx.doi.org/10.1016/j.jhydrol.2005.02.017

Cibin, R., Athira, P., Sudheer, K., & Chaubey, I. (2014). Application of distributed hydrological models for predictions in ungauged basins: a method to quantify predictive uncertainty. *Hydrological Processes, 28*(4), 2033-2045.

Cibin, R., Sudheer, K., & Chaubey, I. (2010). Sensitivity and identifiability of stream flow generation parameters of the SWAT model. *Hydrological Processes, 24*(9), 1133-1148.

Cichota, R., Snow, V., & Tait, A. (2008). A functional evaluation of virtual climate station rainfall data. *New Zealand Journal of Agricultural Research, 51*(3), 317-329.

Coffey, M., Workman, S., Taraba, J., & Fogle, A. (2004). Statistical procedures for evaluating daily and monthly hydrologic model predictions. *Transactions of the ASAE, 47*(1), 59.

Conan, C., de Marsily, G., Bouraoui, F., & Bidoglio, G. (2003). A long-term hydrological modelling of the Upper Guadiana river basin (Spain). *Physics and Chemistry of the Earth, Parts A/B/C, 28*(4), 193-200.

Corong, E., Hensen, M., & Journeaux, P. (2014). *Value of Irrigation in New Zealand- An economy wide assesment*. Retrieved from New Zealand: https://www.mpi.govt.nz/document-vault/5014

Critchley, W., Siegert, K., Chapman, C., & Finkel, M. (1991). Water Harvesting. A manual for the design and construction of water harvesting schemes for plant production.

Curtis, A. (2016). *Cost of Irrigation Scheme Water Supply In New Zealand* Retrieved from Christchurch, New Zealand: http://irrigationnz.co.nz/wp-content/uploads/39238-INZ-CostSurveyReport2016.pdf

DairyNZ. (2010). Average Pasture Growth Data (kg DM/ha/day)-Lower North Island. Retrieved from https://www.dairynz.co.nz/media/323785/average_pasture_growth_data_lower_nth_is_oct_2010.pdf

Douglas-Mankin, K., Srinivasan, R., & Arnold, J. (2010). Soil and Water Assessment Tool (SWAT) model: Current developments and applications. *Transactions of the ASABE, 53*(5), 1423-1431.

Duncan, M. J., & Woods, R. A. (2013). Water regulation. *Ecosystem Services in New Zealand–condition and trends. Manaaki Whenua Press, Lincoln*.

El-Nasr, A. A., Arnold, J. G., Feyen, J., & Berlamont, J. (2005). Modelling the hydrology of a catchment using a distributed and a semi-distributed model. *Hydrological Processes, 19*(3), 573-587.

Geza, M., & McCray, J. E. (2008). Effects of soil data resolution on SWAT model stream flow and water quality predictions. *Journal of Environmental Management, 88*(3), 393-406. doi:http://dx.doi.org/10.1016/j.jenvman.2007.03.016

Gies, L., & Merwade, V. Creating SWAT Soil Database using FAO soil and Terrain Database of East Africa (SOTER) Data. Retrieved from https://web.ics.purdue.edu/~vmerwade/education/fao_soil_tutorial.pdf

Gitau, M. W., & Chaubey, I. (2010). Regionalization of SWAT model parameters for use in ungauged watersheds. *Water, 2*(4), 849-871.

Glendenning, C., Van Ogtrop, F., Mishra, A., & Vervoort, R. (2012). Balancing watershed and local scale impacts of rain water harvesting in India—A review. *Agricultural Water Management, 107*, 1-13.

Goel, A., & Kumar, R. (2005). Economic analysis of water harvesting in a mountainous watershed in India. *Agricultural Water Management, 71*(3), 257-266.

Guse, B., Reusser, D. E., & Fohrer, N. (2014). How to improve the representation of hydrological processes in SWAT for a lowland catchment–temporal analysis of parameter sensitivity and model performance. *Hydrological Processes, 28*(4), 2651-2670.

Hanson, L. S., Vogel, R. M., Kirshen, P., Shanahan, P., & Starrett, S. (2009). *Generalized storage-reliability-yield equations for rainwater harvesting systems.* Paper presented at the Proceedings of the World Environmental & Water Resources Congress.

Harmel, R., Richardson, C., & King, K. (2000). Hydrologic response of a small watershed model to generated precipitation. *Transactions of the ASAE, 43*(6), 1483.

Harris, S. (2015). *Wairarapa Flow Regimes- Economic impact assessment of draft plan changes*. Retrieved from Lyttelton, New Zealand:

Hayhoe, H. N. (1998). Relationship between weather variables in observed and WXGEN generated data series. *Agricultural and Forest Meteorology, 90*(3), 203-214. doi:http://dx.doi.org/10.1016/S0168-1923(97)00093-2

Hedley, C., Laurenson, S., Mclndoe, I., & Reese, P. (2014). *Irrigation on Hills*. Retrieved from New Zealand:

Hendery, S. (2015). Dam plan needs bridging finance. Retrieved from http://www.nzherald.co.nz/hawkes-bay-today/news/article.cfm?c_id=1503462&objectid=11421033

Her, Y., & Chaubey, I. (2015). Impact of the numbers of observations and calibration parameters on equifinality, model performance, and output and parameter uncertainty. *Hydrological Processes, 29*(19), 4220-4237.

Horne, D. (2016). *Water balance spreadsheet*. Palmerston North.

Horne, D., & Gray, D. (2014). *A farmer's Guide: Creating a climate of success- Huatokitoki Landcare Community Project*. Retrieved from

Howell, T., Cuenca, R., & Solomon, K. (1990). Crop Yield Response: Management of Farm Irrigation System. *Edt. Hoffman et al." ASAE, Madison, Wisconsin*.

Howes, J., Horne, D., & Shadbolt, N. (2014). A Calculator for Estimating the Profitability of Irrigation on new Zealand Dairy Farms. *Massey University*.

Jensen, C. R., Battilani, A., Plauborg, F., Psarras, G., Chartzoulakis, K., Janowiak, F., . . . Andersen, M. N. (2010). Deficit irrigation based on drought tolerance and root signalling in potatoes and tomatoes. *Agricultural Water Management, 98*(3), 403-413. doi:http://dx.doi.org/10.1016/j.agwat.2010.10.018

Jobbágy, E. G., & Jackson, R. B. (2000). The vertical distribution of soil organic carbon and its relation to climate and vegetation. *Ecological Applications, 10*(2), 423-436.

Julious, S. A. (2004). Using confidence intervals around individual means to assess statistical significance between two means. *Pharmaceutical Statistics, 3*(3), 217-222. doi:10.1002/pst.126

Kelkar, U., Narula, K. K., Sharma, V. P., & Chandna, U. (2008). Vulnerability and adaptation to climate variability and water stress in Uttarakhand State, India. *Global Environmental Change, 18*(4), 564-574.

Kemp, P., & Lopez, I. (2016). Hill country pastures in the southern North Island of New Zealand: an overview. *Hill Country – Grassland Research and Practice Series, 16*.

Krause, P., Boyle, D. P., & Bäse, F. (2005). Comparison of different efficiency criteria for hydrological model assessment. *Advances in Geosciences, 5*, 89-97.

Lambert, M., Devantler, B., Nes, P., & Penny, P. (1985). Losses of nitrogen, phosphorus, and sediment in runoff from hill country under different fertiliser and grazing management regimes. *New Zealand Journal of Agricultural Research, 28*(3), 371-379.

Lin, S., Jing, C., Chaplot, V., Yu, X., Zhang, Z., Moore, N., & Wu, J. (2010). Effect of DEM resolution on SWAT outputs of runoff, sediment and nutrients. *Hydrology and Earth System Sciences Discussions, 7*(4), 4411-4435.

Machado, C., Morris, S., Hodgson, J., & Fathalla, M. (2005). Seasonal changes of herbage quality within a New Zealand beef cattle finishing pasture.

Mackintosh, L. (2001, 2001). Overview of New Zealand Climate. Retrieved from https://www.niwa.co.nz/education-and-training/schools/resources/climate/overview

Matthews, C. (2016). [New Zealand pasture LAI estimation].
McAneney, K., & Judd, M. (1983). Pasture production and water use measurements in the central Waikato. *New Zealand Journal of Agricultural Research, 26*(1), 7-13.
McBride, S. (1994). *Pasture yield responses to irrigation in Canterbury.* Paper presented at the Proceedings of the New Zealand Grassland Association.
Me, W., Abell, J., & Hamilton, D. (2015a). Effects of hydrologic conditions on SWAT model performance and parameter sensitivity for a small, mixed land use catchment in New Zealand. *Hydrology and Earth System Sciences, 19*(10), 4127-4147.
Me, W., Abell, J., & Hamilton, D. (2015b). Modelling water, sediment and nutrient fluxes from a mixed land-use catchment in New Zealand: effects of hydrologic conditions on SWAT model performance. *Hydrology and Earth System Sciences Discussions, 12*, 4315-4352.
Merz, R., & Blöschl, G. (2004). Regionalisation of catchment model parameters. *Journal of Hydrology, 287*(1), 95-123.
Mockus, V., Werner, J., Woodward, D. E., Nielsen, R., Dobos, R., Hjelmfelt, A., & Hoeft, C. C. (2009). *National Engineering Handbook*. Washington, DC: USDA Retrieved from https://www.wcc.nrcs.usda.gov/ftpref/wntsc/H&H/NEHhydrology/ch7.pdf.
Moir, J. L., Scotter, D. R., Hedley, M. J., & Mackay, A. D. (2000). A climate - driven, soil fertility dependent, pasture production model. *New Zealand Journal of Agricultural Research, 43*(4), 491-500. doi:10.1080/00288233.2000.9513445
Moldan, F., Hultberg, H., Nyström, U., & Wright, R. F. (1995). Nitrogen saturation at Gårdsjön, southwest Sweden, induced by experimental addition of ammonium nitrate. *Forest Ecology and Management, 71*(1-2), 89-97.
Moot, D., Mills, A., Lucas, D., & Scott, W. (2009). Country Pasture/Forage Resource Profiles. *Country Pasture Profiles Retrieved, 28*(9), 2011.
Morcom, C. P. (2013). *Nitrogen Yields into the Tauranga Habour based on sub-catchment land use.* (Master of Science), The Univeristy of Waikato, Hamilton, New Zealand.
Moriasi, D. N., Arnold, J. G., Van Liew, M. W., Bingner, R. L., Harmel, R. D., & Veith, T. L. (2007). Model evaluation guidelines for systematic quantification of accuracy in watershed simulations. *Transactions of the ASABE, 50*(3), 885-900.
Morris, S. T., & Dymond, J. (2013). Sheep and beef cattle production systems. *Ecosystem services in New Zealand: conditions and trends, Lincoln: Landcare Research*, 79-84.
Mullan, B., Porteous, A., Wratt, D., & Hollis, M. (2005). Changes in drought risk with climate change. *National Institute of Water and Atmospheric Research (NIWA), editor: Wellington, New Zealand*.
Munsell Color, C. *Munsell soil color charts*.
Neitsch, S. L., Arnold, J. G., Kiniry, J. R., & Williams, J. R. (2005). Soil and Water Assessment Tool Theoretical Documentation (Version 2005). Retrieved from
Neitsch, S. L., Arnold, J. G., Kiniry, J. R., & Williams, J. R. (2011). *Soil and water assessment tool theoretical documentation version 2009*. Retrieved from
NIWA. (2016). Virtual Climate Station data and products. Retrieved from https://www.niwa.co.nz/climate/our-services/virtual-climate-stations
NZ, D. (2012). Seasonal Nitrogen Use. In D. NZ (Ed.). New Zealand.
Osullivan, P. (2017). Ruataniwha farm water price set - Hawkes Bay Today - Hawke's Bay Today News.
Ouessar, M., Bruggeman, A., Abdelli, F., Mohtar, R., Gabriels, D., & Cornelis, W. (2009). Modelling water-harvesting systems in the arid south of Tunisia using SWAT. *Hydrology and Earth System Sciences, 13*(10), 2003-2021.
Palmer, A. (2016). [Personal Communication Regarding Riverside Farm Water Harvesting Catchment Seepage Rate].
Pollok, J. A., Neall, V. E., & DeRose, R. C. (1994). *A field description of the Soil and Geology of Riverside Farm* (Vol. 14): Massey University.

Ravensdown. (2017). Ravensdown Urea. Retrieved from http://www.ravensdown.co.nz/products/fertiliser/urea

Reeves, E. (2014). *Modelling the hydrological impacts of land use change and intergrating cultural perspectives in the Waikouaiti Catchment, Otago New Zealand.* (Master of Science), University of Otago, Otago, New Zealand.

Riverside Farm. (2016). Retrieved from http://www.massey.ac.nz/massey/about-massey/subsidiaries-commercial-ventures/massey-agricultural-experiment-station/riverside-farm/riverside-farm.cfm

Romanowicz, A. A., Vanclooster, M., Rounsevell, M., & La Junesse, I. (2005). Sensitivity of the SWAT model to the soil and land use data parametrisation: a case study in the Thyle catchment, Belgium. *Ecological Modelling, 187*(1), 27-39. doi:http://dx.doi.org/10.1016/j.ecolmodel.2005.01.025

Saha, P. P., Zeleke, K., & Hafeez, M. (2014). Streamflow modeling in a fluctuant climate using SWAT: Yass River catchment in south eastern Australia. *Environmental Earth Sciences, 71*(12), 5241-5254.

Salinger, M. (1980). New Zealand climate: I. precipitation patterns. *Monthly weather review, 108*(11), 1892-1904.

Saxton, K., Rawls, W. J., Romberger, J., & Papendick, R. (1986). Estimating generalized soil-water characteristics from texture. *Soil Science Society of America Journal, 50*(4), 1031-1036.

Scotter, D., Clothier, B., & Turner, M. (1979). The soil water balance in a gragiaqualf and its effect on pasture growth in central New Zealand. *Soil Research, 17*(3), 455-465.

Shaver, E. (2009). *Small Dam Design*. (4105). Napier: Hawkes Bay regional Council Retrieved from http://www.hbrc.govt.nz/assets/Document-Library/Waterway-Design-guidelines/Small-Dam-Design-20090406.pdf.

Shen, Z., Chen, L., & Chen, T. (2012). Analysis of parameter uncertainty in hydrological and sediment modeling using GLUE method: a case study of SWAT model applied to Three Gorges Reservoir Region, China. *Hydrology and Earth System Sciences, 16*(1), 121-132.

Siddique, K., Belford, R., & Tennant, D. (1990). Root: shoot ratios of old and modern, tall and semi-dwarf wheats in a Mediterranean environment. *Plant and Soil, 121*(1), 89-98.

Snaydon, R. (1972). The effect of total water supply, and frequency of application, upon lucerne. I. Dry matter production. *Crop and Pasture Science, 23*(2), 239-251.

Soltani, A., Latifi, N., & Nasiri, M. (2000). Evaluation of WGEN for generating long term weather data for crop simulations. *Agricultural and Forest Meteorology, 102*(1), 1-12. doi:http://dx.doi.org/10.1016/S0168-1923(00)00100-3

Spruill, C., Workman, S., & Taraba, J. (2000). Simulation of daily and monthly stream discharge from small watersheds using the SWAT model. *Transactions of the ASAE, 43*(6), 1431-1439.

Srinivasan, M., & McDowell, R. (2009). Irrigation and soil physical quality: An investigation at a long-term irrigation site. *New Zealand Journal of Agricultural Research, 52*(2), 113-121.

Srinivasan, R., Zhang, X., & Arnold, J. (2010). SWAT ungauged: hydrological budget and crop yield predictions in the Upper Mississippi River Basin. *Transactions of the ASABE, 53*(5), 1533-1546.

Stephens, T. (2010). *Manual on small earth dams- A guide to siting, design and construction*. Retrieved from Rome, Italy:

Sun, W., Yao, X., Cao, N., Xu, Z., & Yu, J. (2016). Integration of soil hydraulic characteristics derived from pedotransfer functions into hydrological models: evaluation of its effects on simulation uncertainty. *Hydrology Research, 47*(5), 964-978.

Tan, M. L., Ficklin, D. L., Dixon, B., Yusop, Z., & Chaplot, V. (2015). Impacts of DEM resolution, source, and resampling technique on SWAT-simulated streamflow. *Applied Geography, 63*, 357-368.

Thompson, M. (2015). *Minimum flow recommendations for the Wellington region: Technical Report to support the Proposed Natural Resource Plan.* (GW/ESCI-T-15/85). Wellington: Greater Wellington Regional Council.

Turner, N. (1990). Plant water relations and irrigation management. *Agricultural Water Management, 17*(1), 59-73.

Ullrich, A., & Volk, M. (2009). Application of the Soil and Water Assessment Tool (SWAT) to predict the impact of alternative management practices on water quality and quantity. *Agricultural Water Management, 96*(8), 1207-1217.

USDA-NRCS. Soil Texture Calculator. Retrieved from http://www.nrcs.usda.gov/wps/portal/nrcs/detail/soils/survey/?cid=nrcs142p2_054167

Van Griensven, A., Meixner, T., Grunwald, S., Bishop, T., Diluzio, M., & Srinivasan, R. (2006). A global sensitivity analysis tool for the parameters of multi-variable catchment models. *Journal of Hydrology, 324*(1), 10-23.

Wall, A., Stevens, D., Thompson, B., & Goulter, C. (2012). *Winter management practices to optimise early spring pasture production: a review.* Paper presented at the Proceedings of the New Zealand Grassland Association.

Wallis, T. W., & Griffiths, J. F. (1995). An assessment of the weather generator (WXGEN) used in the erosion/productivity impact calculator (EPIC). *Agricultural and Forest Meteorology, 73*(1), 115-133.

Watts, L. (2005). Hydrological monitoring technical report. *Greater Wellington Regional Council, Wellington, New Zealand*.

Waugh, T. (2015). What is the real cost of pasture growth? Retrieved from https://farmersweekly.co.nz/section/dairy/view/what-is-the-real-cost-of-pasture-growth#

Williams, J. R., & Singh, V. (1995). The EPIC model. *Computer models of watershed hydrology.*, 909-1000.

Yang, J., Reichert, P., Abbaspour, K., Xia, J., & Yang, H. (2008). Comparing uncertainty analysis techniques for a SWAT application to the Chaohe Basin in China. *Journal of Hydrology, 358*(1), 1-23.

Zhang, B., Valentine, I., & Kemp, P. D. (2007). Spatially explicit modelling of the impact of climate changes on pasture production in the North Island, New Zealand. *Climatic Change, 84*(2), 203-216.

Zhang, C., Chu, J., & Fu, G. (2013). Sobol''s sensitivity analysis for a distributed hydrological model of Yichun River Basin, China. *Journal of Hydrology, 480*, 58-68.

Zhang, Y., & Chiew, F. H. S. (2009). Relative merits of different methods for runoff predictions in ungauged catchments. *Water Resources Research, 45*(7), n/a-n/a. doi:10.1029/2008WR007504

Appendixes

Appendix I – Excel spreadsheet for calculating command area and pond water balance

The command area water balance was calculated on an excel spreadsheet along with pond water balance. A series of screenshots demonstrated the process of which the water balance is calculated. Figure Appendix-1 gives an overview of the spreadsheet. Figure Appendix-1 is subdivided into 7 parts and a more detailed screen shots are provided for each sub-section.

Part 1 of the spread sheet asked for soil properties of the command area and dam properties. Field capacity (FC) and permanent wilting point (PWP) are given inputs. The total available water content (AWC) is the difference between soil water content between FC and PWP. Therefore, it is calculated as "=F3-F4". Readily available water is the quantity of water that plant can extract from soil profile without any stress to the system. It is set to be half of the AWC or "=F5/2" in the excel spreadsheet. Seepage rate is also given. As to dam properties, embankment height is given, and an excel look up function was used for the maximum water storage volume for a corresponding dam height. The table is the same as Table 6-1

Part 2 of the spreadsheet simply determine whether a given day of the year is in the irrigating season or not. Rain and PET uses the actual climate data as an input.

Part 3 of the spreadsheet models the pond water balance. Results from SWAT modelling was input under the "FLOW_IN" column. The pond is assumed to be empty before the first day and therefore on day one Vpond (pond volume) "=G12", from the second day on, the Vpond is bounded by the maximum dam storage volume determined by the embankment height. The surface area of the pond (SurfPond) is calculated using Equation 3-2, or "=350*H12^(1/2.31)". Evappond is the evaporation from the pond surface. It is calculated as 0.6 PET times the surface area of the pond or "=I12*0.6*F12*0.001" of the previous day times Finally Seepage from the bottom of the pond is equal to the Vpond on the previous day times the seepage rate.

Part 4 of the spread sheet concerns the actual ET of both irrigated and unirrigated soil, irrigation depth and volume, soil water content and readily available soil water content on both the irrigated and unirrigated land. First actual ET is calculated for both the irrigated

scenario and unirrigated scenario. A series of IF functions were used to express the conditionality of calculating the actual ET. Irrigation depth or Irr-Depth is determined by whether there are enough water in the pond for an irrigation event. When the pond has enough water to irrigate the whole command area, an irrigation event will be triggered. Irr-Volume is simply the volume irrigated to the land during a specific irrigation event. SW-1 is simply the soil water content from previous day. SW is bounded by the field capacity and completely dry condition. The soil water content cannot exceed field capacity and cannot go below 0. As with SW-1, SW-1' is the SW' from previous day. SW' is the readily available water content in the soil profile. It is also bounded by conditionality. Finally, SW-Deficit is soil water deficit, it is the difference between field capacity and soil water content. Similar calculation is repeated for the unirrigated scenario.

Part 5 provide the details of irrigation. Irrigation trigger deficit is the soil water deficit that triggers an irrigation. This value is given. Irrigation depth is the depth of water applied to the command area when irrigation was triggered. This value is also given. Command area is the area of which irrigation water is applied to. This value can be changed to test different scenarios. Irrigation day is simply the total number of days when irrigation was applied to the command area, it is calculated using a simple "countif" function. Finally total irrigation volume is the total water applied to the command area in a given period. This value is calculated as the sum of irrigation volume in the given period.

Part 6 model the biomass production under irrigation, dryland, and stressfree conditions. The calculation was conducted using Equation 3-14. Then the final part calculates the failure rate by asking four questions: First, should irrigation water be applied? This decision is determined by the soil water deficit. Second, when the first question's answer is yes, was irrigation actually applied to the soil? In another words, is there enough water in the pond to supply for irrigation? Third, was there an irrigation failure? This was calculated by finding difference between the first question and the second question. And the fourth question calculates failure by its occurrence, 5 days of consecutive water supply failure is counted as one failure.

Part 7 Calculates and count the results from part 6 and provide results to the question asked.

Figure Appendix 1-1

Figure Appendix 1-2 Part 1

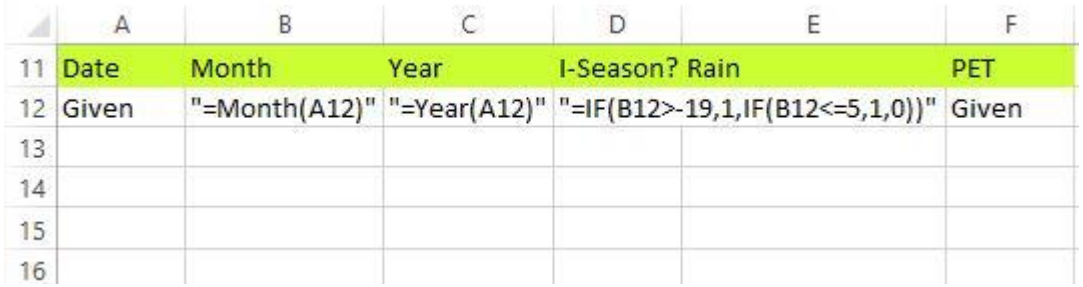

Figure Appendix 1-3 Part 2

	G	H	I	J	K
11	Flow_IN	V_{pond}	$Surf_{pond}$	$Evap_{pond}$	Seepage
12	Given	"=G12"	"=350*H12^(1/2.31)"		
13		"=IF(H12+G13-J11-K11-O11>=$K$4,$K$4,IF(H12+G13-J12-K12-O12<-0,0,H12+G13+J12-K12-O12))"			
14					"=H13*$F$7"
15				"=I15*0.6*F15*0.001"	
16					
17					

Figure Appendix 1-4 Part 3

	L	M	N	O	P	Q	R	S	T	U	V	W	X	Y
8														
9														
10	actual ET		Irrigation Info		Irrigated							Unirrigated		
11	ET(Irr)	ET(non-Irr)	Irr-Depth	Irr-Volume	SW-1	SW	SW-1'	SW'	SW-Deficit	U-SW-1	U-SW	U-SW-1'	U-SW'	U-SW-Def
12	"=IF(R12+E12+N12>=F12,F12,IF(T12<=$F$6,F12,IF(T12>=$F$5,0,F12*($F$5-T12)/$F$6)))"													
13		"=IF(W13+E13>=F13,F13,IF(Y13<=$F$6,F13,IF(Y13>=$F$5,0,F13*($F$5-Y13)/$F$6)))"												
14			"=IF(T14>=$P$3,IF(H14>=$P$4*$P$5*10,$P$4,0),0)"											
15				"=N15*$P$5*10"										
16					"=Q15"	"=IF(P16+E16+N16-L16>=$F$3,$F$3,IF(P16+E16+N16-L16<0,0,P16+E16+N16-L16))"								
17							"=S16"	"=IF(R17+E17-L17+N17>=0,IF(R17+E17-L17+N17>=$F$6,$F$6,R17+E17-L17+N17),0)"						
18								"=F3-P18"						
19														
20														
21														

Figure Appendix 1-5 Part 4

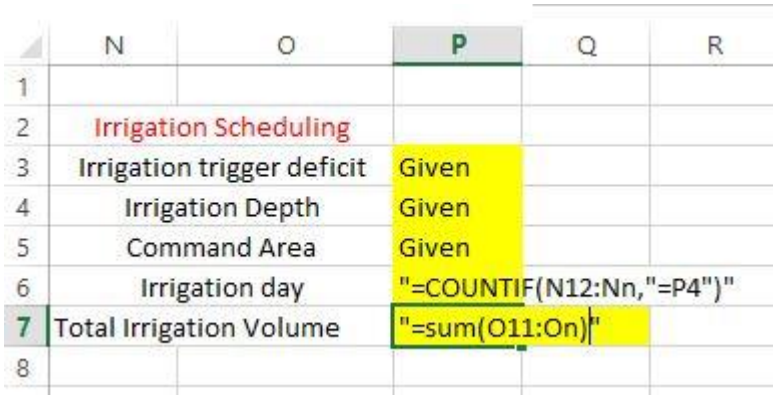

	N	O	P	Q	R
1					
2		Irrigation Scheduling			
3		Irrigation trigger deficit	Given		
4		Irrigation Depth	Given		
5		Command Area	Given		
6		Irrigation day	"=COUNTIF(N12:Nn,"=P4")"		
7		Total Irrigation Volume	"=sum(O11:On)"		
8					

Figure Appendix 1-6 Part 5

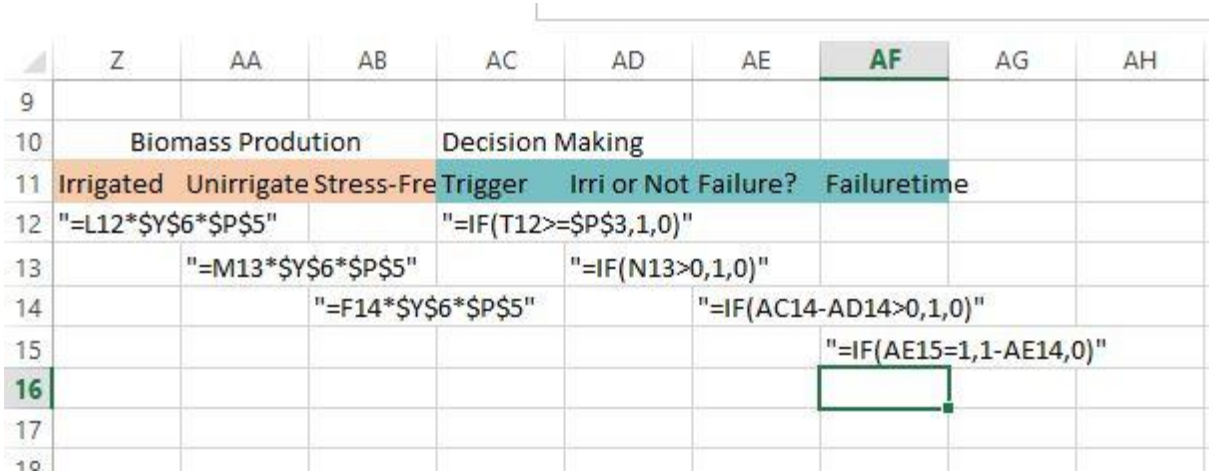

	Z	AA	AB	AC	AD	AE	AF	AG	AH
9									
10	Biomass Prodution			Decision Making					
11	Irrigated	Unirrigate	Stress-Fre	Trigger	Irri or Not	Failure?	Failuretime		
12	"=L12*$Y$6*$P$5"			"=IF(T12>=$P$3,1,0)"					
13		"=M13*$Y$6*$P$5"			"=IF(N13>0,1,0)"				
14			"=F14*$Y$6*$P$5"			"=IF(AC14-AD14>0,1,0)"			
15							"=IF(AE15=1,1-AE14,0)"		
16									
17									

Figure Appendix 1-7 Part 6

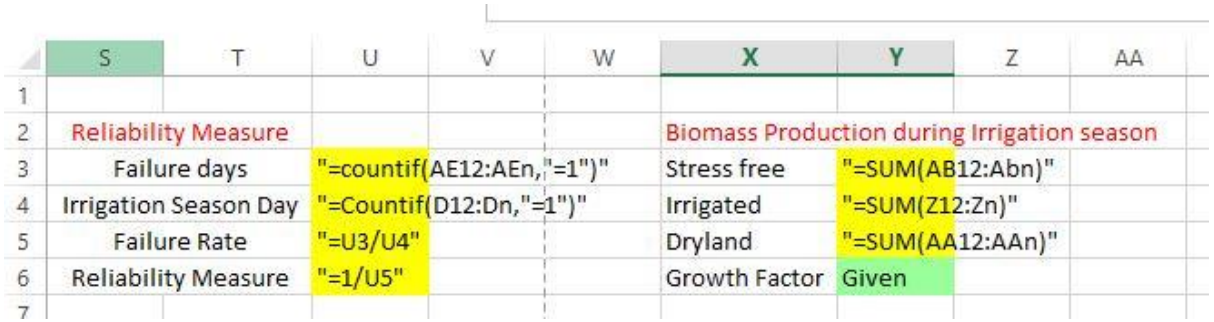

	S	T	U	V	W	X	Y	Z	AA
1									
2	Reliability Measure					Biomass Production during Irrigation season			
3	Failure days		"=countif(AE12:AEn,"=1")"			Stress free	"=SUM(AB12:Abn)"		
4	Irrigation Season Day		"=Countif(D12:Dn,"=1")"			Irrigated	"=SUM(Z12:Zn)"		
5	Failure Rate		"=U3/U4"			Dryland	"=SUM(AA12:AAn)"		
6	Reliability Measure		"=1/U5"			Growth Factor	Given		
7									

Figure Appendix 1-8 Part 7

Appendix II- Validating WGEN weather generator

Weather generator was used to model long term water balance of WHC and to fill missing data points within the data set. WXGEN was built in to SWAT and uses monthly data from WGEN_user database to predict daily weather condition. WXGEN was developed based on WGEN developed by Richardson and Richardson and Wright. Few literatures discussed the quality of these weather generators. (Soltani, Latifi, & Nasiri, 2000) used WGEN generated data to model the long term yield of chickpeas under irrigated and rain-fed conditions. The result from this study demonstrated high degree of similarity between actual and the WGEN generated weather data. (Harmel, Richardson, & King, 2000) studied the effect of the selection of weather generator has on SWAT hydrologic responses, the study shows that WXGEN allows for superior runoff simulation than WGEN. In addition, (Hayhoe, 1998) discovered that the due to the design of WXGEN, the module is able to accurately preserve the relationship between precipitation, temperature, and solar radiation. Despite some positive results, there is a concern that the model generated weather data may fail to represent the actual weather series. For instance, (Wallis & Griffiths, 1995) conducted over 20,000 statstical tests for the weather series generated by WXGEN and observed weather data and found that over 15% of the time the null hypothesis of similarity was rejected.

Precipitation

Precipitation is the driving force behind all hydrological movements. The generated mean monthly precipitation was compared to the recorded precipitation record used to construct WGEN_user database using t-test. F-test was applied to compare the standard deviation of the generated monthly precipitation and that of recorded precipitation. The null hypothesis is that there is no significant difference between the generated and observed data when P value is lower than a threshold value. This threshold value is usually 0.01, 0.05 or 0.10. For this study 0.05 was set to the significance value allowing for a 95% confidence interval. Finally, a polynomial generalized linear regression model was used to fit the generated seasonal precipitation and recorded precipitation on the month. The difference in the estimated parameters between the generated and recorded precipitation models was compared according to Julious (2004), i.e., if the 83.4% confidence limit overlaps, then there is no significant difference in these means between the two models.

The assumption of t-test and F-test is that the sample must be normally distributed. However, the preliminary Shapiro-Wilk normality test shows that for some samples normal distribution assumption is not satisfied. Samples that failed to pass the Shapiro-Wilk normality test are log or square root transformed and the assumption for normal distribution is met. Exception was made for the generated precipitation for the month of April as neither the original data nor the transformed data passed the Shapiro-Wilk normality test. However, since the P-value is 0.024, it can be considered to be near normally distributed.

Months	Transformation
Jan	Square root
Feb	Log
Mar	Square Root
Apr	Square Root
May	Square Root
June	Square Root
July	Square Root
Aug	N/A
Sep	Square Root
Oct	Square Root
Nov	Square Root
Dec	log

Table Appendix 2-1 Transformation taken for each month

After the transformation of data, a series of t-tests was carried out using the transformed data to compare the mean precipitation of each month. The result shows no significant difference between the mean of WXGEN generated and recorded data.

Next, F-tests were applied to the same transformed data to detect any difference in the variance of precipitation for each month in the generated and recorded data. However, while there are no significant difference to the variance of average precipitation for most months, the variance of rainfall for February and September between WXGEN generated and recorded data differs significantly. This result echo the finding of Wallis and Griffiths (1995).

Finally, the polynomial generalized linear regression model was constructed for the observed and simulated precipitation. The regression model is said to be representing the

reality when all parameters are fitted with a P value of less than 0.5. It was found that all of the 83.4% confidence limit of the estimated parameters for the generated precipitation data falls within the 83.4% confidence limit of the estimated parameters for the recorded precipitation data. This result shows that the regression model for the generated precipitation data series is able to predict recorded precipitation in a statistically meaningful way.